



TITLE:

Qualitative Study on the Solutions of Duffing's Equation(Dissertation_全文)

AUTHOR(S):

Kawakami, Hiroshi

CITATION:

Kawakami, Hiroshi. Qualitative Study on the Solutions of Duffing's Equation. 京都大学, 1974, 工学博士

ISSUE DATE:

1974-09-24

URL:

<https://doi.org/10.14989/doctor.r2610>

RIGHT:



QUALITATIVE STUDY ON THE SOLUTIONS OF DUFFING'S EQUATION

HIROSHI KAWAKAMI
DEPARTMENT OF ELECTRONICS
TOKUSHIMA UNIVERSITY

December, 1973

QUALITATIVE STUDY ON THE SOLUTIONS OF DUFFING'S EQUATION

QUALITATIVE STUDY ON THE SOLUTIONS OF DUFFING'S EQUATION

HIROSHI KAWAKAMI

DECEMBER, 1973

INTRODUCTION

This paper deals with some problems concerning the qualitative property of the solutions of Duffing's equation. Recently, interest in the field of nonlinear differential equations has been directed to the study of so-called global problems. Qualitative theory initiated by H. Poincaré and G. D. Birkhoff is useful for the study of those problems and is based on the geometrical property of the phase portrait, i.e., the family of solution curves which fill up the entire phase space. When a differential equation has a cross-section [34]*, the qualitative study of the differential equation reduces to the study of an associated topological mapping of the cross-section. N. Levinson [19] made use of this mapping for the study of second order nonlinear differential equations. The type of the topological mapping in this paper is that of the Euclidean plane into itself. Combining this method of mapping and computer facilities, we investigate the qualitative properties of Duffing's equation.

The text consists of four chapters. In the first two chapters, qualitative properties of certain nonlinear differential equations of the second order are discussed, and the methods of computer analysis are described. The last two chapters are concerned with the qualitative study of the solutions of Duffing's equation.

In Chap. 1, some topological properties of the solutions of Duffing's equation are surveyed. In connection with the equation, fundamental definitions, such as the topological mapping of the phase plane into itself, fixed and periodic points of the mapping, classification of fixed point, dissipative system

* Number in brackets indicates references on pages 77 to 80.

and its maximum invariant set, etc., are stated. Certain properties on the behavior of the solutions of dissipative systems are discussed. Invariant curve of the mapping and its related properties are also discussed.

Chapter 2 deals with the methods of numerical analysis for the solutions of Duffing's equation. Numerical computations are carried out by using both analog and digital computers. From a computational standpoint analog computers are useful for solving the initial value problem of ordinary differential equations. The iterations of the mapping discussed in Chap. 1 are easily carried out by an analog computer with sequential logics. Therefore, analog computers are mostly used to obtain the global properties of the solutions. On the other hand, the location of fixed and periodic points and the correlated periodic solutions are calculated by a digital computer. An example of the numerical solution is illustrated.

Chapter 3 is concerned with the periodic solutions of Duffing's equation. Various types of periodic solutions are investigated by numerical analysis. Namely, harmonic and higher-harmonic solutions and subharmonic solutions of orders 2 and 3 are studied. Certain bifurcation of fixed points and the regions in the parameters plane in which periodic solutions are obtained are investigated. To survey the global aspect of the solutions of Duffing's equation, the phase portrait obtained by the mapping is discussed.

In Chap. 4, doubly asymptotic solution and its related properties are discussed. A doubly asymptotic solution is defined by a solution whose trajectory is the intersection of stable and unstable manifolds for some directly or inversely unstable periodic solutions, [4, 29, 32]. For Duffing's equation, the appearance of doubly asymptotic solutions, especially of homoclinic solutions,

is rarely known up to the present time. The mathematical assertion for the existence of such solutions is still open. Therefore, the homoclinic and heteroclinic solutions and their related properties for dissipative and non-dissipative systems are investigated by numerical computations.

ACKNOWLEDGMENTS

The author owes a lasting debt of gratitude to Professor Dr. C. Hayashi of Kyoto University, who has suggested the field of research of the present thesis and given him constant and generous guidance and encouragement in promoting his work.

In the preparation of the present paper the author has been given many aids and useful advices from Assistant Professor Dr. Y. Ueda of Kyoto University. Acknowledgment must also be made to Assistant Professor Dr. M. Abe of Kyoto University for the use of analog-computer facilities.

The author is also grateful to the staffs and the graduate students of Dr. Hayashi's Laboratory for their excellent cooperation.

The author's thanks are due to Professor Dr. K. Kobayashi of Tokushima University for his valuable suggestions and many good advices of all kinds.

CONTENTS

Introduction	iii
Chapter 1. Topological Properties of the Solutions of Duffing's Equation	
1.1 Introduction	1
1.2 Topological mapping T	2
1.3 Classification of fixed points	3
1.4 Dissipative system and its maximum invariant set	9
1.5 Theorem on the number of fixed and periodic points	11
1.6 Invariant curves of the mapping T and their related properties	12
1.7 Examples of the patterns of invariant curves	16
Chapter 2. Methods of Numerical Analysis	
2.1 Introduction	20
2.2 Procedure of numerical analysis	21
2.3 Analog-computer study	22
2.4 Digital-computer study	25
2.5 An example of numerical solution	26
Chapter 3. Periodic Solutions of Duffing's Equation	
3.1 Introduction	29
3.2 Bifurcation and classification of periodic solutions	30
(a) Generation and branching of fixed points for Eqs. (3.3)	32
(b) Classification of the periodic solutions of Duffing's equation	35
3.3 Harmonic and higher-harmonic solutions	36
(a) Regions in which harmonic and higher-harmonic solutions exist	36
(b) Loci of fixed points and patterns of phase portraits as B varies	38

(c)	Harmonic solutions	40
(d)	Higher-harmonic solutions	42
(e)	Higher-harmonic solutions with subharmonics	44
3.4	Subharmonic solutions of order 2	47
(a)	1/2-harmonic solutions for Eqs. (3.3)	47
(b)	3/2-harmonic solutions for Eqs. (3.3)	50
(c)	Successive multiplication of SI-branching	53
3.5	Subharmonic solutions of order 3	54
(a)	1/3-harmonic solutions for Eqs. (3.3)	54
(b)	5/3-harmonic solutions for Eqs. (3.3)	57
(c)	7/3-harmonic solutions for Eqs. (3.3)	59
3.6	Supplementary remarks	63
Chapter 4. Doubly Asymptotic Solutions of Duffing's Equation		
4.1	Introduction	64
4.2	Homoclinic points correlated with a directly unstable fixed point	65
4. (a)	Homoclinic points in nondissipative systems	65
(b)	Homoclinic points in dissipative systems	69
4.3	Homoclinic points correlated with directly unstable 3-periodic points	71
4.4	Heteroclinic points correlated with directly unstable fixed points	72
4.5	Heteroclinic points correlated with a fixed and 3-periodic points	74
4.6	Supplementary remarks	75
References		77

CHAPTER 1

TOPOLOGICAL PROPERTIES OF THE SOLUTIONS OF DUFFING'S EQUATION

1.1 Introduction

The purpose of this chapter is to briefly survey the qualitative properties of the solutions of Duffing's equation

$$\frac{d^2x}{dt^2} + k\frac{dx}{dt} + c_1x + c_3x^3 = B\cos t + B_0 \quad (1.1)$$

This equation occurs in several different kinds of physical problems. The problem of finding the forced oscillation of an electric oscillatory circuit containing a saturable inductor leads to the solution of Eq. (1.1), [12] Chap.5. As we shall see in the following chapters, the solution of this comparatively simple differential equation possesses a great variety of properties. A considerable number of papers have been published concerning periodic solutions of Eq. (1.1) by using various approximation methods [7, 10, 12, 20]. Still less is known about the nonperiodic solutions. In this chapter the topological mapping based on the qualitative theory of differential equations is considered. The topological mapping, which transfers a representative point on the phase plane at $t = t_0$ to a representative point at $t = t_0 + \tau$ (τ being the period of the external forcing term or its integral multiple), plays an essential role for the numerical analysis in the following chapters. A fixed point of the mapping corresponds to a periodic solution. The behavior of invariant curves in the phase plane reveals the global aspect of the solutions.

1.2 Topological mapping T

In studying the properties of the solutions of Eq. (1.1) it is helpful to use the phase plane, with coordinates x and $y = \frac{dx}{dt}$. Equation (1.1) then becomes the equivalent system

$$\begin{aligned}\frac{dx}{dt} &= y \\ \frac{dy}{dt} &= -ky - c_1x - c_3x^3 + B \cos t + B_0\end{aligned}\tag{1.2}$$

where k, c_1, c_3, B and B_0 are real parameters with $k \geq 0, c_3 > 0$.

The system (1.2) is a particular case of nonautonomous two dimensional system

$$\begin{aligned}\frac{dx}{dt} &= f(t, x, y) \\ \frac{dy}{dt} &= g(t, x, y)\end{aligned}\tag{1.3}$$

where $f(t, x, y)$ and $g(t, x, y)$ defined for all t, x and y in the real numbers R are both periodic in t with period 2π :

$$\begin{aligned}f(t + 2\pi, x, y) &= f(t, x, y) \\ g(t + 2\pi, x, y) &= g(t, x, y)\end{aligned}\tag{1.4}$$

In the following we assume that f and g satisfy the standard conditions for the existence and uniqueness of the solutions for all t in R and moreover for the continuity and differentiability properties of the solutions with respect to any initial condition.

Let us consider the solutions of Eqs. (1.3) in three dimensions x, y and $t: R^{2+1}$. Since the right-hand side of Eqs. (1.3) has period 2π , the equation itself is the same at $t = 0$ and $t = 2\pi$. Then we obtain from the solutions of Eqs. (1.3) a topological mapping T as follows. Let $P_0(x_0, y_0)$ be an arbitrary

point of the xy plane, and $x(t) = x(t; x_0, y_0)$, $y(t) = y(t; x_0, y_0)$ be the solution of Eqs. (1.3) determined by the initial conditions $x(0; x_0, y_0) = x_0$, $y(0; x_0, y_0) = y_0$. We define a mapping T of the xy plane into itself which transforms $P_0(x_0, y_0)$ into $P_1(x_1, y_1)$:

$$T: \begin{array}{ccc} \mathbb{R}^2 & \longrightarrow & \mathbb{R}^2 \\ P_0 & \longmapsto & P_1 \end{array}$$

where $x_1 = x(2\pi, x_0, y_0)$, $y_1 = y(2\pi, x_0, y_0)$.

This mapping is often called the Poincaré mapping. The mapping T has well-known properties, [8]:

1. $T^m \circ T^n = T^m \cdot T^n = T^n \cdot T^m$ for any integers m and n ,
2. T^{-1} is the inverse mapping of T ,
3. T is homeomorphism which preserves the orientation.

If a solution $x(t) = x(t; x_0, y_0)$, $y(t) = y(t; x_0, y_0)$ has period 2π , then the point $P_0(x_0, y_0)$ is a fixed point of the mapping T such that $P_0 = T(P_0)$. If $x(t)$, $y(t)$ is a subharmonic solution of order ν ($\nu = 2, 3, \dots$), i.e., a solution with least period $2\nu\pi$, then P_0 is a point with period ν such that $P_0 = T^\nu(P_0)$ and $P_0 \neq T^{\nu'}(P_0)$ for $\nu' = 1, 2, \dots, \nu - 1$. Hence there are always ν points $P_0, P_1 = T(P_0), \dots, P_{\nu-1} = T^{\nu-1}(P_0)$ which are all fixed points of T^ν and often called ν -periodic points of T .

1.3 Classification of fixed points

There are certain standard types of fixed point of the mapping T and they are significant in the study of periodic solutions of the system (1.3).

Let us consider the change in area in the xy plane under the mapping T . Let $P_0(x_0, y_0)$ be a point of the xy plane and $P_1(x_1, y_1)$ its image by T , and

$x(t)$, $y(t)$ denote the solution of Eqs. (1.3) at P_0 when $t = 0$. Let a neighborhood U_0 of P_0 which has an area $\mu(U_0)$ is carried by T into a neighborhood U_1 of P_1 with an area $\mu(U_1)$. Then the limit of the ratio $\mu(U_1)/\mu(U_0)$ as $\mu(U_0) \rightarrow 0$ is given by the Jacobian

$$\Delta(t) = \frac{\partial(x(t), y(t))}{\partial(x_0, y_0)} = \begin{vmatrix} \frac{\partial x(t)}{\partial x_0} & \frac{\partial x(t)}{\partial y_0} \\ \frac{\partial y(t)}{\partial x_0} & \frac{\partial y(t)}{\partial y_0} \end{vmatrix} \quad (1.5)$$

for $t = 2\pi$. For the system (1.3) we have

$$\dot{\Delta}(t) = \left\{ \frac{\partial}{\partial x} f(t, x(t), y(t)) + \frac{\partial}{\partial y} g(t, x(t), y(t)) \right\} \Delta(t)$$

Since $\Delta(0) = 1$, it follows that

$$\begin{aligned} \Delta(2\pi) &= \frac{\partial(x_1, y_1)}{\partial(x_0, y_0)} = \begin{vmatrix} \frac{\partial x_1}{\partial x_0} & \frac{\partial x_1}{\partial y_0} \\ \frac{\partial y_1}{\partial x_0} & \frac{\partial y_1}{\partial y_0} \end{vmatrix} \\ &= \exp \int_0^{2\pi} \left\{ \frac{\partial}{\partial x} f(t, x, y) + \frac{\partial}{\partial y} g(t, x, y) \right\} dt \end{aligned} \quad (1.6)$$

Thus the element of area $dx_0 dy_0$ is carried by T into $\Delta(2\pi) dx_0 dy_0$.

Now let $P_0(x_0, y_0)$ be a fixed point under T and consider the mapping T in the neighborhood of the fixed point P_0 . Let $x_0(t)$, $y_0(t)$ denote the solution of Eqs. (1.3) at P_0 when $t = 0$. If a point $P(x_0 + u_0, y_0 + v_0)$ is mapped by T into $P'(x_0 + u_1, y_0 + v_1)$, and $x(t)$, $y(t)$ is the solution of Eqs. (1.3) emanating from P , then by the continuity and differentiability of $x(t)$, $y(t)$ with respect to u_0 and v_0 , we have

$$\begin{aligned}
x(t) &= x_0(t) + \xi_1(t)u_0 + \xi_2(t)v_0 + X(t, u_0, v_0) \\
y(t) &= y_0(t) + \eta_1(t)u_0 + \eta_2(t)v_0 + Y(t, u_0, v_0)
\end{aligned}
\tag{1.7}$$

where X, Y and their partial derivatives with respect to u_0 and v_0 vanish at $u_0 = v_0 = 0$. Since $x(2\pi) = x_0 + u_1$, $y(2\pi) = y_0 + v_1$, it follows that

$$\begin{aligned}
u_1 &= au_0 + bv_0 + U(u_0, v_0) \\
v_1 &= cu_0 + dv_0 + V(u_0, v_0)
\end{aligned}
\tag{1.8}$$

where

$$\begin{aligned}
a &= \xi_1(2\pi) = \left. \frac{\partial u_1}{\partial u_0} \right|_{t=2\pi} & b &= \xi_2(2\pi) = \left. \frac{\partial u_1}{\partial v_0} \right|_{t=2\pi} \\
c &= \eta_1(2\pi) = \left. \frac{\partial v_1}{\partial u_0} \right|_{t=2\pi} & d &= \eta_2(2\pi) = \left. \frac{\partial v_1}{\partial v_0} \right|_{t=2\pi}
\end{aligned}$$

and U, V and their partial derivatives with respect to u_0 and v_0 vanish at $u_0 = v_0 = 0$. Therefore by Eqs. (1.8) and Eq. (1.6) it follows that

$$\begin{aligned}
\frac{\partial(x_1, y_1)}{\partial(x_0, y_0)} &= \frac{\partial(u_1, v_1)}{\partial(u_0, v_0)} = ad - bc \\
&= \exp \int_0^{2\pi} \left(\frac{\partial}{\partial x} f(t, x_0(t), y_0(t)) + \frac{\partial}{\partial y} g(t, x_0(t), y_0(t)) \right) dt
\end{aligned}
\tag{1.9}$$

Thus $ad - bc > 0$. In the small neighborhood of $P_0(x_0, y_0)$, the character of the mapping T is determined by the linear terms of Eqs. (1.8). That is, the mapping can be characterized by the roots of the equation

$$\begin{vmatrix} a - \lambda & b \\ c & d - \lambda \end{vmatrix} = 0
\tag{1.10}$$

or

$$\begin{vmatrix} \xi_1(2\pi) - \lambda & \xi_2(2\pi) \\ \eta_1(2\pi) & \eta_2(2\pi) - \lambda \end{vmatrix} = 0 \quad (1.11)$$

It is worth mentioning that $\xi_i(t)$, $\eta_i(t)$ for $i = 1, 2$ coincide with the fundamental set of solutions of the variational system of Eqs. (1.3) for $x_0(t)$, $y_0(t)$:

$$\begin{aligned} \frac{d\xi}{dt} &= \left(\frac{\partial}{\partial x} f(t, x_0(t), y_0(t)) \right) \xi + \left(\frac{\partial}{\partial y} f(t, x_0(t), y_0(t)) \right) \eta \\ \frac{d\eta}{dt} &= \left(\frac{\partial}{\partial x} g(t, x_0(t), y_0(t)) \right) \xi + \left(\frac{\partial}{\partial y} g(t, x_0(t), y_0(t)) \right) \eta \end{aligned} \quad (1.12)$$

with the initial conditions

$$\begin{aligned} \xi_1(0) &= 1 & \xi_2(0) &= 0 \\ \eta_1(0) &= 0 & \eta_2(0) &= 1 \end{aligned}$$

We now consider a vector field in the xy plane which is induced by the Poincaré mapping T , that is, we assign to each point P_0 a vector $\overrightarrow{P_0 P_1}$ directed from P_0 toward and terminating in $T(P_0) = P_1$. Clearly P_0 is a fixed point of T if and only if $\overrightarrow{P_0 P_1} = 0$. For some purposes it is useful to assign a number, called the index, to the fixed points of T or to the simple closed curves in the xy plane.* Consider a simple closed curve C which passes through no fixed

* A curve in the xy plane is the image of a continuous mapping of an interval $a < \theta < b$ into the xy plane. A homeomorphic image of a closed or open line segment is called an arc. A homeomorphic image of the circumference of a circle is called a simple closed curve.

point of T . The number of revolutions made by $\overrightarrow{P_0 P_1}$ as P_0 traces out C must be an integer since P_0 returns to its starting position. This integer is called the index of the curve C and is denoted by $\iota(C)$. This index $\iota(C)$ does not change as C varies continuously without crossing fixed points. Let a fixed point P_0 be enclosed by a small circle containing no fixed point with exception of P_0 itself. Then the index of the circumference of this circle is called the index of P_0 . In this definition the circumference may be replaced by any other simple closed curve containing in its interior the fixed point P_0 but no other fixed points. We write $\iota(P_0)$ for the index of the fixed point P_0 .

Let us consider the roots, λ_1 and λ_2 , of the quadratic equation (1.10). They are either both real, or else are conjugate complex. Moreover, from Eq.(1.9), their product is always positive. A fixed point is called simple if the absolute values of λ_1 and λ_2 are both different from unity. Following G. D. Birkhoff and P. A. Smith [6] and N. Levinson [19], we classify simple fixed points of the mapping T according to the roots of Eq. (1.10). A fixed point and the corresponding periodic solution of Eqs. (1.3) are called:

Completely stable if	$ \lambda_1 < 1$ and $ \lambda_2 < 1$
Completely unstable if	$ \lambda_1 > 1$ and $ \lambda_2 > 1$
Directly unstable if	$0 < \lambda_1 < 1 < \lambda_2$
Inversely unstable if	$\lambda_1 < -1 < \lambda_2 < 0$.

The other case is $|\lambda_1| = |\lambda_2| = 1$. In this case stability is not determined by the linear part of the mapping. This case is also important for the analysis of Duffing's equation without dissipative term. If $k = 0$ for Eqs. (1.2), then from Eq. (1.6) the mapping becomes area-preserving. Therefore in this case possible type of fixed points is directly unstable, inversely unstable, or center

type stable. The same terminology as defined above applies to the periodic point and the corresponding periodic solution, i.e., subharmonic solution of Eqs. (1.3). It is easy to see geometrically, on the basis of above definition, that the completely stable or unstable, and the inversely unstable fixed points have index +1, while the directly unstable fixed point has index -1 (see Fig. 1.1). Clearly an inversely unstable fixed point under T becomes a directly unstable fixed point under T^2 .

Let a point S be a completely stable fixed point. Then there exists an open neighborhood V of S such that $T(V) \subset V$. Hence we define a set, called the domain of attraction of S , as follows:

$$\text{ATTR}(S) = \bigcup_{v=1}^{\infty} T^{-v}(V)$$

Clearly $\text{ATTR}(S)$ is open and each point in $\text{ATTR}(S)$ tends to the fixed point S under repeated applications of the mapping T .

For convenience' sake we introduce the notation of fixed and periodic points as follows: the symbols S , U , D and I denote a completely stable, a completely unstable, a directly unstable and an inversely unstable fixed points, respectively. When there are many fixed points of the same type, we number them from one and upward in an appropriate manner and write j -th fixed point by jS , $j = 1, 2, \dots$. In the case of v -periodic points we denote S_i^v , $i = 1, 2, \dots, v$, that is, $T(S_i^v) = S_{i+1}^v \pmod{i = v}$. If there exist other v -periodic points of the same type, we say that S_i^v , $i = 1, 2, \dots, v$, is a v -periodic group and we write the j -th v -periodic group by $^jS_i^v$, $i = 1, 2, \dots, v$,

$$T(^jS_i^v) = ^jS_{i+1}^v, \quad T(^jS_i^v) = ^jS_i^v.$$

1.4 Dissipative system and its maximum invariant set

For Duffing's equation (1.2), if the dissipative constant k is positive, it can be shown that the equation satisfies the following dissipative property.

Let $P_0(x_0, y_0)$ be an arbitrary point in the xy plane and $x(t) = x(t; x_0, y_0)$, $y(t) = y(t; x_0, y_0)$ be a solution of Eqs. (1.3) with initial condition $x(0) = x_0$, $y(0) = y_0$. We shall say, following N. Levinson [19] and J. L. Massera [21], that system (1.3) is dissipative, or D-system, if there exist an $r > 0$, and an integer $n > 0$ such that the solution $x(t) = x(t; x_0, y_0)$, $y(t) = y(t; x_0, y_0)$ satisfies $x^2(t_0) + y^2(t_0) < r^2$ at a certain $t = t_0 > 0$ and it remains in this same circular region for all $t > t_0 + 2n\pi$.

There are various results known for the D-system [26]. Here we show several properties of them which will be encountered for the analysis of the system (1.2). Consider the Poincaré mapping T introduced at the preceding sections. In the D-system this mapping has the property that any circular region with its center at the origin and sufficiently large radius is mapped into itself by an application of a sufficiently large power of T . In this case of Eqs. (1.2), it can be shown that a more restricted condition is satisfied [19], that is, if we consider a simple closed curve C_0 , which is sufficiently remote from the origin and contains the origin in its interior, it follows that under iterations of T all points exterior to C_0 are transformed into interior points. Moreover if $T^n(C_0)$ be denoted by C_n , it follows that $C_1 \subset C_0$. Thus $C_{n+1} \subset C_n$, $n = 1, 2, \dots$

For the numerical analysis of Eqs. (1.2), we choose as C_0 a limit cycle of the equations

$$\begin{aligned}\frac{dx}{dt} &= y \\ \frac{dy}{dt} &= -ky - c_1x - c_3x^3 + B \operatorname{sgn} y\end{aligned}\tag{1.13}$$

where

$$\operatorname{sgn} y = \begin{cases} +1 & y > 0 \\ -1 & y < 0 \end{cases}$$

In fact, if $k > 0$, $c_1 > 0$, and $c_3 > 0$, it is easily proved that Eqs. (1.13) has a limit cycle. Comparing the vectorfield defined by Eqs. (1.2) with that defined by Eqs. (1.13), we get the above assertion.

Let us consider a closed set Δ_0 whose boundary is the simple closed curve C_0 described above, let $T^n(\Delta_0) = \Delta_n$, $n = 1, 2, \dots$. Then we can define a set

$$\Delta = \bigcap_{n=0}^{\infty} \Delta_n.$$

The set Δ is called to be the maximum invariant set of the system (1.2). It is shown that the set Δ is independent of the choice of the simple closed curve C_0 and has the following properties:

1. Δ is bounded, closed and connected set such that $T(\Delta) = \Delta$,
2. The compliment of Δ is a simply connected domain if the point at infinity is included in it,
3. If $P \notin \Delta$, then $\lim_{n \rightarrow \infty} d(T^n(P), \Delta) = 0$, where $d(T^n(P), \Delta) = \inf_{Q \in \Delta} (T^n(P), Q)$,
4. If S is a bounded set such that $T(S) = S$, then $S \subset \Delta$,
5. Δ has at least one fixed point under the mapping T ,
6. Δ contains all fixed points, periodic points and recurrent points, if they exist.

For Eqs. (1.2), if $k > 0$, then by Eq. (1.6) each sufficiently small area $dx dy$ goes into an area $\exp(-2k\pi) dx dy$. Thus for all bounded set S the area $\mu(S)$ tends to zero under T^n as $n \rightarrow \infty$. In particular Δ has zero area and cannot contain a simple closed curve which is invariant under T .

1.5 Theorem on the number of fixed and periodic points

N. Levinson [19] and J. L. Massera [21] have discussed the number of fixed and periodic points of the dissipative system (1.3). We assume that there are only a finite number of fixed points or periodic points which all present the simple case. Let $N(v)$ be the total number of fixed points of the mapping T^v . Let $C(v)$ be the total number of completely stable and completely unstable fixed points under T^v ; similarly, let $D(v)$ and $I(v)$ be the number of directly and inversely unstable fixed points of T^v , respectively. Then the following equations hold:

$$\begin{aligned}
 \text{For } v = 1, \quad & C(1) + I(1) = D(1) + 1 \\
 & N(1) = C(1) + I(1) + D(1) = 2D(1) + 1 \\
 \text{For } v = 2n + 1, \quad & C(v) + I(v) = D(v) = mv \quad n, m; \text{ positive integers} \\
 & N(v) = 2D(v) = 2mv \\
 \text{For } v = 2n, \quad & C(v) + I(v) = D(v) + 2I(v/2) \\
 & N(v) = 2\{D(v) + I(v/2)\}
 \end{aligned}$$

In these equations we count the number of fixed points only with respect to the lowest power of T ; therefore, for instance, the number of directly unstable fixed points under T^2 is not counted if they are inversely unstable fixed points under T .

1.6 Invariant curves of the mapping T and their related properties

We now summarize some definitions and properties concerning invariant curves of the mapping T with respect to a directly or an inversely unstable fixed point under the mapping. In the following a curve C in the xy plane is called invariant under T if for any integer n and any point $P \in C$, $T^n(P) \in C$.

Let D be a directly unstable fixed point of the mapping T and let consider the mapping in a small neighborhood of the point D . From the assumption of f and g in Eqs. (1.3), if u, v are appropriately taken coordinates with the point D at $u = v = 0$, the mapping T may be represented as follows:

$$\begin{aligned} u_1 &= \lambda_1 u + U(u, v) \\ v_1 &= \lambda_2 v + V(u, v) \end{aligned} \tag{1.14}$$

where $0 < \lambda_1 < 1 < \lambda_2$ and $U(u, v), V(u, v)$ and their first order partial derivatives vanish at $u = v = 0$. Under this situation, it is known, see for example [11] Chap. IX, that there exist a neighborhood of D and two differentiable arcs* ζ^+ and ζ^- which have the following properties:

$$T(\zeta^+) \subset \zeta^+, \quad T^{-1}(\zeta^-) \subset \zeta^-, \quad \zeta^+ \cap \zeta^- = D$$

where ζ^+ and ζ^- are not tangent at D . Following H. Poincaré [29] and G. D. Birkhoff [4], the arc ζ^+ is called an ω -branch or a stable arc passing through D and the ζ^- is called an α -branch or an unstable arc passing through D . The arc ζ^+ or ζ^- may be decomposed as two branches:

$$\begin{aligned} \zeta^+ &= \zeta_1^+ \cup \zeta_2^+ \cup D, & \zeta_1^+ \cap \zeta_2^+ &= \emptyset \\ \zeta^- &= \zeta_1^- \cup \zeta_2^- \cup D, & \zeta_1^- \cap \zeta_2^- &= \emptyset \end{aligned}$$

* An arc or a curve is said to be differentiable if the associated mapping is differentiable.

It is clear that $T(\zeta_i^+) \subset \zeta_i^+$, $T^{-1}(\zeta_i^-) \subset \zeta_i^-$ for $i = 1, 2$. It is worthwhile consider the following qualitative properties; there about at D four invariant branches, that is, two ω -branches ζ_1^+ and ζ_2^+ whose points converge toward D on indefinite iteration of T , and two α -branches ζ_1^- and ζ_2^- whose points converge toward D on iteration of T^{-1} .

We now define global invariant branches under T with respect to the point D as follows:

$$\omega_i(D) = \bigcup_{n=0}^{\infty} T^{-n}(\zeta_i^+)$$

$$\alpha_i(D) = \bigcup_{n=0}^{\infty} T^n(\zeta_i^-)$$

for $i = 1, 2$.

These branches are also called ω - and α -branches with respect to D which are invariant under T . It is clear that the following properties are satisfied:

1. $\lim_{n \rightarrow \infty} T^n(P) = D$ for $P \in \omega_i(D)$,
 $\lim_{n \rightarrow \infty} T^{-n}(P) = D$ for $P \in \alpha_i(D)$,
2. $\omega_1(D) \cap \omega_2(D) = \phi$, $\alpha_1(D) \cap \alpha_2(D) = \phi$,
3. For every neighborhood U of any point $P \in \omega_{1 \text{ or } 2}(D)$ and for every neighborhood V of any point $Q \in \alpha_{1 \text{ or } 2}(D)$, there exist a point $R \in U$ and a positive integer n such that $T^n(R) \in V$.

Notice that, however, an α -branch may intersect an ω -branch, and the points of intersection in such a case are called doubly asymptotic points. If the two branches which intersect at a doubly asymptotic point P actually cross, i.e., are not coincident or merely tangent at P , then P will be said to be transversal or of general type; in contrary case, P is of special type.

We introduce some terminology defined by H. Poincaré [29] and G. D. Birkhoff [4] under more general situation. Let D_i^n , $i = 1, 2, \dots, n$, be directly unstable n -periodic point and let $\omega_k(D_i^n)$ and $\alpha_k(D_i^n)$, $k = 1, 2$; $i = 1, 2, \dots, n$, be ω - and α -branches with respect to D_i^n under the mapping T^n . A doubly asymptotic point P is called homoclinic if

$$P = \omega_{1 \text{ or } 2}(D_i^n) \cap \alpha_{1 \text{ or } 2}(D_i^n)$$

for some i ($1 < i < n$), or

$$P = \omega_{1 \text{ or } 2}(D_i^n) \cap \alpha_{1 \text{ or } 2}(D_j^n)$$

for some i, j ($i \neq j$, $1 < i < n$, $1 < j < n$).

For convenience, let us say that the homoclinic points of the former type are simple. In addition to the points D_i^n above, let D_j^m , $j = 1, 2, \dots, m$, be another directly unstable m -periodic point and $\omega_k(D_j^m)$ and $\alpha_k(D_j^m)$, $k = 1, 2$; $j = 1, 2, \dots, m$, be ω - and α -branches with respect to D_j^m . Then a doubly asymptotic point P is called heteroclinic point correlated with D_i^n and D_j^m if

$$P = \omega_{1 \text{ or } 2}(D_i^n) \cap \alpha_{1 \text{ or } 2}(D_j^m)$$

or

$$P = \alpha_{1 \text{ or } 2}(D_i^n) \cap \omega_{1 \text{ or } 2}(D_j^m)$$

for some i, j ($1 < i < n$; $1 < j < m$).

The solutions of Eqs. (1.3) correlated with the homoclinic and heteroclinic points are called the homoclinic and heteroclinic solutions, respectively.

Let 1D and 2D be directly unstable fixed points and H be a transversal heteroclinic point correlated with 1D and 2D . Then by definition one of ω -branches (or α -branches) of 1D intersects at H with one of α -branches (or ω -branches) of 2D . If $\omega_1({}^1D)$, which is one of ω -branches of 1D , intersects at H

with $\alpha_1(^2D)$, which is one of α -branches of 2D , we shall say that 1D is chained to 2D and two arcs $^2D\alpha_1(^2D)H$ and $H\omega_1(^1D)^1D$ which are connected at H are a transition chain from 2D to 1D through H (see Fig. 1.2). Note that the assertion that 1D is chained to 2D does not implies that 2D is chained to 1D . If 1D is chained to 2D and 2D is also chained to 1D , the transition chains from 2D to 1D and from 1D to 2D will be said to form a cycle. More precisely, let $H_1 = \alpha_1(^2D) \cap \omega_1(^1D)$ and $H_2 = \alpha_1(^1D) \cap \omega_1(^2D)$ be two heteroclinic points correlated with 1D and 2D , and let $^2D\alpha_1(^2D)H_1$ and $H_1\omega_1(^1D)^1D$ be the transition chain from 2D to 1D and $^1D\alpha_1(^1D)H_2$ and $H_2\omega_1(^2D)^2D$ be the transition chain from 1D to 2D , then the two fixed points 1D and 2D have a cycle property with a cycle $^2D\alpha_1(^2D)H_1\omega_1(^1D)^1D\alpha_1(^1D)H_2\omega_2(^2D)^2D$, or simply $^2DH_1^1DH_2^2D$ (see Fig. 1.3). More generally, let $^1D, ^2D, \dots, ^nD$ be directly unstable fixed points. We shall call that $^1D, ^2D, \dots, ^nD$ form a cycle if $\alpha_{1or2}(^1D) \cap \omega_{1or2}(^2D) \neq \phi$, $\alpha_{1or2}(^2D) \cap \omega_{1or2}(^3D) \neq \phi$, \dots , $\alpha_{1or2}(^nD) \cap \omega_{1or2}(^1D) \neq \phi$. Notice that a directly unstable fixed point with a homoclinic point has always a cycle which will be called homoclinic cycle.

We now summarize some properties of doubly asymptotic points and ω - and α -branches. Let $^1D, ^2D$ and 3D be directly unstable fixed points. In the following we assume that doubly asymptotic points, if they exist, are all transversal.

1. If H is a homoclinic point of 1D (or a heteroclinic point correlated with 1D and 2D), then there exist infinitely many homoclinic points of 1D (or heteroclinic points correlated with 1D and 2D).
2. If 2D is chained to 1D and 3D is chained to 2D , then 3D is chained to 1D .
3. If 2D is chained to 1D , then there neighborhood U of any point $P \in \omega_{1or2}(^1D)$ and for a neighborhood V of any point $Q \in \alpha_{1or2}(^2D)$, there exist a point $R \in U$ and a positive integer n such that $T^n(R) \in V$.

4. If 1D and 2D have a cycle property, then there exist homoclinic points of 1D and homoclinic points of 2D .
5. In every neighborhood of a homoclinic point there exist infinitely many periodic points.

For many more details on this subject, see H. Poincaré [29], G. D. Birkhoff [4, 5], G. D. Birkhoff and P. A. Smith [6], S. Smale [32, 33], Y. I. Neimark [23, 24], L. P. Silnikov [30, 31], V. I. Arnold [2], V. I. Arnold and A. Avez [3], V. A. Pliss [27, 28], and H. Kawakami [17].

1.7 Examples of the patterns of invariant curves

In this section we shall discuss some examples of the behavior of invariant curves, of which the simplest possible cases will be treated, of the Poincaré mapping T defined by Duffing's equation (1.1) with a positive dissipative constant k . In this case, since the maximum invariant set of the system (1.2) is bounded and has zero area, the possible types of fixed points or periodic points are completely stable, directly unstable or inversely unstable ones. Using the theorem of N. Levinson and J. L. Massera in Sec. 1.5, we find the following results. It is noted that, in the following examples, only fixed point under T will be considered although the mapping T may have many periodic points.

(a) T has only one fixed point: $N(1) = 1$

Two different cases listed in Table 1.1 are considered. For the case 1 in Table 1.1, the simplest structure of the maximum invariant set Δ is that Δ has a single point which is completely stable. In this case Eqs. (1.2) has one periodic solution of period 2π toward which all other solutions tend. On the other hand, for the latter case in Table 1.1, Δ has at least two 2-periodic points of completely stable or inversely unstable type.

Table 1.1 Number of fixed points (f.p.)
of different types.

Type of f.p. No. of f.p.	S	I	D
Case 1	1	0	0
Case 2	0	1	0

(b) T has three fixed points: $N(1) = 3$; An example of the appearance of homoclinic points.

In this case, we have always a directly unstable fixed point as listed in Table 1.2. Let us consider briefly the possible behavior of invariant branches of the directly unstable fixed point D. Let H_{ij} be a set of homoclinic points, which will be assumed transversal, with respect to $\omega_i(D)$ and $\alpha_j(D)$:

$$H_{ij} = \omega_i(D) \cap \alpha_j(D)$$

Table 1.2 Number of fixed points of
different types.

Type of f.p. No. of f.p.	S	I	D
Case 1	2	0	1
Case 2	1	1	1
Case 3	0	2	1

for $i, j = 1, 2$. Then there are sixteen different combinations of H_{ij} as follows:

1. $H_{ij} = \phi$ for $i, j = 1, 2$
2. $H_{11} \neq \phi, H_{12} = H_{21} = H_{22} = \phi$
3. $H_{12} \neq \phi, H_{11} = H_{21} = H_{22} = \phi$
4. $H_{21} \neq \phi, H_{11} = H_{12} = H_{22} = \phi$
5. $H_{22} \neq \phi, H_{11} = H_{12} = H_{21} = \phi$
6. $H_{11} \neq \phi, H_{12} \neq \phi, H_{21} = H_{22} = \phi$
7. $H_{11} \neq \phi, H_{21} \neq \phi, H_{12} = H_{22} = \phi$
8. $H_{12} \neq \phi, H_{22} \neq \phi, H_{11} = H_{21} = \phi$
9. $H_{21} \neq \phi, H_{22} \neq \phi, H_{11} = H_{12} = \phi$
10. $H_{12} \neq \phi, H_{21} \neq \phi, H_{11} = H_{22} = \phi$
11. $H_{11} \neq \phi, H_{22} \neq \phi, H_{12} = H_{21} = \phi$
12. $H_{12} \neq \phi, H_{21} \neq \phi, H_{22} \neq \phi, H_{11} = \phi$
13. $H_{11} \neq \phi, H_{21} \neq \phi, H_{22} \neq \phi, H_{12} = \phi$
14. $H_{11} \neq \phi, H_{12} \neq \phi, H_{22} \neq \phi, H_{21} = \phi$
15. $H_{11} \neq \phi, H_{12} \neq \phi, H_{21} \neq \phi, H_{22} = \phi$
16. $H_{ij} \neq \phi$ for $i, j = 1, 2$.

By the assumptions of uniqueness of solutions and transversal homoclinic points, the cases from 10 to 15 cannot occur. Hence we have ten different combinations.

As an example, we consider the case 1 in Table 1.2. Combining the results of the sets of homoclinic points above, we obtain some different patterns of invariant branches illustrated in Fig. 1.4. In this figure, the pattern (a) shows that the maximum invariant set Δ consists of three fixed points and α -branches of D , while the boundary of the domain of attraction for 1S or 2S is the directly unstable fixed point D and its ω -branches. All other cases

show the appearance of homoclinic points. Therefore, it may be expected that there appear infinitely many periodic points in the neighborhood of a homoclinic point.

(c) T has five fixed points: $N(1) = 5$; An example of the appearance of heteroclinic points.

In this case, heteroclinic points may appear in addition to a possibility of sets of homoclinic points, since we have always two directly unstable fixed points. As an example, we consider the case 1 in Table 1.3. Some different patterns of invariant curves are illustrated in Fig. 1.5. The patterns (a), (b), and (c) show that the maximum invariant set Δ consists of five fixed points and α -branches of two directly unstable fixed points, although heteroclinic points appear in the patterns (b) and (c). The pattern (d) is an example with cycle property. In this case homoclinic points appear and Δ have complex structure. Further discussion will be made in Chap. 4.

Table 1.3 Number of fixed points of different types.

Type of f.p. No. of f.p.	S	I	D
Case 1	3	0	2
Case 2	2	1	2
Case 3	1	2	2
Case 4	0	3	2

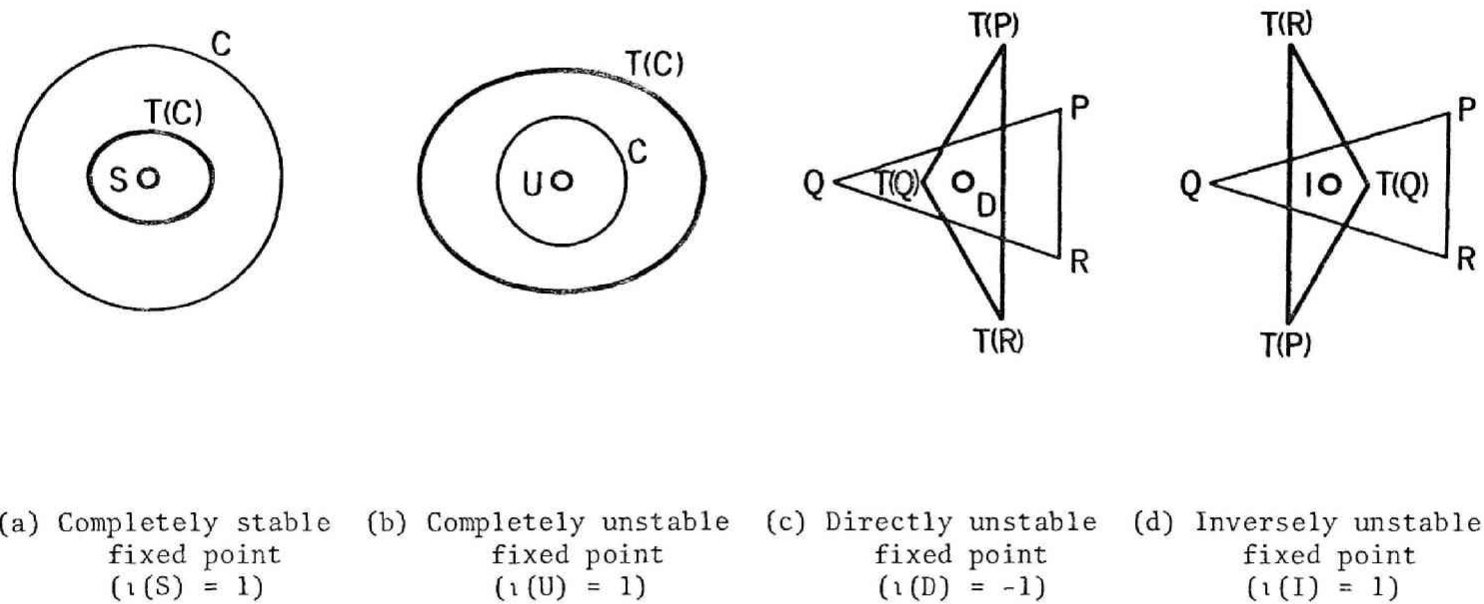


Fig. 1.1. Types of simple fixed points in the xy plane.

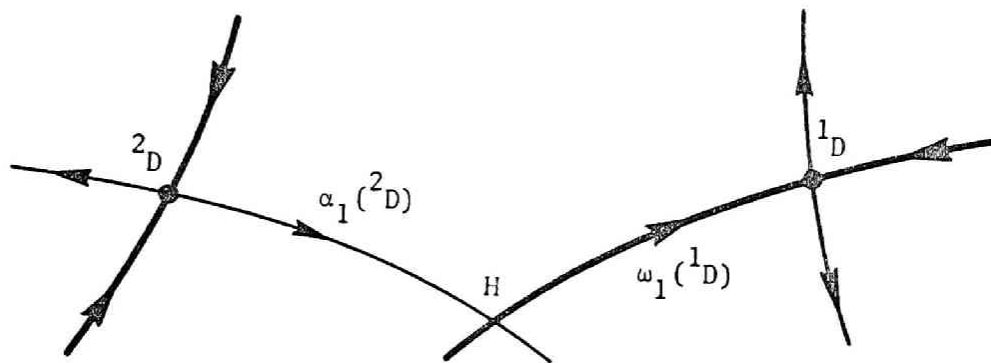


Fig. 1.2. Transition chain from 2_D to 1_D through H : $2_D \alpha_1(2_D) H \omega_1(1_D) 1_D$.

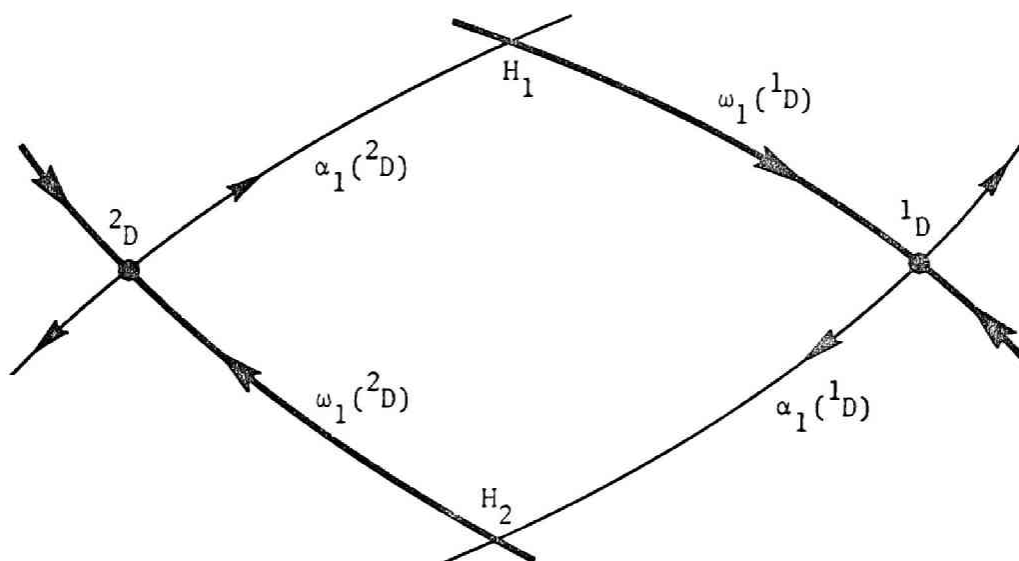
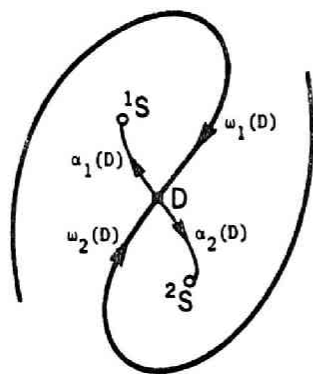
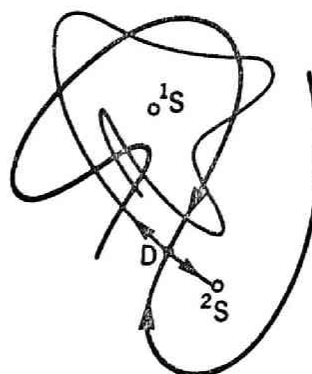


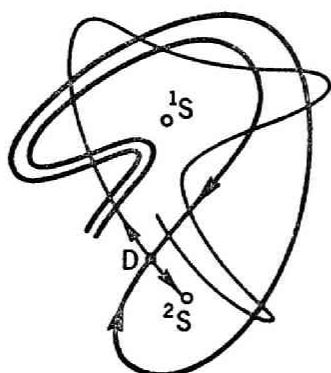
Fig. 1.3. Cycle ${}^2_D\alpha_1({}^2_D)H_1\omega_1({}^1_D){}^1_D\alpha_1({}^1_D)H_2\omega_1({}^2_D){}^2_D$.



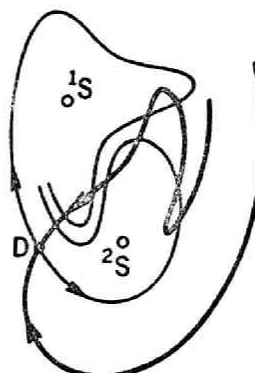
(a)



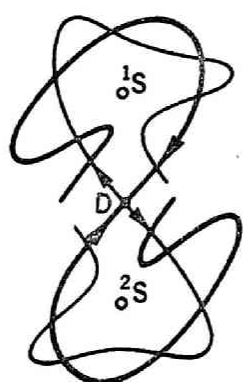
(b)



(c)



(d)

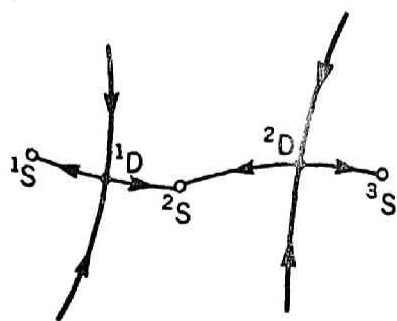


(e)

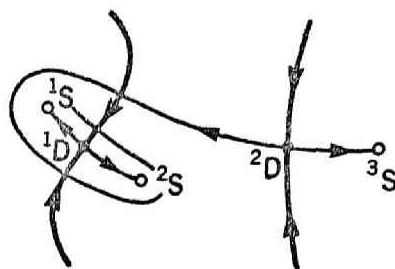


(f)

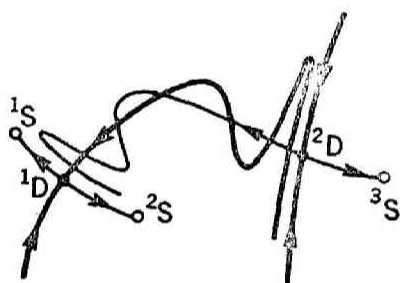
Fig. 1.4. Some different configurations of invariant curves.



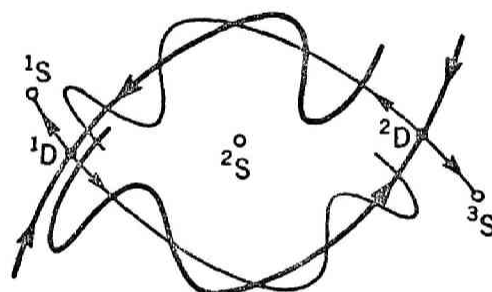
(a)



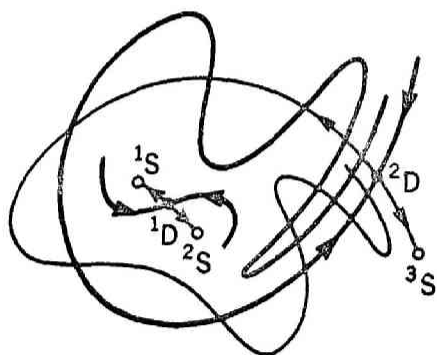
(b)



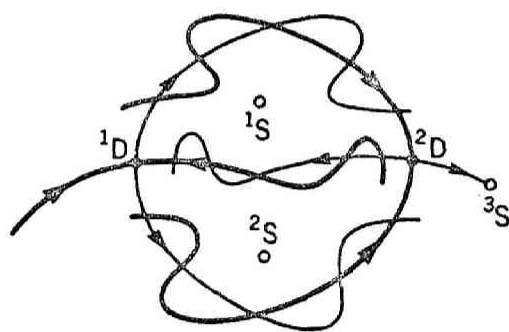
(c)



(d)



(e)



(f)

Fig. 1.5. Some different configurations of invariant curves.

CHAPTER 2

METHODS OF NUMERICAL ANALYSIS

2.1 Introduction

The present short chapter is concerned with the methods of numerical computation for the solutions of Duffing's equation. These methods will be used in the following chapters. Numerical analysis are carried out by using both analog and digital computers. The iterations of the Poincaré mapping discussed in the previous chapter are easily accomplished by using an analog computer with memories and sequential logics. From a computational standpoint analog computers are quite available for solving the initial value problem of ordinary differential equations, but the accuracy of computation is poorer than in digital computers. Therefore calculations will be done in the following manner. First, an analog-computer study is carried out with the aid of the qualitative properties of Duffing's equation and with the aid of various approximate solutions which are stated in Ref. [12]. Secondly, if it is needed, a digital computation is carried out with the aid of the results of the analog-computer study.

In Sec. 2.2, the procedure of numerical analysis is stated. Sections 2.3 and 2.4 deal with an analog-computer study and a digital-computer study, respectively. An example of numerical solution is shown in Sec. 2.5.

2.2 Procedure of numerical analysis

The purpose of numerical analysis is at the first place to find the maximum invariant set of a given equation and to find ω -branches of directly or inversely unstable fixed or periodic points. These behaviors in the phase plane reveal the global aspect of the qualitative properties of the given equation. Secondly, fixed and periodic points will be found in the maximum invariant set and periodic solutions corresponding to the fixed or periodic points will be calculated. Stability of the periodic solution is also investigated by the calculation of characteristic multipliers of the variational system of the periodic solution. Hence for the D-system, in particular for Eqs. (1.2) with $k > 0$, the procedure of numerical analysis is as follows:

1. By using Eqs. (1.13), calculate the limit cycle C_0 of this equations. This simple closed curve is satisfied the condition of D-system:

$$T(C_0) \subset C_0.$$
2. Apply several iterations of the Poincaré mapping T to this curve C_0 :

$$T(C_0) = C_1, T(C_1) = C_2, \dots, T(C_{m-1}) = C_m.$$
 After some repetitions of this process the area of interior domain of C_m which contains the maximum invariant set Δ is now properly small.
3. Find the fixed and periodic points in the interior domain of C_m .
 In this step completely stable fixed or periodic points are found automatically. On the contrary it may be difficult to find directly or inversely unstable points. After several trials we can obtain these points because the interior domain of C_m is not so large.
4. Calculate the invariant curves of each directly or inversely unstable point. Small changes of initial conditions in the neighborhood of the point lead to find these curves.

For finding ω -branches, we set the inverse time system, that is, for Eqs. (1.2) we set

$$\begin{aligned}\frac{dx}{dt} &= y \\ \frac{dy}{dt} &= ky - c_1 x - c_3 x^3 + B \cos t + B_0\end{aligned}\tag{2.1}$$

Equations (2.1) has the same fixed and periodic points and invariant curves as Eqs. (1.2), but the stability and the direction of successive points on the invariant curves under T are converse in comparison with Eqs. (1.2). Therefore we can find ω -branches of the original equation as α -branches of the inverse time equation.

5. Calculate periodic solutions corresponding to fixed or periodic points. And investigate the stability of the periodic solutions, i.e., calculate the characteristic multipliers of the variational equations.

From step 1 to step 4 we generally use an analog computer and for step 5 we use a digital computer. In step 3, if the accuracy of computation is needed, a digital computation is carried out after the finding the results of an analog computation.

For nondissipative system, that is, for Eqs. (1.2) with $k = 0$, we have no information for step 1. In this case the analysis is done as a limiting case of dissipative system, i.e., as $k \rightarrow 0$.

2.3 Analog-computer study

By nature analog computers do not require a detailed programming of the individual mathematical operations as digital computers. Each operational element may be considered as a fixed subroutine for execution of prescribed

mathematical operation, where the algorithm is fixed and determined by the design principle of the operational elements (integrator, adder, function generator, etc.).

An algorithm for the Poincaré mapping defined by nonautonomous system with periodic forcing term is shown in Fig. 2.1. This diagram consists of a system equation with harmonic oscillator, samplers with analog memory, and a logical control elements which control the samplers and a recorder pen.

(a) System equation

Let us consider the system (1.2)

$$\begin{aligned}\frac{dx}{dt} &= y \\ \frac{dy}{dt} &= -ky - c_1x - c_3x^3 + B \cos t + B_0\end{aligned}\tag{1.2}$$

The initial dependent variables x, y and the independent variable t are represented in an analog computer by the machine variables X, Y and τ :

$$\begin{aligned}X &= \alpha x \\ Y &= \beta y \\ \tau &= \theta t\end{aligned}\tag{2.2}$$

To reduce the error it is desirable that the scale factors α, β are chosen so that the machine variables X, Y are as closed as possible to the maximum possible voltage in the working range (± 100 volts in our machine). For this reason we select the scale factors α, β from the conditions

$$\begin{aligned}\alpha &= \frac{100}{x_{\max}} \\ \beta &= \frac{100}{y_{\max}}\end{aligned}\tag{2.3}$$

where x_{\max} and y_{\max} are the maximum values of x and y . As for the time scale θ , the characteristics of the operational elements impose constraints on the choice of minimum and maximum values. The time scale is therefore chosen $1 \leq \theta \leq 4$ in our problem. Substituting Eqs. (2.2) into Eqs. (1.2) we obtain the machine equations:

$$\begin{aligned} \frac{dX}{d\tau} &= \frac{y_{\max}}{\theta x_{\max}} Y \\ \frac{dY}{d\tau} &= -\frac{k}{\theta} Y - \frac{c_1 x_{\max}}{\theta y_{\max}} X - \frac{c_3 x_{\max}^3}{\theta y_{\max}} \frac{X^3}{100^2} + \frac{B}{\theta y_{\max}} 100 \cos \frac{\tau}{\theta} + \frac{B_0}{\theta y_{\max}} 100 \end{aligned} \quad (2.4)$$

Figure 2.2 shows a block diagram of an analog-computer setup for the solutions of Eqs. (2.4).

(b) Control circuit

Control circuit for the mapping is divided into two parts; samplers with analog memory and a control circuit of a recorder pen. Fig. 2.3 shows the block diagram of samplers with analog memory. This circuit is achieved by a sample-and-hold circuit of mode controlled integrators. The $X(\tau)$ and $Y(\tau)$ of Eqs. (2.4) are sampled at the instants of $\tau = 2n\theta\pi$ ($n = 1, 2, \dots$) and holded in integrators I-1 and I-2. Mode controlled integrators I-1 and I-2 operate according to the logical input signals R and C listed in the table under the figure. The values $X(2n\theta\pi)$ and $Y(2n\theta\pi)$ which are holded in I-1 and I-2 are successively plotted on an X-Y recorder by a circuit shown in Fig. 2.4. In this figure a recorder pen marks its input values when relay RY is energized.

In this way, for any initial point, we obtain its successive images under the mapping on X-Y recorder. Another circuit for automatic plotting device is found in Ref. [13].

2.4 Digital-computer study

Digital computations are mainly carried out for the following purposes:

1. To find accurate location of a fixed or periodic point,
2. To calculate the periodic solution corresponding to a fixed or periodic point, and to calculate harmonic components for the periodic solution,
3. To calculate the characteristic multipliers of the variational equation (1.12) corresponding to the periodic solution.

The procedure for the purpose 1 is as follows:

1. By using the results of analog-computer study, choose an initial point P_0 on the xy plane which gives the initial condition for Eqs. (1.2).
2. Calculate the successive images of P_0 under T until the following convergent condition is fulfilled

$$| P_n - P_{n+v} | < \epsilon \quad (2.5)$$

where ϵ is a small positive constant, $v = 1$ for fixed point, and $v = m$ for m -periodic point.

Numerical examples of the following chapters will be developed using a TOSBAC 3400 and single-precision arithmetic with ten significant digits. The algorithm is programmed in FORTRAN IV. Numerical integration is carried out by the Runge-Kutta-Gill method. The interval of integration 2π is divided 60 steps for examples with the parameter $B < 0.5$ and 120 steps for that with $B > 0.5$. The value of ϵ in the inequality (2.5) is taken equal to $10^{-4} \sim 10^{-5}$.

It is noted that for a completely stable fixed or periodic point the successive images of step 2 above are automatically convergent; for a directly or

inversely unstable point it will be divergent generally, but several number of trials lead to obtain satisfactory results. Once the fixed or periodic point is determined, the corresponding trajectory and periodic solution are easily obtained. Hence the calculations 2 and 3 are achieved easily.

2.5 An example of numerical solution

As a specific example of Eqs. (1.2), we consider

$$\begin{aligned}\frac{dx}{dt} &= y \\ \frac{dy}{dt} &= -0.2y - x^3 + 0.3 \cos t\end{aligned}\tag{2.6}$$

In this example Eqs. (1.13) becomes

$$\begin{aligned}\frac{dx}{dt} &= y \\ \frac{dy}{dt} &= -0.2y - x^3 + 0.3 \operatorname{sgn} y\end{aligned}\tag{2.7}$$

Following the procedure described in Sec. 2.2, we obtain a limit cycle C_0 of Eqs. (2.7), and obtain the successive images $T(C_0) = C_1$, $T(C_1) = C_2$. After this procedure we find two completely stable fixed point 1S , 2S and a directly unstable fixed point D . Figure 2.5 shows the limit cycle C_0 , its images C_1 and C_2 , three fixed points 1S , 2S and D , and α -branches of the point D . For the ω -branches of D we set the inverse time equation (2.1) and we obtain these branches. Then we find the complete phase portrait for the system (2.6) under the mapping T . Figure 2.6 shows a photograph of the phase portrait on the xy plane obtained by analog computation. In Fig. 2.7, which is the copy of Fig. 2.6, the arrows on the invariant curves indicate the direction of the movement

of successive images under T . The trajectories of the corresponding three fixed points are shown in Fig. 2.8. The waveforms of these periodic solutions are illustrated in Fig. 2.9. In this figure the periodic solution correlated with the directly unstable fixed point D is shown by $x_D(t)$ and the periodic solutions correlated with completely stable fixed points 1S and 2S are shown by $x_{1S}(t)$ and $x_{2S}(t)$, respectively. They are given by

$$\begin{aligned} x_D(t) = & - 0.7394 \cos t + 0.6752 \sin t \\ & + 0.0223 \cos 3t + 0.0250 \sin 3t \\ & + 0.0009 \cos 5t - 0.0007 \sin 5t \\ & + \dots \end{aligned}$$

$$\begin{aligned} x_{1S}(t) = & - 0.3100 \cos t + 0.0671 \sin t \\ & - 0.0007 \cos 3t + 0.0006 \sin 3t \\ & + \dots \end{aligned}$$

$$\begin{aligned} x_{2S}(t) = & 0.6864 \cos t + 0.9841 \sin t \\ & - 0.0597 \cos 3t + 0.0215 \sin 3t \\ & - 0.0001 \cos 5t - 0.0032 \sin 5t \\ & + 0.0002 \cos 7t + 0.0000 \sin 7t \\ & + \dots \end{aligned}$$

The fixed points and related properties are listed in Table 2.1 below.

Table 2.1 Fixed points and related properties correlated with the periodic solutions for Eqs. (2.6).

Fixed point	Periodic solution	x	y	λ_1, λ_2	Classification
D	Harmonic	- 0.7163	0.7464	2.457, 0.116	Directly unstable
¹ S	Harmonic	- 0.3107	0.0689	- 0.389 \pm 0.365i	Completely stable
² S	Harmonic	0.6267	1.0331	0.098 \pm 0.524i	Completely stable

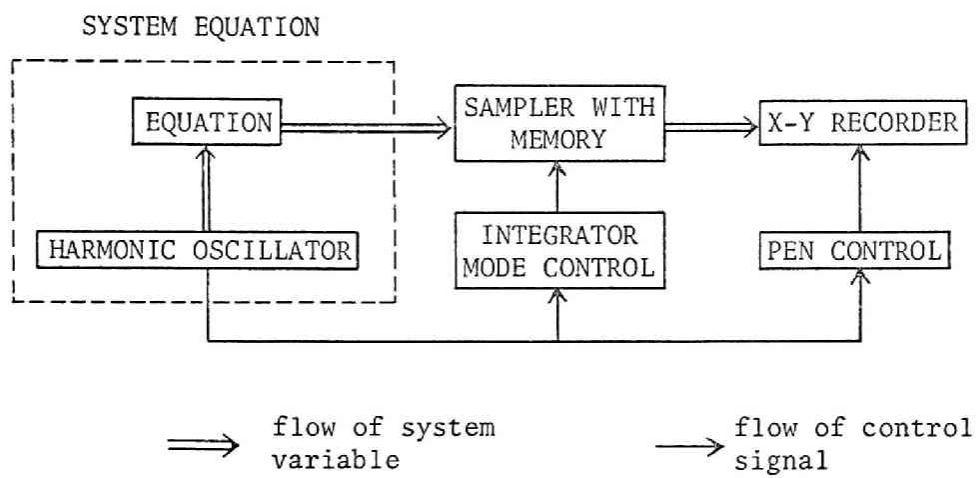


Fig. 2.1. Block diagram describing the Poincaré mapping of nonautonomous system with the periodic forcing term.

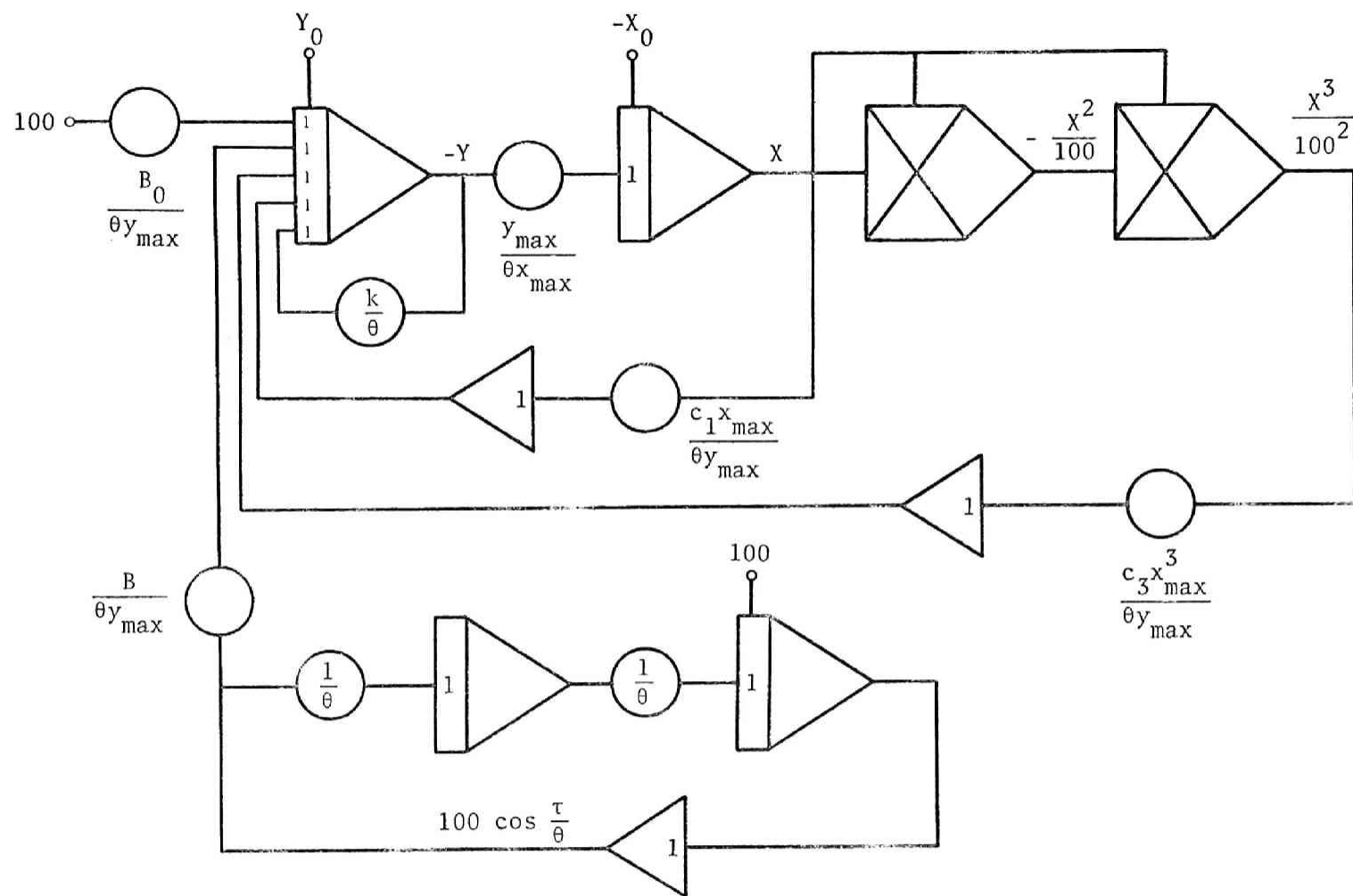
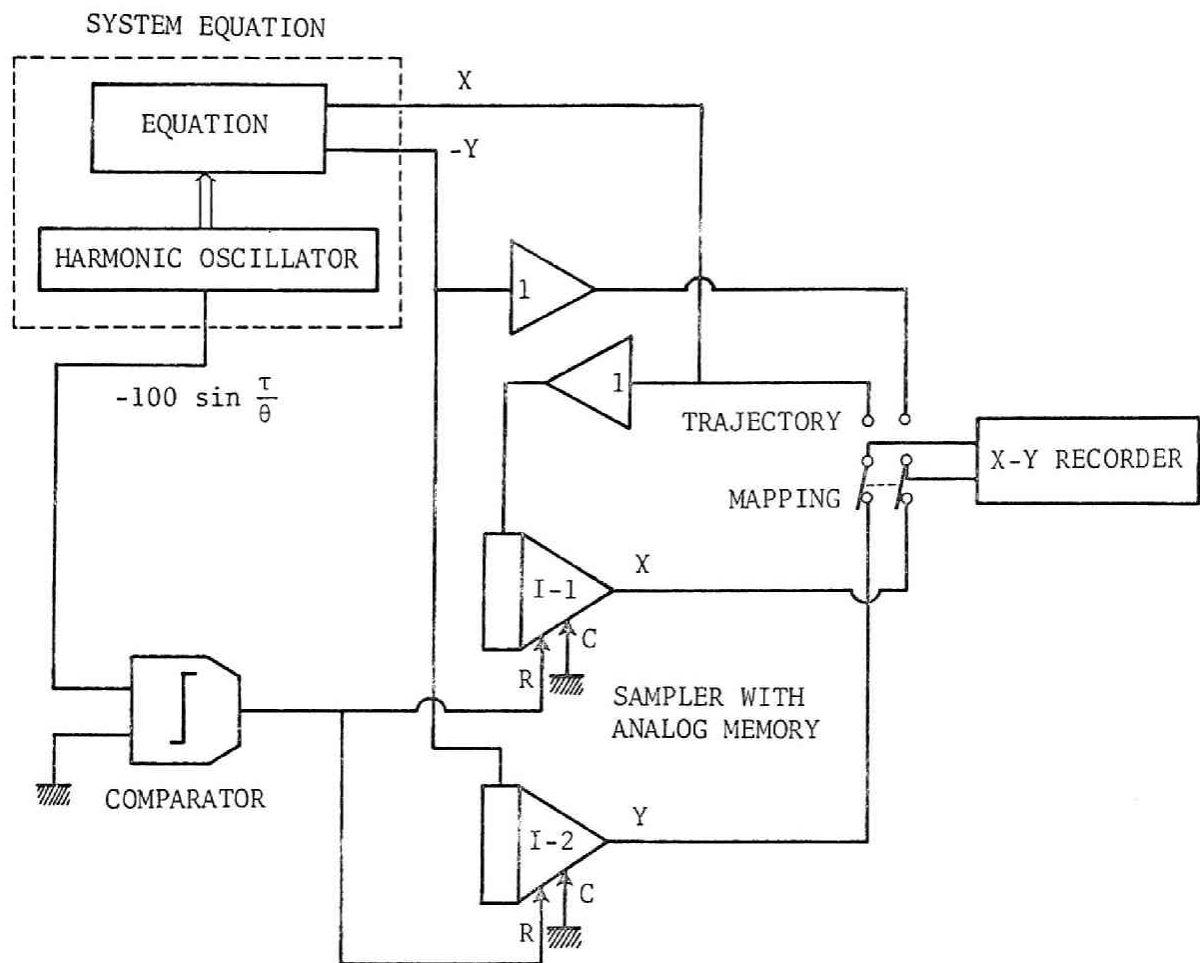


Fig. 2.2. Analog computer implementation of Duffing's equation.



Operational modes of integrators I-1, I-2.

Operational Modes	Logical Signals	
	R	C
Compute	0	1
Reset	1	0
Hold	0	0

Fig. 2.3. Block diagram of samplers with analog memory.

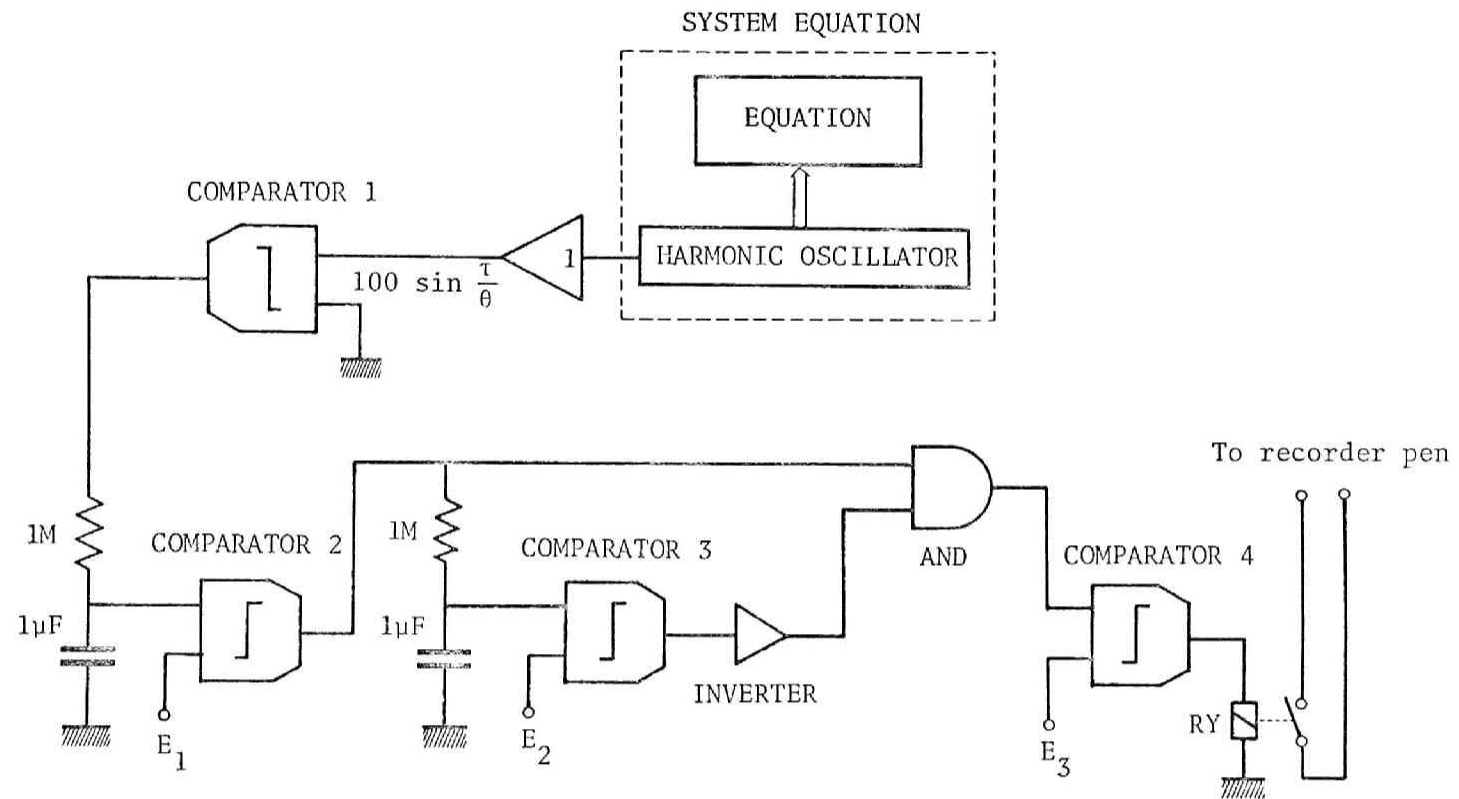


Fig. 2.4. Block diagram of a control circuit of a recorder pen.

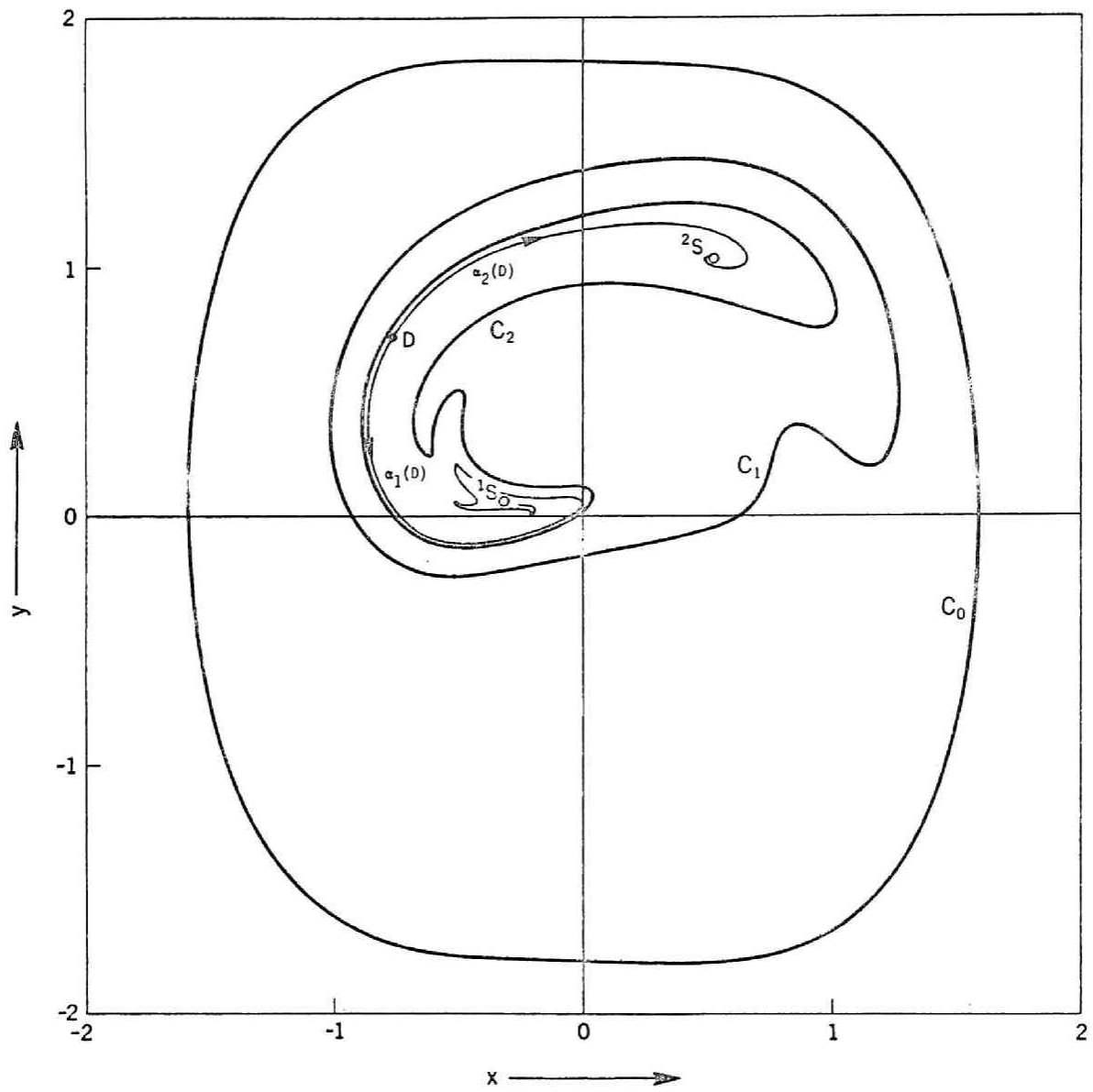


Fig. 2.5. Limit cycle C_0 for Eqs. (2.7) and its successive images $T(C_0) = C_1$, $T(C_1) = C_2$, and invariant set for Eqs. (2.6).

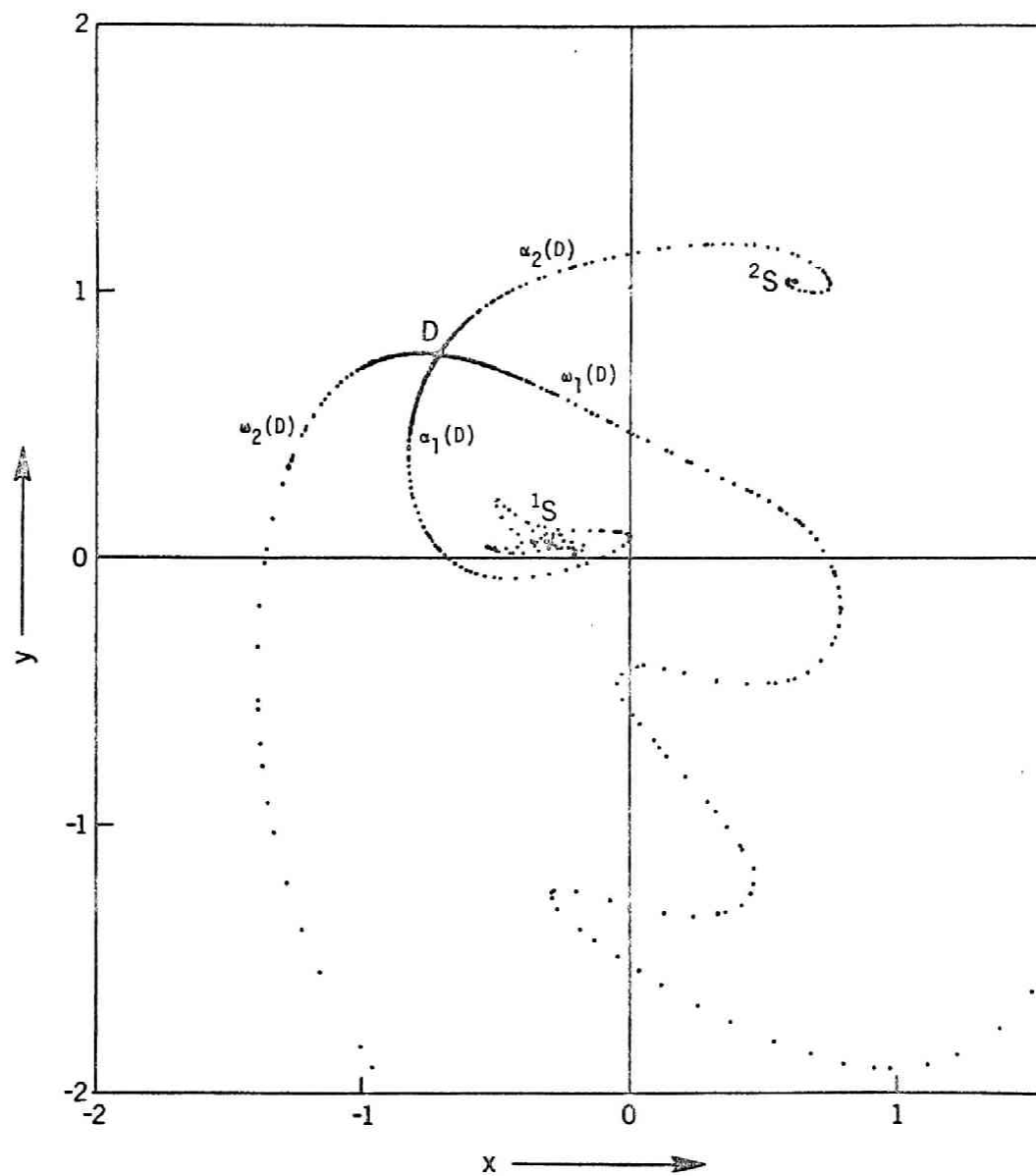


Fig. 2.6. Fixed points and invariant curves for Eqs. (2.6)
by using an analog computer.

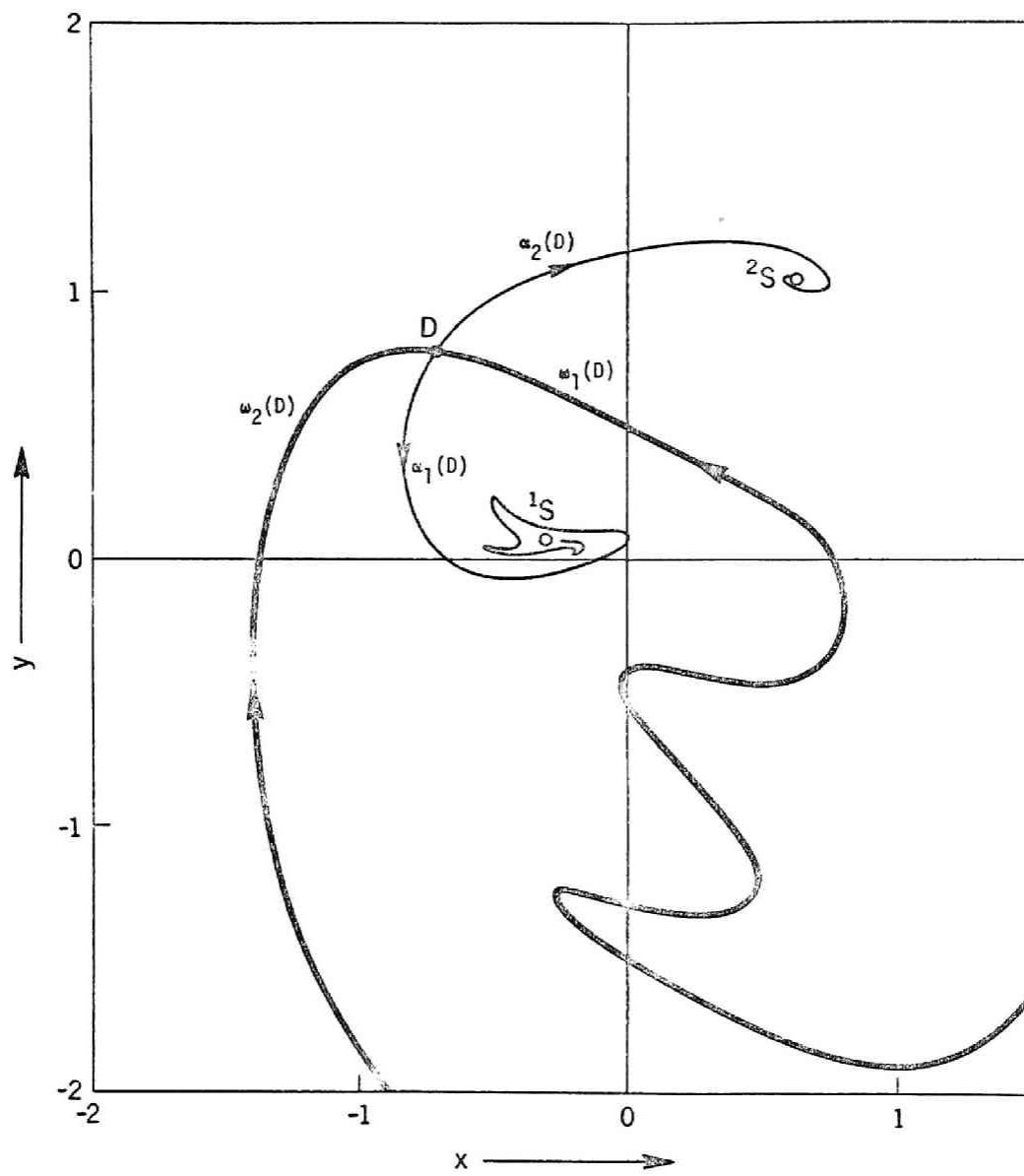


Fig. 2.7. Fixed points and invariant curves for Eqs. (2.6).

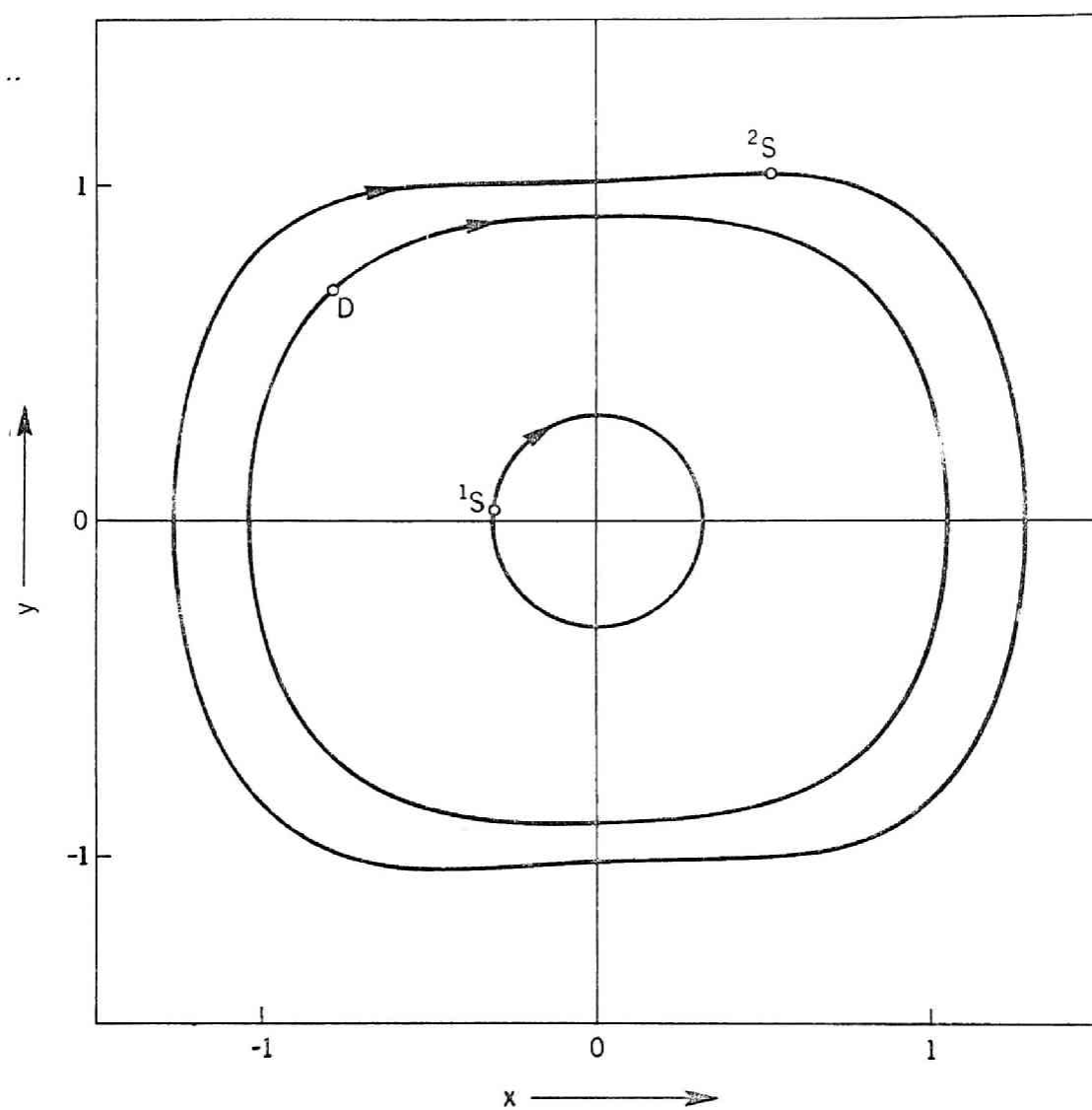


Fig. 2.8. Trajectories of the periodic solutions for Eqs. (2.6).

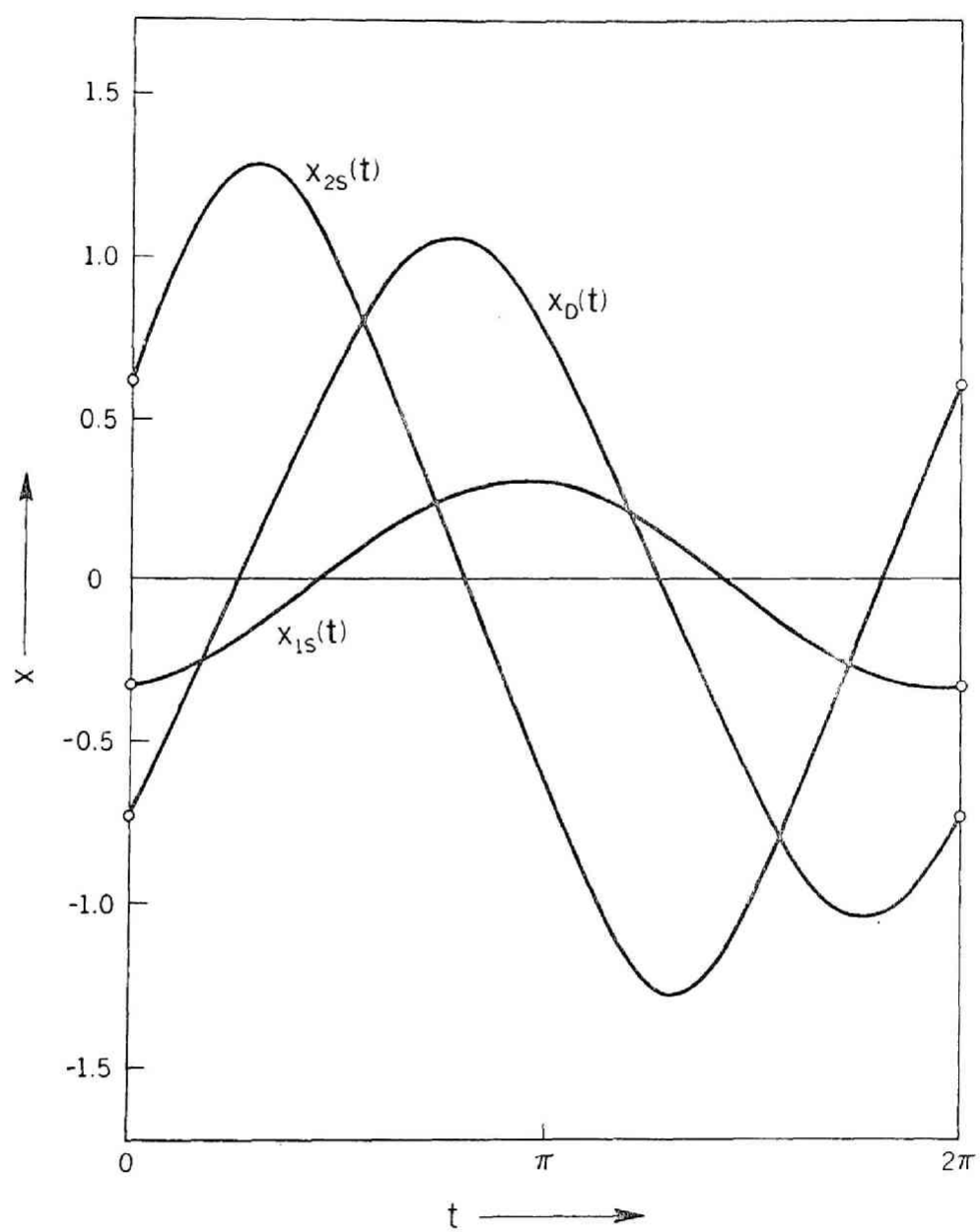


Fig. 2.9. Time responses of the periodic solutions for Eqs. (2.6).

CHAPTER 3

PERIODIC SOLUTIONS OF DUFFING'S EQUATION

3.1 Introduction

In this chapter we deal with the periodic solutions of the following simple but typical case of Eq. (1.1), [12]:

$$\frac{d^2x}{dt^2} + k\frac{dx}{dt} + x^3 = B \cos t + B_0 \quad (3.1)$$

where $k > 0$, B and B_0 are real parameters.* Since the external forcing term of Eq. (3.1) has period 2π , any periodic solution must have a period commensurable with 2π . We shall see that the equation can possess a wide variety of periodic solutions in addition to harmonic solutions which have the period 2π . Namely, the equation has subharmonic solutions the smallest period of which may be some integral multiple of the period 2π . The investigation is conducted with the aid of computer facilities discussed in Chap. 2.

In Sec. 3.2, certain bifurcation of fixed points is discussed and a conventional classification of the periodic solutions is introduced. In Sec. 3.3, numerical results for harmonic and higher-harmonic solutions are considered. Similarly, subharmonic solutions of orders 2 and 3 are discussed in Secs. 3.4 and 3.5, respectively.

* The nonlinearity in Eq. (3.1) is simply given by a cubic function of x . The inclusion of a linear term and/or higher-degree terms in x does not essentially alter the numerical analysis in what follows.

3.2 Bifurcation and classification of periodic solutions

Before going into detailed discussion for the periodic solutions of Eq.(3.1), we consider some basic properties for the nature of the system (3.1) and its periodic solutions with respect to the system parameters. In the most part of this and next chapters, we shall consider Duffing's equation of the form:

$$\frac{d^2x}{dt^2} + k\frac{dx}{dt} + x^3 = B \cos t \quad (3.2)$$

This equation is unchanged if the sign of x is reversed and t is shifted by π radians. Therefore the system (3.2) is called the symmetrical system. On the other hand, the system (3.1) is called the unsymmetrical system because of the external forcing term with the unidirectional component B_0 . Equation (3.1) may readily be transformed to one with unsymmetrical nonlinearity but with symmetrical external forcing term. Throughout the following, we shall treat unsymmetrical system only in order to obtain some typical numerical examples.*

Let us consider the symmetrical system (3.2), or the equivalent system:

$$\begin{aligned} \frac{dx}{dt} &= y \\ \frac{dy}{dt} &= -ky - x^3 + B \cos t \end{aligned} \quad (3.3)$$

Let $x(t) = x(t; x_0, y_0)$, $y(t) = y(t; x_0, y_0)$ be a periodic solution of Eqs.(3.3) with the period 2π determined by the initial conditions $x(0; x_0, y_0) = x_0$ and $y(0; x_0, y_0) = y_0$. Let T denote the Poincaré mapping defined by Eqs. (3.3). Then the solution $-x(t+\pi; x_0, y_0)$, $-y(t+\pi; x_0, y_0)$ is also a periodic solution of Eqs. (3.3). For convenience in the following discussion, if a periodic

* A subharmonic solution of the even order may exist for Eq. (3.2), but this type of solution is apt to occur when the system is unsymmetrical [12].

solution $x(t)$, $y(t)$ satisfies the equalities

$$\begin{aligned} x(t; x_0, y_0) &= -x(t+\pi; x_0, y_0) \\ y(t; x_0, y_0) &= -y(t+\pi; x_0, y_0) \end{aligned} \quad (3.4)$$

then we call the solution primary. And the corresponding fixed point $P(x_0, y_0)$ will be called primary fixed point. Any primary solution can be equivalently defined by Fourier-series expansion in the following form:

$$\begin{aligned} x(t) &= \sum_{n=1}^{\infty} [a_{2n+1} \cos (2n+1)t + b_{2n+1} \sin (2n+1)t] \\ y(t) &= \sum_{n=1}^{\infty} [(2n+1)b_{2n+1} \cos (2n+1)t - (2n+1)a_{2n+1} \sin (2n+1)t] \end{aligned} \quad (3.5)$$

If a periodic solution does not satisfy the equalities (3.4), or equivalently, is expressed by Fourier-series expansion containing the even order components, then the periodic solution is referred to as non-primary solution. Corresponding to a non-primary solution $x(t) = x(t; x_0, y_0)$, $y(t) = y(t; x_0, y_0)$, we can find two fixed points $P(x_0, y_0)$ and $Q(-x(\pi), -y(\pi))$ in xy plane. For Eqs. (3.3) with $k > 0$, since the total index is always unity, this equation possesses at least one primary solution for any value of B . Furthermore, a primary solution is either completely stable or directly unstable, since the coefficients of the variational system of Eqs. (3.3) for the primary solution have period π .

We now consider the variation of the qualitative structure of the phase portrait when the system parameter varies. The qualitative structure of the phase portrait is determined by the maximum invariant set Δ and invariant curves with respect to directly and/or inversely unstable points introduced in Chap. 1. That is, for Eqs. (3.3), the qualitative change of the phase portrait may be occurred by the appearance and disappearance of fixed and periodic points and

by the variation of invariant curves. In this section we shall discuss the appearance and disappearance of fixed and periodic points. The nature of invariant curves will be treated in the next chapter.

(a) Generation and branching of fixed points for Eqs. (3.3)

Bifurcation theory in nonlinear two dimensional autonomous system was studied in standard treatises by A.A. Andronov, A.A. Vitt and S.E. Khaikin [1], N. Minorsky [22] and others. Analogically, we discuss the appearance and disappearance of fixed and periodic points under the Poincaré mapping T defined by Eqs. (3.3).

Let us consider the system (3.3) under a fixed dissipative constant $k > 0$. In this case, the system has a parameter B : the amplitude of the external forcing term. It may be expected that for a sufficiently small value of B , the system has only one completely stable fixed point. For a large value of B , however, the system possesses a various type of fixed and periodic points. By reason of this fact, we discuss the possibility of the bifurcation for Eqs. (3.3). For simplicity, let us consider the bifurcation of fixed points. Similar discussion is applied to the bifurcation of periodic points.

If for some changes of B the solution varies without undergoing any qualitative changes in its topological structure, such values B are called ordinary values. If, however, for some special value $B = B_c$, the topological structure of the phase portrait undergoes a qualitative change, such a special value is called critical value, [1].

On the other hand, for any closed curve C in xy plane, the index of C is continuous on the parameter B provided that no fixed points appear on the curve C . Thus, a fixed point with non-zero index cannot either appear or disappear for the variation of B . A completely stable fixed point whose characteristic

multipliers are both real and positive, can disappear only after having previously merged with a directly unstable fixed point, thus forming a non-simple fixed point with an index equal to zero. Conversely, a directly unstable fixed point or a completely stable fixed point can appear or generate from the splitting up of non-simple fixed point with an index equal to zero. Therefore, for fixed and periodic points of Eqs. (3.3), the possible types of the qualitative change of the phase portrait are as follows:

TYPE I (Generation of fixed points or SD-generation)

Let $\Delta(B)$ be the maximum invariant set of Eqs. (3.3) for an ordinary value of B . Consider the variations of the parameter B . If a non-simple fixed point stated above appears at $B = B_g$ and the topological structure of $\Delta(B_g)$ is the same as $\Delta(B)$ except the non-simple fixed point and α -branch with respect to this point and for further changes of B this non-simple fixed point splits into a completely stable and a directly unstable fixed points, then we say that this phenomenon is that of the generation of a stable and a directly unstable fixed points, or simply, SD-generation. This situation is illustrated in Fig. 3.1 (a). In this figure $\Delta(B)$ is sketched by a hatched area but for Eqs. (3.3) $\Delta(B)$ has evidently zero measure. The disappearance phenomenon is defined conversely.

In accordance with the change of stability of a fixed point, there appear or disappear other fixed or 2-periodic points. These phenomena will be referred to as branchings. Two different types, i.e. Type II and Type III, of branching can be considered.

TYPE II (SD-branching)

Let a point S be a completely stable fixed point for an ordinary value of B . Under the variations of B , at $B = B_b$, if the corresponding fixed point S is

changed into a non-simple fixed point with an index equal to unity, and further variations of B cause this point to split into three fixed points: two completely stable and one directly unstable fixed points, then we say that this phenomenon is SD-branching. This process is simply regarded as follows: During the variations of B , a fixed point, say an original fixed point, continues to exist and changes its stability at $B = B_b$ and puts forth to branches of two fixed points, say branched fixed points, after the critical value of $B = B_b$. The passage of B through its critical value B_b is illustrated in Fig. 3.1 (b). In this figure the points S and D denote the original fixed point, and 1S and 2S are branched fixed points.

TYPE III (SI-branching)

Let a point S be a completely stable fixed point for an ordinary value of B . Consider the variations of the parameter B . If at some special value $B = B_b$ the corresponding fixed point S is changed into a non-simple fixed point with an index equal to unity, and further variations of B cause this point to split into an inversely unstable fixed point and two completely stable 2-periodic points, then this phenomenon is called SI-branching. In this case, the original fixed point is changed into an inversely unstable fixed point, while the branched points are two completely stable 2-periodic points. Figure 3.1 (c) shows SI-branching. In this figure S and I denote a completely stable and an inversely unstable fixed points, respectively. S_1^2 and $S_2^2(= T(S_1^2))$ are branched 2-periodic points.

We now summarize the relation between the bifurcation and primary or non-primary solutions for Eqs. (3.3).

1. For SD-generation, there are two cases: primary fixed points genera-

tion and non-primary fixed points generation. If generated fixed point are non-primary, then four fixed points, two completely stable and two directly unstable fixed points appear.

2. No SI-branching can occur in a primary fixed point.
3. Branched fixed points by SD-branching always appear in pair.

(b) Classification of the periodic solutions of Duffing's equation

From the numerical analysis which will be discussed in the next sections, we shall see that the system (3.2) possesses a various types of periodic solutions. This fact impels us to distinguish those periodic solutions into several types despite of the lack of theoretical background. From the physical point of view, an oscillatory system governed by Duffing's equation may have a periodic response the fundamental period of which is either equal to that of the external forcing term or equal to its integral multiple. The terms harmonic and subharmonic oscillations are applied to those responses, respectively, [12]. Corresponding to such a periodic oscillation, a solution of period 2π of Eq. (3.2) is called harmonic solution. A periodic solution with period $2m\pi$, i.e., m times the period of the forcing term is called subharmonic solution of order m .

On the other hand, a periodic solution is expressed by a Fourier-series expansion. For the purpose of notational convenience, comparing the coefficients in the expansion, various harmonic and subharmonic solutions will be distinguished as follows: From the numerical results if the coefficient of the terms $\cos t$ or/and $\sin t$ is predominant and the other coefficients are relatively small, then we say the periodic solution harmonic. If the coefficient of the terms $\cos mt$ or/and $\sin mt$ is dominant in the periodic solution, then the solution is called

higher-harmonic solution of order m or m -harmonic solution. Similarly, if the coefficient of the terms $\cos nt/m$ or/and $\sin nt/m$ is dominant in a subharmonic solution, then we call the solution subharmonic solution of order m/n or n/m -harmonic solution. In the case of weak nonlinear system, one can find more persuasive classification in Ref. [18].

3.3 Harmonic and higher-harmonic solutions

This section describes numerical results on the harmonic and higher-harmonic solutions for Eqs. (3.3) as the parameters in the equation are varied over large intervals.

(a) Regions in which harmonic and higher-harmonic solutions exist

Before going into a detailed computation for specific parameters B and k , we shall investigate the regions of the parameters in Bk plane in which harmonic and higher-harmonic solutions are obtained. Figure 3.2 shows these regions obtained by analog computations. The six regions in Fig. 3.2 are as follows: In the regions I and III, there exists a harmonic solution correlated with a completely stable fixed point. In the sense of nonlinear physical phenomena, the harmonic solutions in the region I and III are often called nonresonant and resonant responses, respectively. Between the regions I and III, an overlapped region II exists in which there are three harmonic solutions. Two of them are completely stable and the third one is directly unstable. Therefore, under the variations of B from the region I to III, we see that, at left side boundary of the region II, SD-generation appears, the generated fixed points are primary; while at right side boundary, the disappearance phenomenon, i.e. SD-disappearance, occurs. Transfer from the region III into IV gives rise to SD-branching. Hence a harmonic solution changes into three periodic solutions, two of which

are completely stable and the third one is directly unstable. The two stable solutions contain even harmonics in addition to the fundamental and odd harmonics, i.e. these solutions are non-primary. In the region V, seven periodic solutions appear: four completely stable and three directly unstable solutions. That is, for the entrance to the region V from left side boundary, SD-generations occur, while for leaving the region V along right side boundary, SD-disappearance are observed. In the region VI, there are three harmonic solutions: one directly and two inversely unstable solutions. Hence on the boundary between the regions IV and VI, SI-branching appears. Thus in the region VI, subharmonic solutions of order 2 appear. Above situation are summarized in Tables 3.1 and 3.2. It is to be noted that Fig. 3.2 and also Table 3.1 show only harmonic solutions. When the parameter k is sufficiently small, subharmonic solutions may appear in every region. This will be stated in the following sections.

Table 3.1 Number and type of harmonic solutions in the different regions in the Bk plane illustrated in Fig. 3.2

Region	Number of harmonic solutions	Type of fixed point correlated with the harmonic solution
I	1	S
II	3	$S \times 2, D \times 1$
III	1	S
IV	3	$S \times 2, D \times 1$
V	7	$S \times 4, D \times 3$
VI	3	$I \times 2, D \times 1$

Table 3.2 Types of bifurcation when B is increased

Boundary between	Types of bifurcation	Generated, disappeared or branched points
I II	SD-generation	primary
II III	SD-disappearance	primary
III IV	SD-branching	non-primary
IV V (left side)	SD-generation	non-primary
V IV (right side)	SD-disappearance	non-primary
IV VI	SI-branching	2-periodic points

(b) Loci of fixed points and patterns of phase portraits as B varies

To get more specific information on the nature of the harmonic solutions, we consider Eqs. (3.3) with a fixed parameter k . The loci of fixed points are schematically illustrated in Fig. 3.3, as the parameter B varies. The locus of the fixed point correlated with the primary solution is shown by heavy line $OA_1A_2\dots$ in Fig. 3.3. As B increases the fixed point moves along this curve in the direction of the arrows. The fixed point starts from the origin O (for which $B = 0$) and moves toward A_1 . When it reaches A_1 , another fixed point appear at A_3 , i.e., SD-generation occurs. With a further increase in B , three fixed points appear, moving from A_1 to A_2 , from A_3 to A_2 , and from A_3 to A_4 , respectively. When the first two fixed points coalesce at A_2 , the third point reaches A_4 . A further increase in B results in the disappearance of the coalesced fixed point, i.e., SD-disappearance, and the remaining fixed point moves

from A_4 to A_5, A_6, \dots . Investigating the stability of the fixed point, one see that the fixed points on the solid-line portions of the curve are completely stable and those on the dashed portions are directly unstable.

When B is increased beyond A_5 , the locus breaks into three; namely, the original locus $A_5A_6\dots$, B-branch $A_5B_6\dots$, and C-branch $A_5C_6\dots$, that is, SD-branching occurs. The loci of the branched fixed points are shown by fine lines in Fig. 3.3. Periodic solutions on B-branch and C-branch are non-primary, i.e., they are characterized by the presence of even harmonics in addition to the fundamental and odd harmonics. Thus, for a given value of B , there exist three fixed points, say A_6, B_6 , and C_6 ; A_6 is directly unstable while B_6 and C_6 are completely stable. When B is increased further, fixed points on B-branch and C-branch proceed to B_7 and C_7 , respectively.* Then the subdivision of the two branches occurs simultaneously at those points, i.e., SI-branching occurs. Fixed points on $B_7D_8\dots, B_7E_8\dots, C_7F_8\dots, C_7G_8\dots$ are obtained under every second iterate of the mapping T ; therefore, the corresponding periodic solutions contain subharmonic component of order 2 and its higher-harmonics. Thus we obtain three fixed points and four 2-periodic points: a directly unstable A_8 , two inversely unstable B_8 and C_8 , and four completely stable 2-periodic points D_8, E_8, F_8 and G_8 .

The phase portraits for some fixed B and k are pictorially shown in Fig. 3.4. This figure shows schematically the location of fixed points and invariant

* When k is large the jump phenomenon, i.e., SD-generation and SD-disappearance, of fixed points on the original locus (from A_2 to A_4 and from A_3 to A_1) disappears. On the contrary, if k is very small the jump phenomenon occurs also on B- and C-branches.

curves which pass through the directly and inversely unstable fixed points. The arrows in the figure indicate the direction of the movement of successive images of the mapping T . Figure 3.4 (a) shows the pattern of a phase portrait obtained in the parameter region II in Fig. 3.2. The patterns (b), (c) and (d) in Fig. 3.4 show the phase portraits obtained in the regions IV, V and VI, respectively. It is to be noted that for small k subharmonic solutions may exist. For example, in the region II subharmonic solutions of order 3 exist. The phase portrait is sketched in Fig. 3.4 (e). This situation will be discussed in the next sections.

(c) Harmonic solutions

We now discuss more completely representative cases of Eqs. (3.3). To begin with, let us consider a case in which the parameters are chosen in the region II in Fig. 3.2, i.e., $k = 0.1$ and $B = 0.3$. Thus we are dealing with

$$\frac{d^2x}{dt^2} + 0.1 \frac{dx}{dt} + x^3 = 0.3 \cos t \quad (3.6)$$

In this case, there are three fixed points corresponding to the periodic solutions of Eq. (3.6).^{*} One of them is directly unstable and the other two are completely stable; details of the fixed points are given in Table 3.3. Figure 3.5 shows the location of the fixed points and a pair of invariant curves which pass through the unstable fixed point D. The arrows in the figure indicate the direction of successive images of points on the invariant curves under T . For this example one of the invariant curves, i.e., ω -branches drawn in heavy line, along which the successive images approach the point D is the boundary of the

^{*} These fixed points are situated on the original locus $OA_1A_2\dots$ in Fig. 3.3.

Table 3.3 Fixed points and related properties correlated with the periodic solutions for Eq. (3.6).

Fixed point	Periodic solution	x	y	λ_1, λ_2	Classification
D	Harmonic	-0.9170	0.3812	3.763, 0.142	Directly unstable
1S	Harmonic	-0.3228	0.0360	$-0.586 \pm 0.436i$	Completely stable
2S	Harmonic	1.1381	0.7447	$-0.170 \pm 0.710i$	Completely stable

two domains of attraction. On the other hand, α -branches of D, drawn in fine line, with two fixed points 1S and 2S form the maximum invariant set of this equation. The periodic solution correlated with the directly unstable fixed point D is found to be

$$\begin{aligned}
 x_D(t) = & -0.9022 \cos t + 0.3046 \sin t \\
 & -0.0149 \cos 3t + 0.0241 \sin 3t \\
 & + 0.0001 \cos 5t + 0.0008 \sin 5t \\
 & + \dots
 \end{aligned}$$

The stable periodic solutions $x_{1S}(t)$ and $x_{2S}(t)$ correlated with points 1S and 2S are respectively given by

$$\begin{aligned}
 x_{1S}(t) = & -0.3219 \cos t + 0.0350 \sin t \\
 & -0.0009 \cos 3t + 0.0003 \sin 3t \\
 & + \dots
 \end{aligned}$$

$$\begin{aligned}
 x_{2S}(t) = & 1.1193 \cos t + 0.5246 \sin t \\
 & + 0.0211 \cos 3t + 0.0679 \sin 3t \\
 & - 0.0020 \cos 5t + 0.0032 \sin 5t
 \end{aligned}$$

$$\begin{aligned}
& - 0.0002 \cos 7t + 0.0000 \sin 7t \\
& + \dots
\end{aligned}$$

The values λ_1 and λ_2 in Table 3.3 are calculated by the solutions of the variational equations of Eq. (3.6) with respect to the above periodic solutions.

(d) Higher-harmonic solutions

We consider the second case in which B is increased (in the region IV in Fig. 3.2) and the equation becomes

$$\frac{d^2x}{dt^2} + 0.1 \frac{dx}{dt} + x^3 = 2.6 \cos t \quad (3.7)$$

Corresponding to the periodic solutions of Eq. (3.7), we have three fixed points under the mapping T, the details of which are listed in Table 3.4. These fixed points and the invariant curves are shown in Fig. 3.6. The ω - and α -branches are drawn in heavy and fine lines, respectively. The periodic solution correlated with the directly unstable fixed point D is found to be

$$\begin{aligned}
x_D(t) = & 1.6672 \cos t + 0.1328 \sin t \\
& + 0.2609 \cos 3t + 0.0446 \sin 3t \\
& + 0.0302 \cos 5t + 0.0091 \sin 5t \\
& + 0.0036 \cos 7t + 0.0016 \sin 7t \\
& + 0.0004 \cos 9t + 0.0003 \sin 9t \\
& + \dots
\end{aligned}$$

The stable periodic solutions $x_{1S}(t)$ and $x_{2S}(t)$ correlated with points 1S and 2S are respectively given by

$$\begin{aligned}
x_{1S}(t) &= -x_{2S}(t + \pi) \\
&= -0.0468
\end{aligned}$$

Table 3.4 Fixed points and related properties correlated with the periodic solutions for Eq. (3.7).

Fixed point	Periodic solution	x	y	λ_1, λ_2	Classification
D	3-harmonic	1.9625	0.3261	2.000, 0.267	Directly unstable
1S	2-harmonic	1.4083	2.0971	$0.061 \pm 0.728i$	Completely stable
2S	2-harmonic	1.6975	-1.7049	$0.061 \pm 0.728i$	Completely stable

$$\begin{aligned}
 &+ 1.4999 \cos t + 0.1771 \sin t \\
 &- 0.0627 \cos 2t + 0.7037 \sin 2t \\
 &+ 0.0870 \cos 3t + 0.0256 \sin 3t \\
 &- 0.0315 \cos 4t + 0.1156 \sin 4t \\
 &- 0.0274 \cos 5t - 0.0067 \sin 5t \\
 &- 0.0042 \cos 6t + 0.0071 \sin 6t \\
 &- 0.0061 \cos 7t - 0.0029 \sin 7t \\
 &+ 0.0003 \cos 8t - 0.0010 \sin 8t \\
 &- 0.0005 \cos 9t - 0.0004 \sin 9t \\
 &+ 0.0002 \cos 10t - 0.0003 \sin 10t \\
 &+ \dots
 \end{aligned}$$

We now consider the cases in which B is varied in the region V in Fig. 3.2. Figure 3.7 shows schematically the location of fixed points and invariant curves of directly unstable fixed points when the parameter $B = 2.8, 3.2, 3.5$ and 3.8 with $k = 0.1$. From this figure one can see how to change the pattern of phase

portrait in the region V. It is noted that for sufficiently small k the fixed points 1S and 2S change into inversely unstable fixed points. But under the variation of the system parameters, these inversely unstable fixed points disappear after the passage of the left side boundary of the region V in Fig. 3.2. Thus the appearance of inversely unstable fixed points in the region VI means the SI-branching of the fixed points 3S and 4S illustrated in Fig. 3.7.

(e) Higher-harmonic solutions with subharmonics

We consider the fourth case in which B is still further increased and the equation becomes

$$\frac{d^2x}{dt^2} + 0.1 \frac{dx}{dt} + x^3 = 5.0 \cos t \quad (3.8)$$

This example illustrates the interpretation of SI-branching. As the result of this phenomenon, three fixed points: two inversely and one directly unstable fixed points, and four completely stable 2-periodic points are obtained. Their details are shown in Table 3.5. The locations of fixed and 2-periodic points and invariant curves are sketched in Fig. 3.8.

The periodic solution correlated with the directly unstable fixed point D is found to be

$$\begin{aligned} x_D(t) = & 1.8319 \cos t + 0.1189 \sin t \\ & + 0.5105 \cos 3t + 0.0470 \sin 3t \\ & + 0.8710 \cos 5t + 0.0151 \sin 5t \\ & + 0.0162 \cos 7t + 0.0039 \sin 7t \\ & + 0.0030 \cos 9t + 0.0010 \sin 9t \\ & + 0.0006 \cos 11t + 0.0002 \sin 11t \\ & + \dots \end{aligned}$$

Table 3.5 Fixed points and related properties correlated with the periodic solutions for Eq. (3.8).

Fixed point	Periodic solution	x	y	λ_1, λ_2	Classification
D	5-harmonic	2.4493	0.3750	1.166, 0.458	Directly unstable
1I	2-harmonic	2.7130	1.2598	-1.146, -0.465	Inversely unstable
2I	2-harmonic	1.7131	-0.3496	-1.146, -0.465	Inversely unstable
$^1S_1^2$	2-harmonic	2.5359	2.5433	$0.387 \pm 0.366i$	Completely stable
$^1S_2^2$	2-harmonic	2.7507	-0.1816	$0.387 \pm 0.366i$	Completely stable
$^2S_1^2$	2-harmonic	1.5100	-0.3099	$0.387 \pm 0.366i$	Completely stable
$^2S_1^2$	2-harmonic	1.9278	-0.3709	$0.387 \pm 0.366i$	Completely stable

The inversely unstable periodic solutions $x_{1I}(t)$ and $x_{2I}(t)$ correlated with the points 1I and 2I are respectively given by

$$\begin{aligned}
 x_{1I}(t) &= -x_{2I}(t + \pi) \\
 &= -0.4508 \\
 &\quad + 1.8171 \cos t + 0.1445 \sin t \\
 &\quad + 0.7435 \cos 2t + 0.1909 \sin 2t \\
 &\quad + 0.3034 \cos 3t + 0.0174 \sin 3t \\
 &\quad + 0.1623 \cos 4t + 0.0624 \sin 4t \\
 &\quad + 0.0719 \cos 5t + 0.0285 \sin 5t \\
 &\quad + 0.0353 \cos 6t + 0.0166 \sin 6t \\
 &\quad + 0.0162 \cos 7t + 0.0097 \sin 7t
 \end{aligned}$$

$$\begin{aligned}
& + 0.0076 \cos 8t + 0.0052 \sin 8t \\
& + 0.0035 \cos 9t + 0.0028 \sin 9t \\
& + 0.0016 \cos 10t + 0.0015 \sin 10t \\
& + 0.0007 \cos 11t + 0.0008 \sin 11t \\
& + 0.0003 \cos 12t + 0.0004 \sin 12t \\
& + \dots
\end{aligned}$$

The periodic solutions correlated with the 2-periodic points are as follows:

$$\begin{aligned}
x_{1S1}(t) &= x_{1S2}(t + 2\pi) = -x_{2S1}(t + \pi) = -x_{2S2}(t - \pi) \\
&= 0.4384 \\
&+ 0.0026 \cos \frac{1}{2}t - 0.0204 \sin \frac{1}{2}t \\
&+ 1.8061 \cos t + 0.1475 \sin t \\
&+ 0.0613 \cos \frac{3}{2}t + 0.0106 \sin \frac{3}{2}t \\
&- 0.7174 \cos 2t - 0.1924 \sin 2t \\
&- 0.2534 \cos \frac{5}{2}t - 0.0174 \sin \frac{5}{2}t \\
&+ 0.2927 \cos 3t + 0.0200 \sin 3t \\
&+ 0.0162 \cos \frac{7}{2}t + 0.0174 \sin \frac{7}{2}t \\
&- 0.1491 \cos 4t - 0.0603 \sin 4t \\
&- 0.0523 \cos \frac{9}{2}t - 0.0111 \sin \frac{9}{2}t \\
&+ 0.0667 \cos 5t + 0.0266 \sin 5t \\
&+ 0.0251 \cos \frac{11}{2}t + 0.0135 \sin \frac{11}{2}t \\
&- 0.0277 \cos 6t - 0.0148 \sin 6t \\
&- 0.0132 \cos \frac{13}{2}t - 0.0059 \sin \frac{13}{2}t \\
&+ 0.0130 \cos 7t + 0.0080 \sin 7t \\
&+ 0.0073 \cos \frac{15}{2}t + 0.0047 \sin \frac{15}{2}t
\end{aligned}$$

$$\begin{aligned}
& - 0.0053 \cos 8t - 0.0042 \sin 8t \\
& - 0.0037 \cos \frac{17}{2}t - 0.0027 \sin \frac{17}{2}t \\
& + 0.0022 \cos 9t + 0.0020 \sin 9t \\
& + 0.0018 \cos \frac{19}{2}t + 0.0016 \sin \frac{19}{2}t \\
& - 0.0009 \cos 10t - 0.0010 \sin 10t \\
& + \dots
\end{aligned}$$

where the subscript for $x(t)$ means that $x_{jSi}(t)$, for example, is the periodic solution correlated with the point jS_i^2 .

3.4 Subharmonic solutions of order 2

In the preceding section we have seen that, as B increases for Eqs. (3.3), higher-harmonics (odd and even) and subharmonics develop in the periodic solution. In a system with small dissipative constant k , however, we have a situation considerably different from that described in Sec. 3.3, i.e., subharmonic solution may occur. As already reported in Refs. [25] App. V and [12] Chap. 10, the system (3.3) has subharmonic solutions of order 2 in some parameter regions. In this section we investigate subharmonic solutions of order 2 for Eqs. (3.3).

(a) 1/2-harmonic solutions for Eqs. (3.3)

In Ref. [25] App. V, the region of 1/2-harmonic solutions for Eqs. (3.3) was investigated. We reproduce the result in Fig. 3.9 with some additional results. The figure shows the regions of harmonic, 1/2-harmonic and 1/3-harmonic solutions for Eqs. (3.3). In this figure the region of 1/2-harmonic solutions is divided roughly into two: the region in which four completely stable and four directly unstable 2-periodic points are obtained (surrounding

narrow region in the figure), and the region in which four inversely unstable and four directly unstable 2-periodic points are obtained (surrounded region).

As representative examples of two cases stated above, we consider first the equation:

$$\frac{d^2x}{dt^2} + 0.09 \frac{dx}{dt} + x^3 = 0.26 \cos t \quad (3.9)$$

The pattern of phase portrait for 2-periodic points is sketched in Fig. 3.10.

In this figure two groups of 2-periodic points of the same types are seen, i.e.,

$$\begin{aligned} {}^1S_1^2, {}^1S_2^2 (= T({}^1S_1^2)) \quad \text{and} \quad {}^2S_1^2, {}^2S_2^2 (= T({}^2S_1^2)) \\ {}^1D_1^2, {}^1D_2^2 (= T({}^1D_1^2)) \quad \text{and} \quad {}^2D_1^2, {}^2D_2^2 (= T({}^2D_1^2)). \end{aligned}$$

Their details are given in Table 3.6. The invariant curves which pass through the directly unstable 2-periodic point ${}^jD_i^2$ ($j = 1, 2; i = 1, 2$) are obtained by the mapping T^2 .

The periodic solutions correlated with the 2-periodic points are as follows:

$$\begin{aligned} x_{1D1}(t) &= x_{1D2}(t + 2\pi) = -x_{2D1}(t + \pi) = -x_{2D2}(t - \pi) \\ &= 0.0522 \\ &\quad + 0.3127 \cos \frac{1}{2}t + 0.1281 \sin \frac{1}{2}t \\ &\quad - 0.3455 \cos t + 0.0523 \sin t \\ &\quad + 0.0046 \cos \frac{3}{2}t - 0.0081 \sin \frac{3}{2}t \\ &\quad - 0.0044 \cos 2t - 0.0052 \sin 2t \\ &\quad + 0.0056 \cos \frac{5}{2}t + 0.0003 \sin \frac{5}{2}t \\ &\quad - 0.0013 \cos 3t + 0.0007 \sin 3t \\ &\quad + \dots \end{aligned}$$

Table 3.6 Fixed and 2-periodic points and related properties for Eq. (3.8).

Fixed point	Periodic solution	x	y	λ_1, λ_2	Classification
D	Harmonic	-0.9389	0.4281	3, 481, 0.153	Directly unstable
1S	Harmonic	-0.2737	0.0266	$-0.386 \pm 0.647i$	Completely stable
2S	Harmonic	1.1162	0.7449	$-0.077 \pm 0.750i$	Completely stable
$^1D_1^2$	1/2-harmonic	0.0238	0.0968	3.271, 0.099	Directly unstable
$^1D_2^2$	1/2-harmonic	-0.6220	-0.0086	3.271, 0.099	Directly unstable
$^2D_1^2$	1/2-harmonic	-0.5309	0.2283	3.271, 0.099	Directly unstable
$^2D_2^2$	1/2-harmonic	-0.2579	-0.0981	3.271, 0.099	Directly unstable
$^1S_1^2$	1/2-harmonic	0.0961	0.0737	$-0.391 \pm 0.412i$	Completely stable
$^1S_2^2$	1/2-harmonic	-0.6616	0.0364	$-0.391 \pm 0.412i$	Completely stable
$^2S_1^2$	1/2-harmonic	-0.5063	0.2578	$-0.391 \pm 0.412i$	Completely stable
$^2S_2^2$	1/2-harmonic	-0.3697	-0.1252	$-0.391 \pm 0.412i$	Completely stable

$$x_{1S1}(t) = x_{1S2}(t = 2\pi) = -x_{2S1}(t + \pi) = -x_{2S2}(t - \pi)$$

$$= 0.0341$$

$$\begin{aligned}
& + 0.3669 \cos \frac{1}{2}t + 0.0631 \sin \frac{1}{2}t \\
& - 0.3590 \cos t + 0.0580 \sin t \\
& + 0.0052 \cos \frac{3}{2}t - 0.0065 \sin \frac{3}{2}t \\
& - 0.0063 \cos 2t - 0.0023 \sin 2t \\
& + 0.0065 \cos \frac{5}{2}t - 0.0012 \sin \frac{5}{2}t
\end{aligned}$$

$$\begin{aligned}
& - 0.0014 \cos 3t + 0.0009 \sin 3t \\
& + \dots
\end{aligned}$$

where the subscript for $x(t)$ means that $x_{jDi}(t)$, for example, is the periodic solution correlated with the point j_{Di}^2 .

For the second example, we consider Eqs. (3.3) with $k = 0.05$, $B = 0.22$. Figure 3.11 shows the phase portrait in this case. When compared with Fig. 3.10, one sees that the completely stable 2-periodic points change into the inversely unstable 2-periodic points, that is, SI-branching for 2-periodic points is observed. For instance, j_{Si}^2 in Fig. 3.10 changes into j_{Ii}^2 in Fig. 3.11. In this case it may appear inversely unstable v -periodic points ($v = 4, 8, 16, \dots$), i.e., SI-branching may proceed successively. Moreover, simple homoclinic points with respect to j_{Di}^2 exist. It is difficult, however, to observe clearly this qualitative change in the phase portrait by numerical computation. In this example, we also observe 3-periodic points which will be discussed in the next section.

(b) 3/2-harmonic solutions for Eqs. (3.3)

The phase portraits of the above examples are concerned with the 2-periodic points around the fixed point correlated with a nonresonant harmonic solution. For the parameters k small, $0 < k < 0.07$, and B large, $0.7 < B < 1.2$, 2-periodic points around the stable fixed point correlated with a resonant harmonic solution appear. As an example, let us consider the equation

$$\frac{d^2x}{dt^2} + 0.04 \frac{dx}{dt} + x^3 = 0.9 \cos t \quad (3.10)$$

The phase portrait is shown in Fig. 3.12. The details of fixed and 2-periodic

points are listed in Table 3.7. The periodic solutions correlated with the 2-periodic points are as follows, where the subscript notation is the same as stated in (a):

$$\begin{aligned}
 x_{1D1}(t) &= x_{1D2}(t + 2\pi) = -x_{2D1}(t + \pi) = -x_{2D2}(t - \pi) \\
 &= 0.0797 \\
 &\quad - 0.3761 \cos \frac{1}{2}t + 0.0304 \sin \frac{1}{2}t \\
 &\quad + 1.1316 \cos t + 0.1233 \sin t \\
 &\quad + 0.6666 \cos \frac{3}{2}t + 0.3082 \sin \frac{3}{2}t \\
 &\quad + 0.1711 \cos 2t + 0.0646 \sin 2t
 \end{aligned}$$

Table 3.7 Fixed and 2-periodic points and related properties for Eq. (3.10).

Fixed point	Periodic solution	x	y	λ_1, λ_2	Classification
S	Harmonic	1.5318	0.1727	$-0.858 \pm 0.206i$	Completely stable
$1D_1^2$	3/2-harmonic	1.7231	1.1579	1.819, 0.333	Directly unstable
$1D_2^2$	3/2-harmonic	1.1122	-0.3203	1.819, 0.333	Directly unstable
$2D_1^2$	3/2-harmonic	0.5706	1.2309	1.819, 0.333	Directly unstable
$2D_2^2$	3/2-harmonic	1.1289	-1.5448	1.819, 0.333	Directly unstable
$1S_1^2$	3/2-harmonic	1.1192	2.1311	$-0.057 \pm 0.776i$	Completely stable
$1S_2^2$	3/2-harmonic	0.6022	-0.7620	$-0.057 \pm 0.776i$	Completely stable
$2S_1^2$	3/2-harmonic	0.1420	0.8130	$-0.057 \pm 0.776i$	Completely stable
$2S_2^2$	3/2-harmonic	1.4111	-1.8669	$-0.057 \pm 0.776i$	Completely stable

$$\begin{aligned}
& - 0.0388 \cos \frac{5}{2}t + 0.0122 \sin \frac{5}{2}t \\
& + 0.0028 \cos 3t - 0.0078 \sin 3t \\
& + 0.0438 \cos \frac{7}{2}t + 0.0342 \sin \frac{7}{2}t \\
& + 0.0322 \cos 4t + 0.0359 \sin 4t \\
& + 0.0097 \cos \frac{9}{2}t + 0.0187 \sin \frac{9}{2}t \\
& - 0.0006 \cos 5t + 0.0035 \sin 5t \\
& - 0.0001 \cos \frac{11}{2}t + 0.0005 \sin \frac{11}{2}t \\
& + 0.0011 \cos 6t + 0.0023 \sin 6t \\
& + 0.0007 \cos \frac{13}{2}t + 0.0029 \sin \frac{13}{2}t \\
& - 0.0001 \cos 7t + 0.0017 \sin 7t \\
& - 0.0002 \cos \frac{15}{2}t + 0.0005 \sin \frac{15}{2}t \\
& + \dots
\end{aligned}$$

$$\begin{aligned}
x_{1S1}(t) &= x_{1S2}(t + 2\pi) = -x_{2S1}(t + \pi) = -x_{2S2}(t - \pi) \\
&= 0.0579
\end{aligned}$$

$$\begin{aligned}
& - 0.3345 \cos \frac{1}{2}t + 0.1358 \sin \frac{1}{2}t \\
& + 0.8607 \cos t + 0.1495 \sin t \\
& + 0.6306 \cos \frac{3}{2}t + 0.7913 \sin \frac{3}{2}t \\
& + 0.0040 \cos 2t + 0.1989 \sin 2t \\
& - 0.0185 \cos \frac{5}{2}t + 0.0242 \sin \frac{5}{2}t \\
& - 0.0283 \cos 3t - 0.0172 \sin 3t \\
& + 0.0142 \cos \frac{7}{2}t + 0.0255 \sin \frac{7}{2}t \\
& - 0.0205 \cos 4t + 0.0539 \sin 4t \\
& - 0.0292 \cos \frac{9}{2}t + 0.0163 \sin \frac{9}{2}t \\
& - 0.0116 \cos 5t - 0.0021 \sin 5t
\end{aligned}$$

$$\begin{aligned}
& - 0.0017 \cos \frac{11}{2}t - 0.0041 \sin \frac{11}{2}t \\
& + 0.0003 \cos 6t - 0.0003 \sin 6t \\
& - 0.0023 \cos \frac{13}{2}t + 0.0005 \sin \frac{13}{2}t \\
& - 0.0022 \cos 7t - 0.0013 \sin 7t \\
& - 0.0005 \cos \frac{15}{2}t - 0.0014 \sin \frac{15}{2}t \\
& + 0.0003 \cos 8t - 0.0006 \sin 8t \\
& + \dots
\end{aligned}$$

(c) Successive multiplication of SI-branching

We have seen in Fig. 3.4 (d) and also stated (a) above that, when SI-branching occur, i.e., a fixed point of the mapping T becomes inversely unstable, the invariant curve emanating from this point tends to a pair of completely stable, 2-periodic points. We may say that, when completely stable v -periodic points change into inversely unstable v -periodic points, v pairs of completely stable $2v$ -periodic points appear. Under certain circumstances, such multiplication of SI-branching proceeds successively as the parameters vary. If we denote the number of completely stable v -periodic points by $S(v)$ and that of inversely unstable v -periodic points by $I(v)$, then the number of periodic points thus produced is given by the formula:

$$\begin{aligned}
S(2^v) &= 2^v \\
I(2^{v-i}) &= 2^{v-i} \quad (i = 1, 2, \dots, v)
\end{aligned}$$

v being 0, 1, 2,

As a specific example we consider the equations

$$\begin{aligned}\frac{dx}{dt} &= y \\ \frac{dy}{dt} &= -0.2y - x^3 + B \cos t + B_0\end{aligned}\tag{3.11}$$

Figure 3.13 shows the regions in BB_0 plane in which harmonic, 1/2- and 1/4-harmonic solutions are obtained. Under varying B and B_0 successive multiplication of 2-periodic points occurs as illustrated in Fig. 3.14. The system parameters in the respective cases are given by

- | | |
|----------------------------|----------------------------|
| (a) $B = 0.3, B_0 = 0.2$ | (b) $B = 0.3, B_0 = 0.14$ |
| (c) $B = 0.3, B_0 = 0.105$ | (d) $B = 0.3, B_0 = 0.08.$ |

3.5 Subharmonic solutions of order 3

As mentioned earlier and reported in Ref. [12] Chap. 10, subharmonic solutions of order 3 are obtained in Eqs. (3.3). We now investigate three types of subharmonic solutions of order 3, i.e., 1/3-, 5/3- and 7/3-harmonic solutions for the system (3.3).

- (a) 1/3-harmonic solutions for Eqs. (3.3)

Under the parameter k small, 1/3-harmonic solutions are obtained in the situation $0 < B < 0.27$ as sketched in Fig. 3.9. As an example, we consider the equation

$$\frac{d^2x}{dt^2} + 0.1 \frac{dx}{dt} + x^3 = 0.15 \cos t\tag{3.12}$$

This equation has three fixed points 1S , 2S and D , and six 3-periodic points S_1^3 , S_2^3 , S_3^3 , D_1^3 , D_2^3 and D_3^3 . Their details are given in Table 3.8. Figure 3.15 shows these fixed and periodic points and invariant curves which pass through

Table 3.8 Fixed and 3-periodic points and related properties for Eq. (3.12).

Fixed point	Periodic solution	x	y	λ_1, λ_2	Classification
D	Harmonic	-0.7032	0.8532	2.144, 0.249	Directly unstable
1S	Harmonic	-0.1511	0.0155	$0.313 \pm 0.660i$	Completely stable
2S	Harmonic	0.6547	0.9869	$0.383 \pm 0.622i$	Completely stable
D_1^3	1/3-harmonic	0.0510	0.0675	4.911, 0.031	Directly unstable
D_2^3	1/3-harmonic	-0.1497	-0.0628	4.911, 0.031	Directly unstable
D_3^3	1/3-harmonic	-0.4146	0.0719	4.911, 0.031	Directly unstable
S_1^3	1/3-harmonic	0.1766	0.0480	$-0.369 \pm 0.126i$	Completely stable
S_2^3	1/3-harmonic	-0.2920	-0.0886	$-0.369 \pm 0.126i$	Completely stable
S_3^3	1/3-harmonic	-0.4167	0.1348	$-0.369 \pm 0.126i$	Completely stable

the point D. The α -branches of D_i^3 ($i = 1, 2, 3$) under the mapping T^3 are also illustrated in the same figure. The ω -branches of D_i^3 are already reported in Ref. [12], p. 250.

The periodic solution correlated with the point D is found to be

$$\begin{aligned}
 x_D(t) = & -0.7380 \cos t + 0.7817 \sin t \\
 & + 0.0340 \cos 3t + 0.0262 \sin 3t \\
 & + 0.0009 \cos 5t - 0.0014 \sin 5t \\
 & - 0.0001 \cos 7t + 0.0000 \sin 7t \\
 & + \dots
 \end{aligned}$$

The stable periodic solutions $x_{1S}(t)$ and $x_{2S}(t)$ correlated with points 1S and 2S are respectively given by

$$\begin{aligned} x_{1S}(t) = & - 0.1511 \cos t + 0.0154 \sin t \\ & - 0.0001 \cos 3t + 0.0000 \sin 3t \\ & + \dots \end{aligned}$$

$$\begin{aligned} x_{2S}(t) = & 0.7075 \cos t + 0.9287 \sin t \\ & - 0.0525 \cos 3t + 0.0238 \sin 3t \\ & - 0.0005 \cos 5t - 0.0027 \sin 5t \\ & + 0.0001 \cos 7t + 0.0000 \sin 7t \\ & + \dots \end{aligned}$$

The periodic solutions correlated with the 3-periodic points are as follows:

$$\begin{aligned} x_{D1}(t) = x_{D2}(t - 2\pi) = x_{D3}(t + 2\pi) \\ = & 0.2216 \cos \frac{1}{3}t + 0.1478 \sin \frac{1}{3}t \\ & - 0.1709 \cos t + 0.0252 \sin t \\ & - 0.0007 \cos \frac{5}{3}t - 0.0048 \sin \frac{5}{3}t \\ & + 0.0012 \cos \frac{7}{3}t + 0.0003 \sin \frac{7}{3}t \\ & - 0.0001 \cos 3t + 0.0001 \sin 3t \\ & + \dots \end{aligned}$$

$$\begin{aligned} x_{S1}(t) = x_{S2}(t - 2\pi) = x_{S3}(t + 2\pi) \\ = & 0.3550 \cos \frac{1}{3}t + 0.0672 \sin \frac{1}{3}t \\ & - 0.1760 \cos t + 0.0310 \sin t \\ & - 0.0040 \cos \frac{5}{3}t - 0.0029 \sin \frac{5}{3}t \\ & + 0.0017 \cos \frac{7}{3}t - 0.0004 \sin \frac{7}{3}t \\ & - 0.0001 \cos 3t + 0.0001 \sin 3t \\ & + \dots \end{aligned}$$

where the subscript for $x(t)$ means that $x_{D1}(t)$, for example, is the periodic solution correlated with the point D_1^3 .

(b) 5/3-harmonic solutions for Eqs. (3.3)

We now discuss the 5/3-harmonic solutions of Eqs. (3.3). This periodic solutions are obtained in the parameter regions sketched in Fig. 3.16. Roughly speaking, the region is divided into two: surrounded by bolded full lines. In every region one obtains a pair of 3-periodic points: three completely stable and three directly unstable 3-periodic points. Hence in the overlapped region there exist six stable and six directly unstable 3-periodic points.

As an example, we consider the equation:

$$\frac{d^2x}{dt^2} + 0.1 \frac{dx}{dt} + x^3 = 1.5 \cos t \quad (3.13)$$

This equation has a stable fixed point S and three completely stable and three directly unstable 3-periodic points. Their details are given in Table 3.9.

The phase portrait of this equation is shown in Fig. 3.17.

The periodic solution correlated with the point S is found to be

$$\begin{aligned} x_S(t) = & 1.5142 \cos t + 0.1719 \sin t \\ & + 0.1601 \cos 3t + 0.0464 \sin 3t \\ & + 0.0134 \cos 5t + 0.0070 \sin 5t \\ & + 0.0011 \cos 7t + 0.0009 \sin 7t \\ & + 0.0001 \cos 9t + 0.0001 \sin 9t \\ & + \dots \end{aligned}$$

The periodic solution correlated with the 3-periodic points are given by

$$x_{D1}(t) = x_{D2}(t - 2\pi) = x_{D3}(t + 2\pi)$$

Table 3.9 Fixed and 3-periodic points and related properties for Eq. (3.13).

Fixed point	Periodic solution	x	y	λ_1, λ_2	Classification
S	Harmonic	1.6889	0.3530	$-0.209 \pm 0.700i$	Completely stable
D_1^3	5/3-harmonic	1.8648	-0.5214	2.292, 0.066	Directly unstable
D_2^3	5/3-harmonic	1.1673	1.5815	2.292, 0.066	Directly unstable
D_3^3	5/3-harmonic	1.4919	-0.4211	2.292, 0.066	Directly unstable
S_1^3	5/3-harmonic	2.0966	0.4839	$-0.147 \pm 0.361i$	Completely stable
S_2^3	5/3-harmonic	0.2472	1.3564	$-0.147 \pm 0.361i$	Completely stable
S_3^3	5/3-harmonic	0.9377	-1.1306	$-0.147 \pm 0.361i$	Completely stable

$$\begin{aligned}
&= 0.1535 \cos \frac{1}{3}t - 0.1796 \sin \frac{1}{3}t \\
&\quad + 1.4148 \cos t + 0.1981 \sin t \\
&\quad + 0.4596 \cos \frac{5}{3}t - 0.1492 \sin \frac{5}{3}t \\
&\quad - 0.0476 \cos \frac{7}{3}t - 0.1292 \sin \frac{7}{3}t \\
&\quad + 0.0904 \cos 3t + 0.0204 \sin 3t \\
&\quad + 0.0754 \cos \frac{11}{3}t - 0.0007 \sin \frac{11}{3}t \\
&\quad + 0.0134 \cos \frac{13}{3}t - 0.0255 \sin \frac{13}{3}t \\
&\quad + 0.0021 \cos 5t - 0.0063 \sin 5t \\
&\quad + 0.0056 \cos \frac{17}{3}t + 0.0011 \sin \frac{17}{3}t \\
&\quad + 0.0033 \cos \frac{19}{3}t - 0.0021 \sin \frac{19}{3}t \\
&\quad + \dots
\end{aligned}$$

$$\begin{aligned}
x_{S1}(t) &= x_{S2}(t - 2\pi) = x_{S3}(t + 2\pi) \\
&= -0.2446 \cos \frac{1}{3}t - 0.2558 \sin \frac{1}{3}t \\
&\quad + 1.0645 \cos t + 0.2828 \sin t \\
&\quad + 0.9909 \cos \frac{5}{3}t + 0.1097 \sin \frac{5}{3}t \\
&\quad + 0.1225 \cos \frac{7}{3}t - 0.0346 \sin \frac{7}{3}t \\
&\quad + 0.0019 \cos 3t + 0.0281 \sin 3t \\
&\quad + 0.0618 \cos \frac{11}{3}t + 0.0282 \sin \frac{11}{3}t \\
&\quad + 0.0595 \cos \frac{13}{3}t + 0.0269 \sin \frac{13}{3}t \\
&\quad + 0.0237 \cos 5t + 0.0037 \sin 5t \\
&\quad + 0.0059 \cos \frac{17}{3}t - 0.0021 \sin \frac{17}{3}t \\
&\quad + 0.0035 \cos \frac{19}{3}t + 0.0016 \sin \frac{19}{3}t \\
&\quad + \dots
\end{aligned}$$

Under varying k and B , the qualitative change of the phase portrait occurs as illustrated in Fig. 3.18. The system parameters in the respective cases are given by

- | | |
|-------------------------|----------------------------|
| (a) $k = 0.05, B = 1.4$ | (b) $k = 0.05, B = 1.52$ |
| (c) $k = 0.05, B = 1.6$ | (d) $k = 0.05, B = 1.67$. |

(c) $7/3$ -harmonic solutions for Eqs. (3.3)

When B is largely increased, $7/3$ -harmonic solutions appear in Eq. (3.3). As an example we consider the equation

$$\frac{d^2x}{dt^2} + 0.1 \frac{dx}{dt} + x^3 = 5.8 \cos t \quad (3.14)$$

By numerical computation, we observe that the equation has one directly and two inversely unstable fixed points, and three completely stable and three

directly unstable 3-periodic points. These fixed and periodic points and invariant curves for the directly unstable points are illustrated in Fig. 3.19. From this figure the invariant curves with respect to the point D exhibit complex structure, i.e., homoclinic points appear. Fixed and 3-periodic points are listed in Table 3.10. Homoclinic points and their related properties will be discussed in the next chapter.

The periodic solution correlated with the point D is found to be

$$\begin{aligned}
 x_D(t) = & 1.8543 \cos t + 0.1218 \sin t \\
 & + 0.6002 \cos 3t + 0.0484 \sin 3t \\
 & + 0.1115 \cos 5t + 0.0174 \sin 5t \\
 & + 0.0229 \cos 7t + 0.0050 \sin 7t \\
 & + 0.0047 \cos 9t + 0.0013 \sin 9t \\
 & + 0.0010 \cos 11t + 0.0003 \sin 11t \\
 & + 0.0002 \cos 13t + 0.0001 \sin 13t \\
 & + \dots
 \end{aligned}$$

The inversely unstable periodic solutions $x_{1I}(t)$ and $x_{2I}(t)$ correlated with the points 1I and 2I are respectively given by

$$\begin{aligned}
 x_{1I}(t) &= x_{2I}(t + \pi) \\
 &= 0.4700 \\
 &+ 1.8669 \cos t + 0.1368 \sin t \\
 &+ 0.7121 \cos 2t + 0.1566 \sin 2t \\
 &+ 0.4028 \cos 3t + 0.0027 \sin 3t \\
 &+ 0.1689 \cos 4t + 0.0581 \sin 4t \\
 &+ 0.0897 \cos 5t + 0.0221 \sin 5t
 \end{aligned}$$

Table 3.10 Fixed and 3-periodic points and related properties for Eq. (3.14).

Fixed point	Periodic solution	x	y	λ_1, λ_2	Classification
D	3-harmonic	2.5948	0.4063	7.854, 0.068	Directly unstable
1I	2-harmonic	2.8567	1.0652	-1.614, -0.330	Inversely unstable
2I	2-harmonic	1.9353	-0.2828	-1.614, -0.330	Inversely unstable
D_1^3	7/3-harmonic	1.7254	4.4215	7.678, 0.020	Directly unstable
D_2^3	7/3-harmonic	2.2106	-3.4370	7.678, 0.020	Directly unstable
D_3^3	7/3-harmonic	1.0987	0.0251	7.678, 0.020	Directly unstable
S_1^3	7/3-harmonic	2.3088	4.7863	$-0.322 \pm 0.219i$	Completely stable
S_2^3	7/3-harmonic	1.8855	-3.0752	$-0.322 \pm 0.219i$	Completely stable
S_3^3	7/3-harmonic	1.1395	1.1239	$-0.322 \pm 0.219i$	Completely stable

$$\begin{aligned}
& + 0.0441 \cos 6t + 0.0163 \sin 6t \\
& + 0.0215 \cos 7t + 0.0087 \sin 7t \\
& + 0.0107 \cos 8t + 0.0052 \sin 8t \\
& + 0.0052 \cos 9t + 0.0029 \sin 9t \\
& + 0.0025 \cos 10t + 0.0016 \sin 10t \\
& + 0.0012 \cos 11t + 0.0009 \sin 11t \\
& + 0.0006 \cos 12t + 0.0005 \sin 12t \\
& + 0.0003 \cos 13t + 0.0003 \sin 13t \\
& + 0.0001 \cos 14t + 0.0001 \sin 14t \\
& + \dots
\end{aligned}$$

The periodic solutions correlated with the 3-periodic points are as follows:

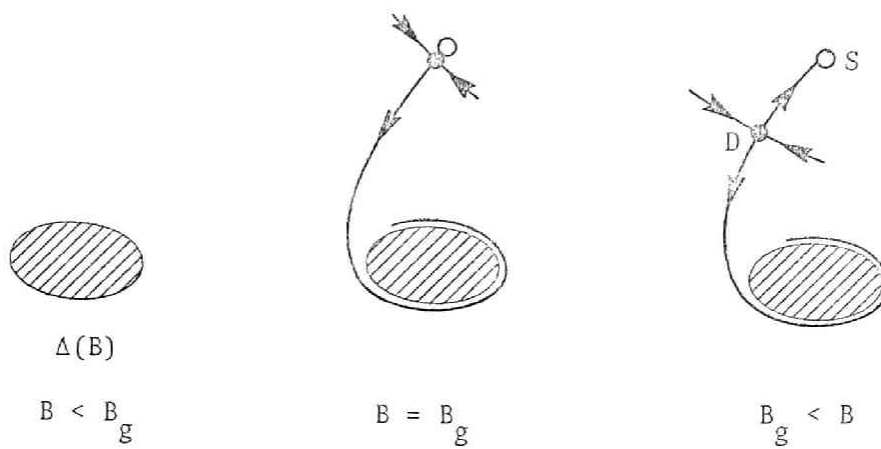
$$\begin{aligned}
 x_{D1}(t) &= x_{D2}(t - 2\pi) = x_{D3}(t + 2\pi) \\
 &= 0.3989 \cos \frac{1}{3}t - 0.3120 \sin \frac{1}{3}t \\
 &\quad + 1.6890 \cos t + 0.2036 \sin t \\
 &\quad + 0.0137 \cos \frac{5}{3}t + 0.1621 \sin \frac{5}{3}t \\
 &\quad + 0.5280 \cos \frac{7}{3}t + 1.0588 \sin \frac{7}{3}t \\
 &\quad + 0.0288 \cos 3t + 0.0642 \sin 3t \\
 &\quad - 0.0684 \cos \frac{11}{3}t + 0.0578 \sin \frac{11}{3}t \\
 &\quad + 0.0612 \cos \frac{13}{3}t + 0.1849 \sin \frac{13}{3}t \\
 &\quad - 0.0117 \cos 5t + 0.0063 \sin 5t \\
 &\quad - 0.0641 \cos \frac{17}{3}t + 0.0662 \sin \frac{17}{3}t \\
 &\quad - 0.0081 \cos \frac{19}{3}t + 0.0101 \sin \frac{19}{3}t \\
 &\quad + \dots
 \end{aligned}$$

$$\begin{aligned}
 x_{S1}(t) &= x_{S2}(t - 2\pi) = x_{S3}(t + 2\pi) \\
 &= -0.6613 \cos \frac{1}{3}t - 0.1462 \sin \frac{1}{3}t \\
 &\quad + 1.6732 \cos t + 0.2228 \sin t \\
 &\quad + 0.1613 \cos \frac{5}{3}t + 0.2012 \sin \frac{5}{3}t \\
 &\quad + 0.9633 \cos \frac{7}{3}t + 0.7759 \sin \frac{7}{3}t \\
 &\quad + 0.1342 \cos 3t + 0.1550 \sin 3t \\
 &\quad - 0.0415 \cos \frac{11}{3}t + 0.0630 \sin \frac{11}{3}t \\
 &\quad + 0.1269 \cos \frac{13}{3}t + 0.1394 \sin \frac{13}{3}t \\
 &\quad - 0.0051 \cos 5t + 0.0203 \sin 5t \\
 &\quad + 0.0040 \cos \frac{17}{3}t + 0.0914 \sin \frac{17}{3}t \\
 &\quad - 0.0028 \cos \frac{19}{3}t + 0.0342 \sin \frac{19}{3}t \\
 &\quad + \dots
 \end{aligned}$$

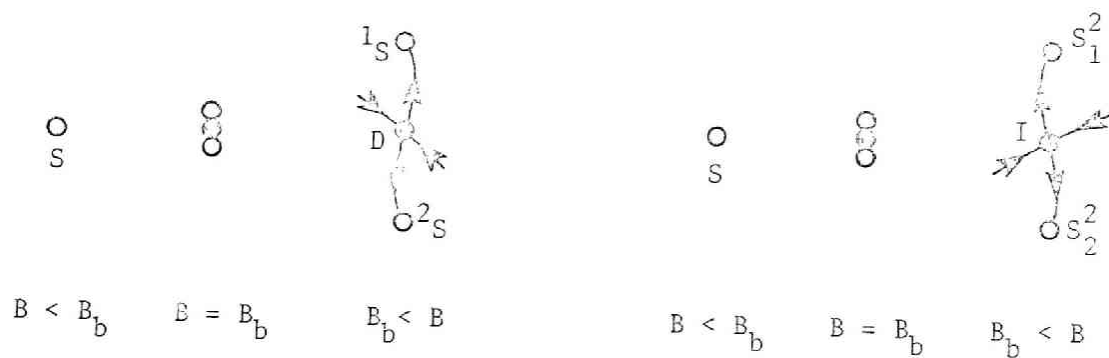
3.6 Supplementary remark

The periodic solutions of Duffing's equation (3.3) have been investigated by using the Poincaré mapping and its computer realization. Bifurcation of fixed or periodic points was also discussed for Eqs. (3.3) with a positive dissipative constant k . As we have seen in several examples, if Eqs. (3.3) has no homoclinic solution, the phase portrait obtained by the mapping T is relatively simple, i.e., the qualitative structure of the phase portrait is characterized by fixed and periodic points, and invariant curves of directly and inversely unstable points. Qualitative change of the phase portrait may occur only by the bifurcation of fixed or periodic points, or by a change of the global behavior of invariant curves. However, if a homoclinic solution appears, the structure of the phase portrait becomes very complex one; for example, infinitely many periodic solutions appear.

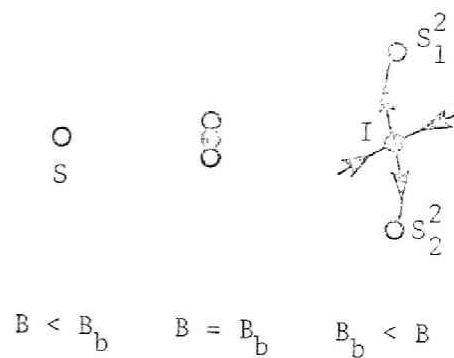
Several examples of harmonic, higher-harmonic and subharmonic solutions have been illustrated. In addition to these examples, however, it will be expected that other periodic solutions, especially subharmonic solutions, may appear in Eqs. (3.3) when the dissipative constant k is sufficiently small.



(a) Generation of fixed points or SD-generation



(b) SD-branching



(c) SI-branching

Fig. 3.1. Types of the bifurcation for Eqs. (3.3).

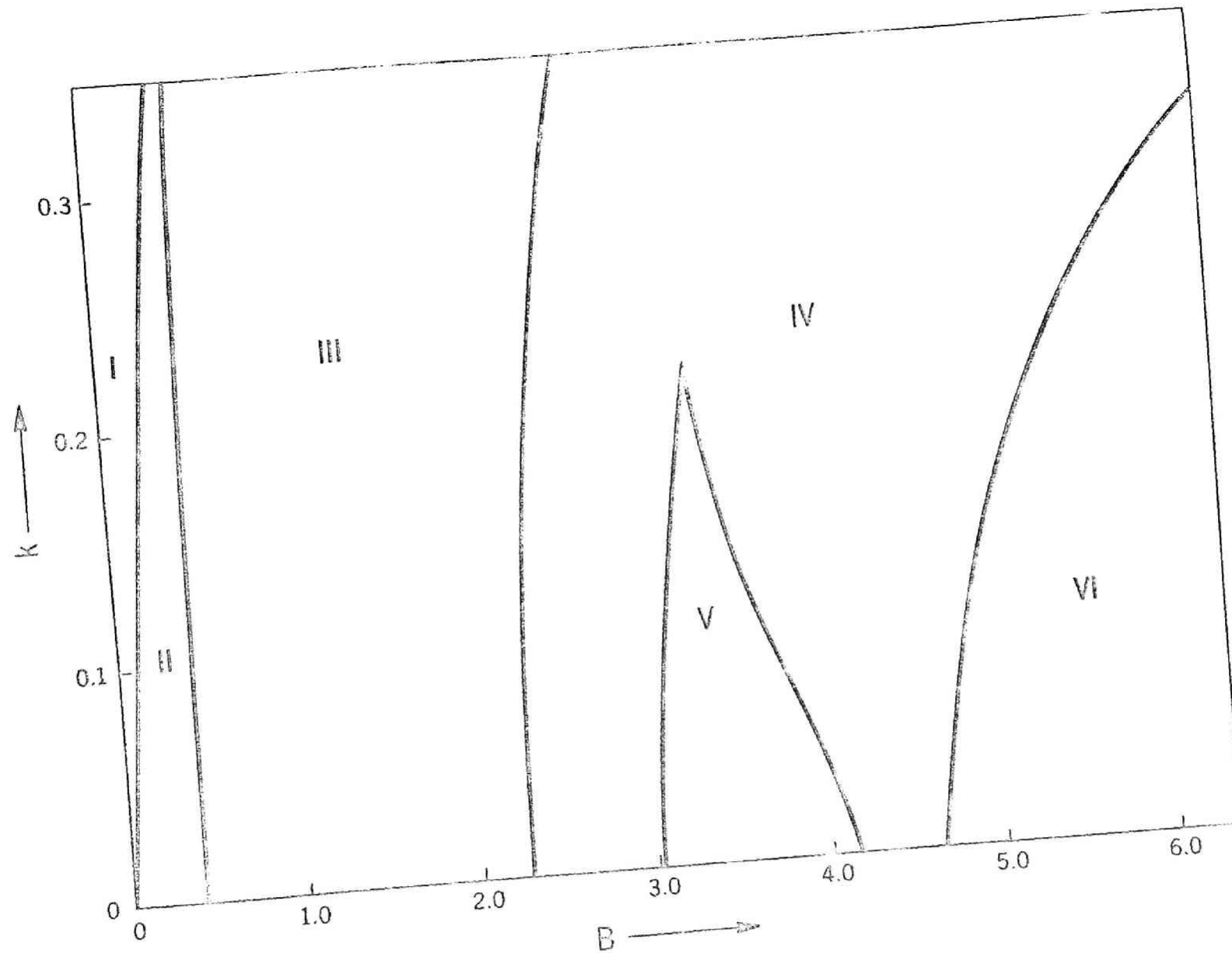


Fig. 3.2. Regions in which harmonic solutions of different types are obtained for Eqs. (3.3).

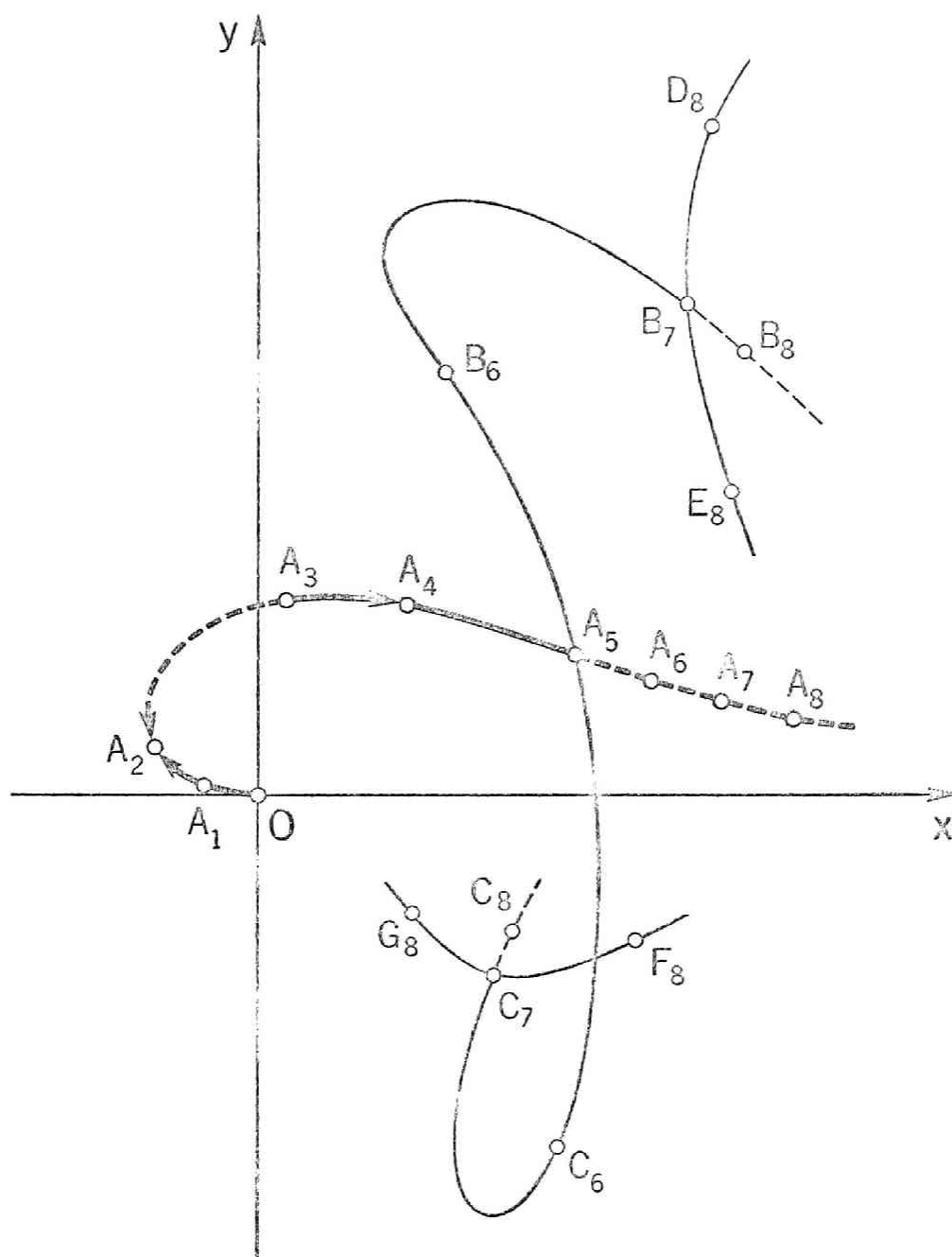


Fig. 3.3. Loci of fixed points under variation of the parameter B
(harmonic solutions).

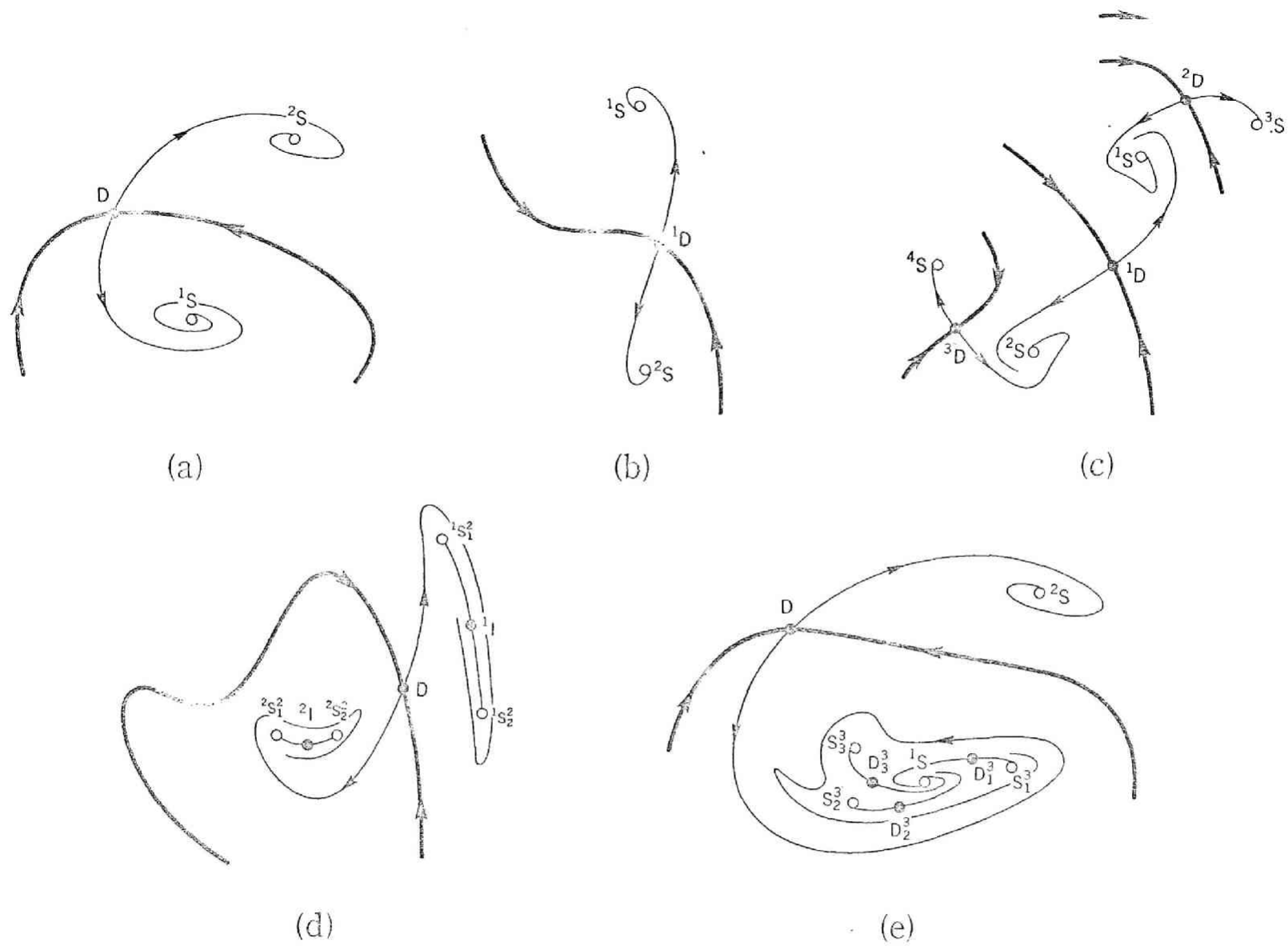


Fig. 3.4. Some representative patterns of phase portrait of Eqs. (3.3).

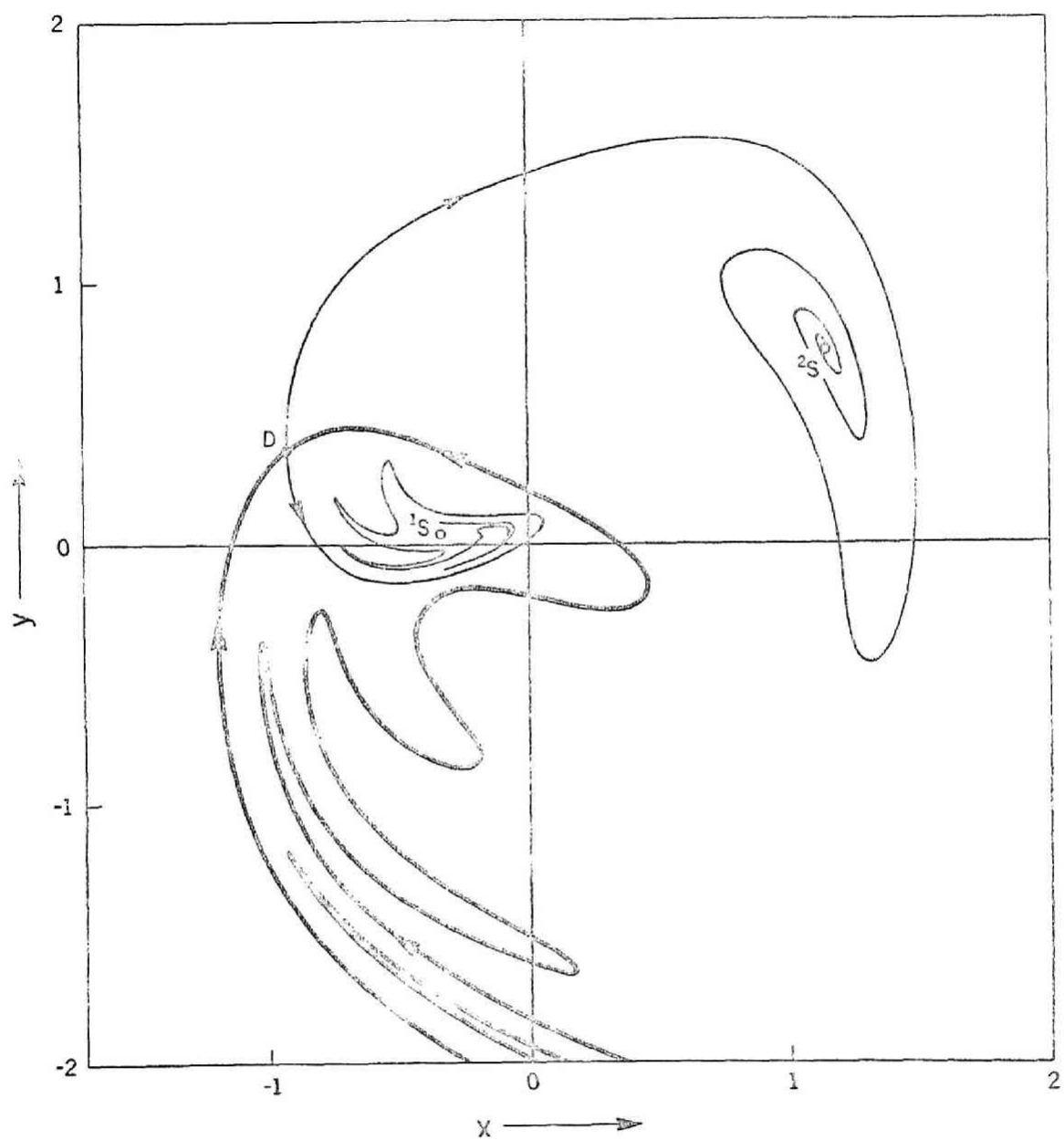


Fig. 3.5. Fixed points and invariant curves of the mapping for Eq. (3.6).

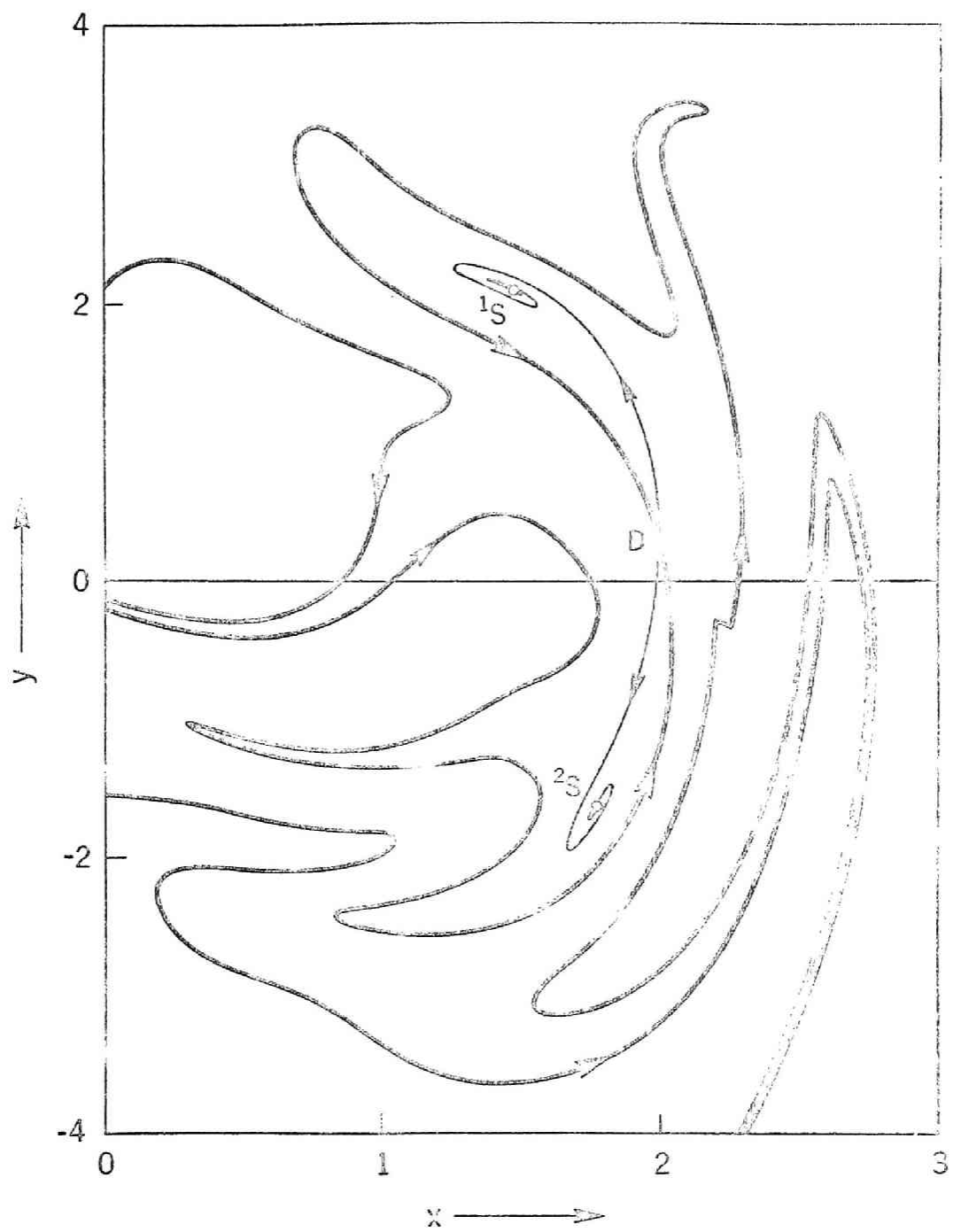
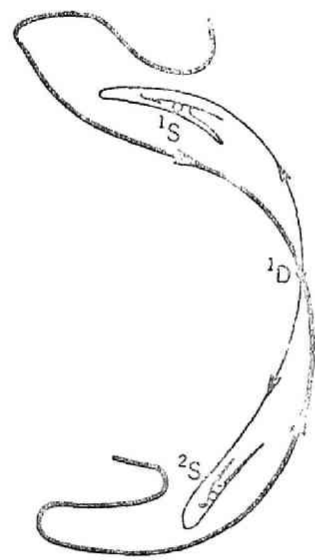
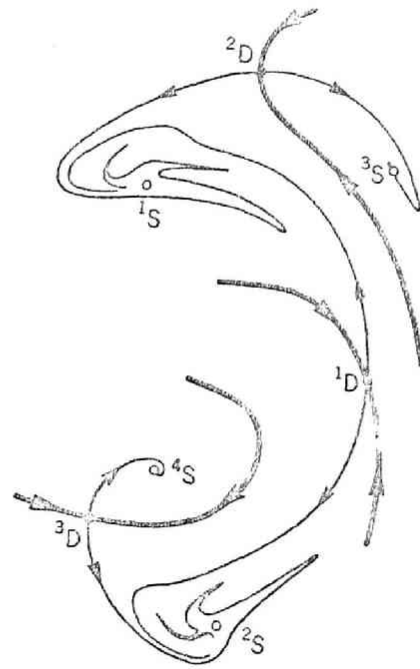


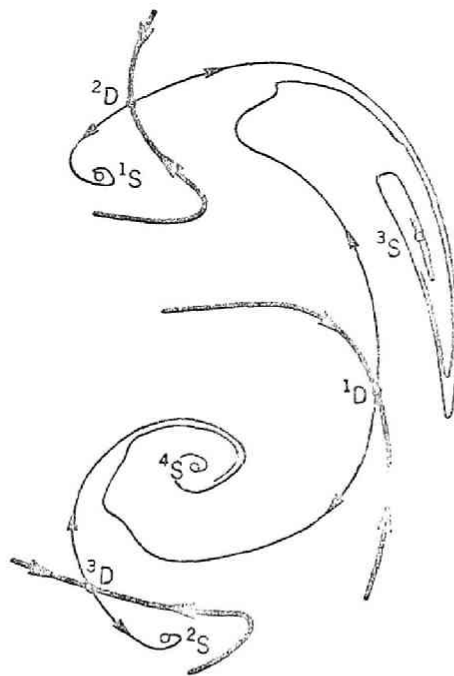
Fig. 3.6. Fixed points and invariant curves of the mapping for Eq. (3.7).



(a)



(b)



(c)



(d)

Fig. 3.7. Some representative patterns of phase portrait in the regions IV and V in Fig. 3.2.

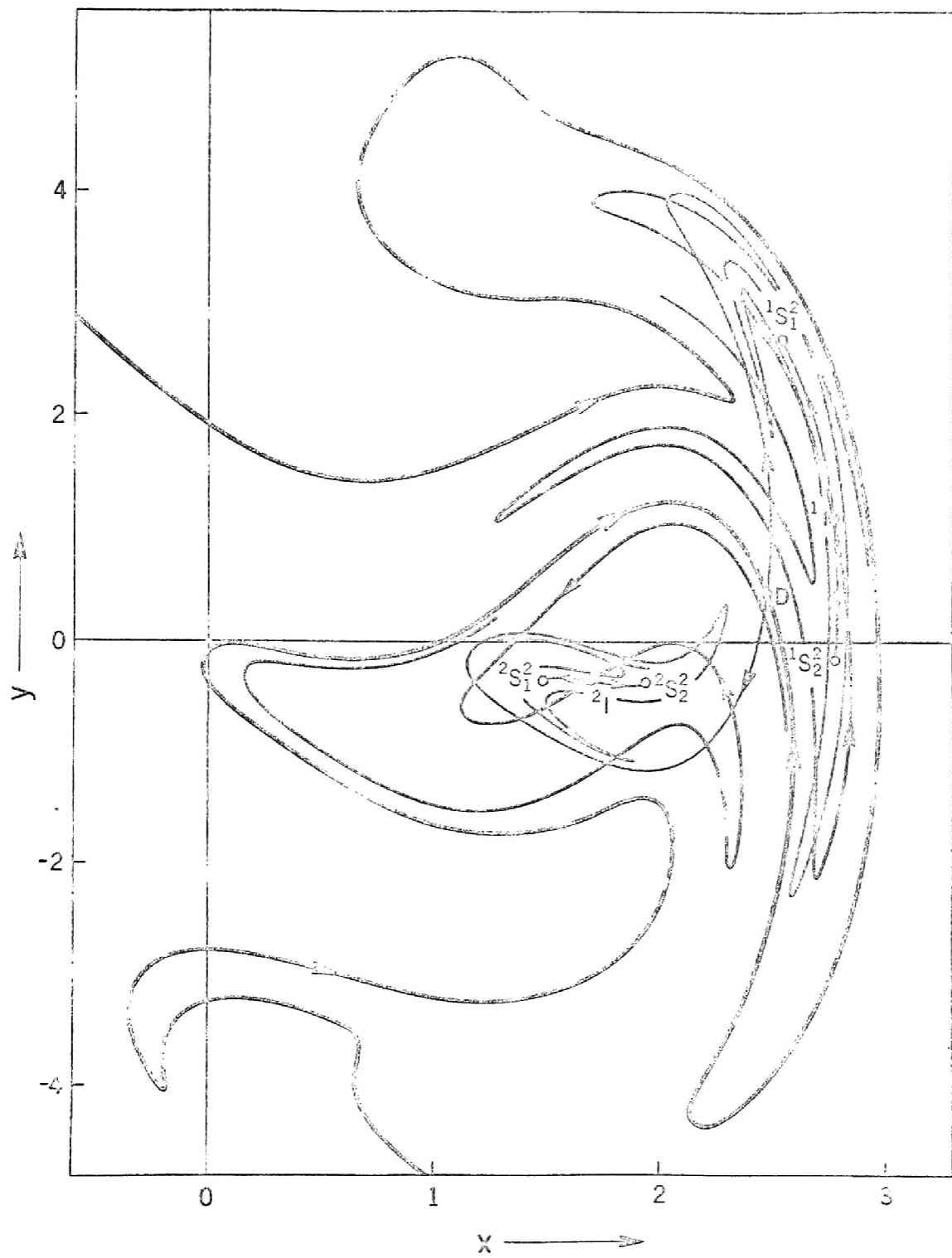


Fig. 3.8. Fixed and 2-periodic points and invariant curves of the mapping for Eq. (3.8).

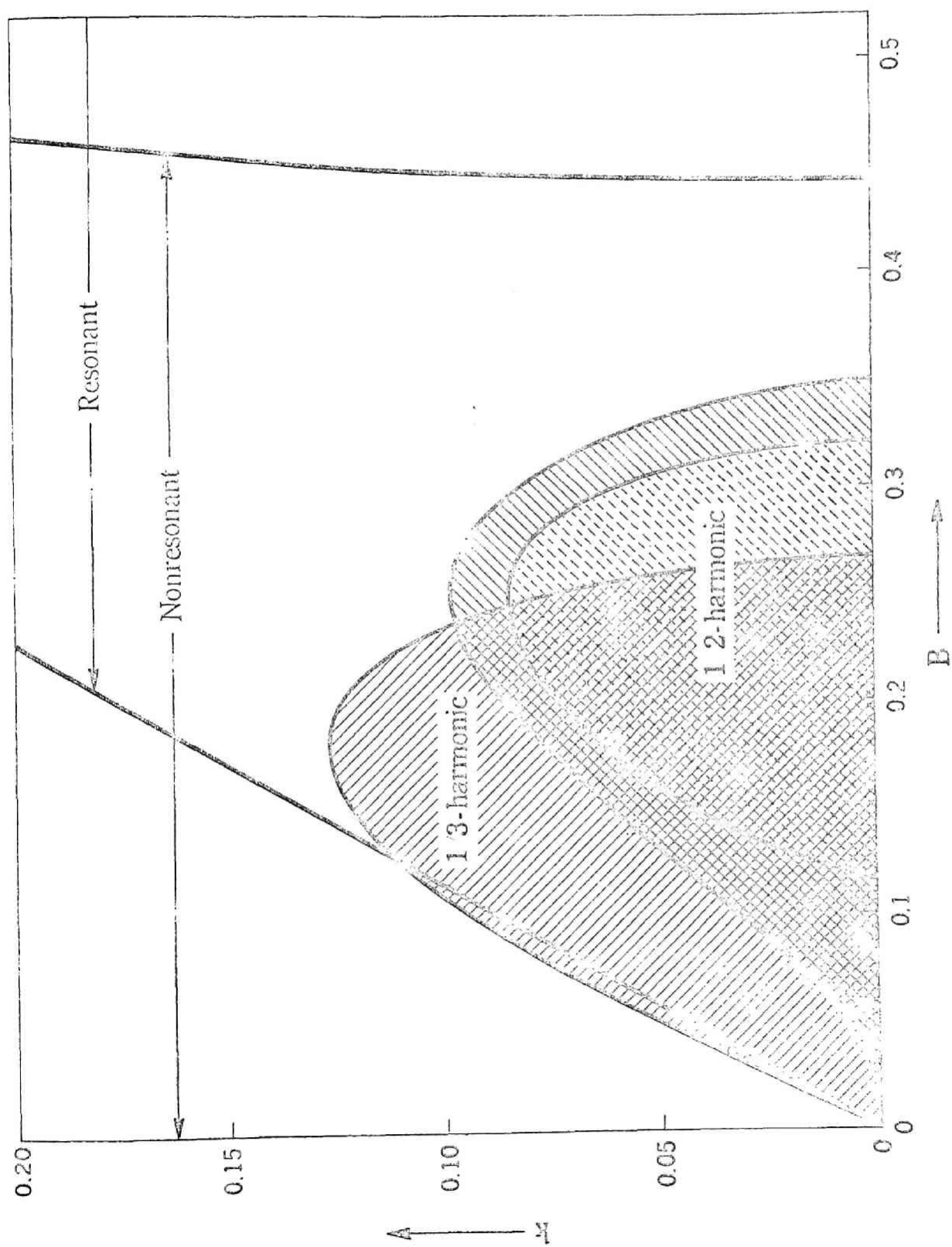


Fig. 3.9. Regions in which harmonic (resonant and nonresonant) and subharmonic solutions are obtained.

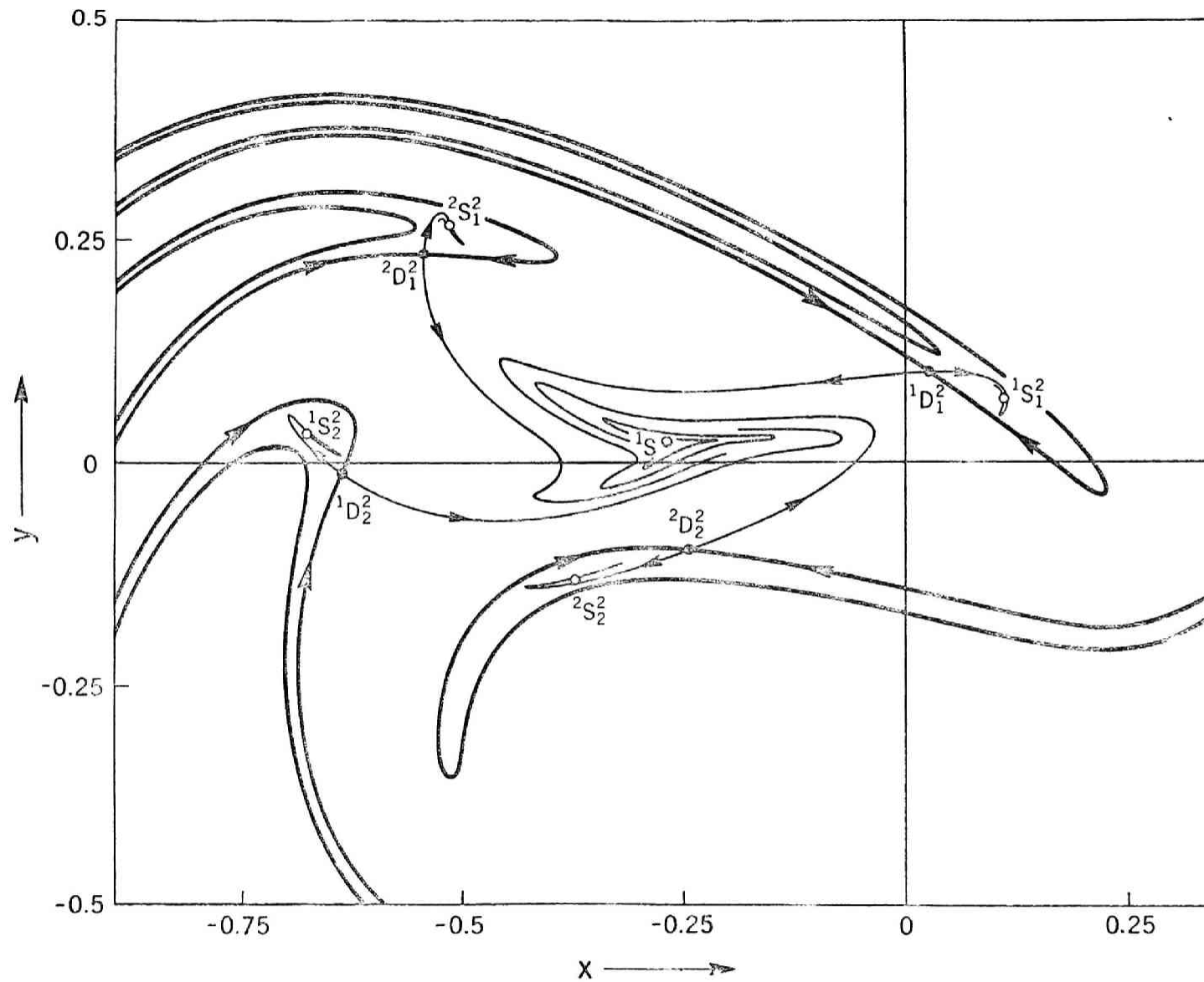


Fig. 3.10. 2-periodic points and invariant curves of the mapping for Eq. (3.9).

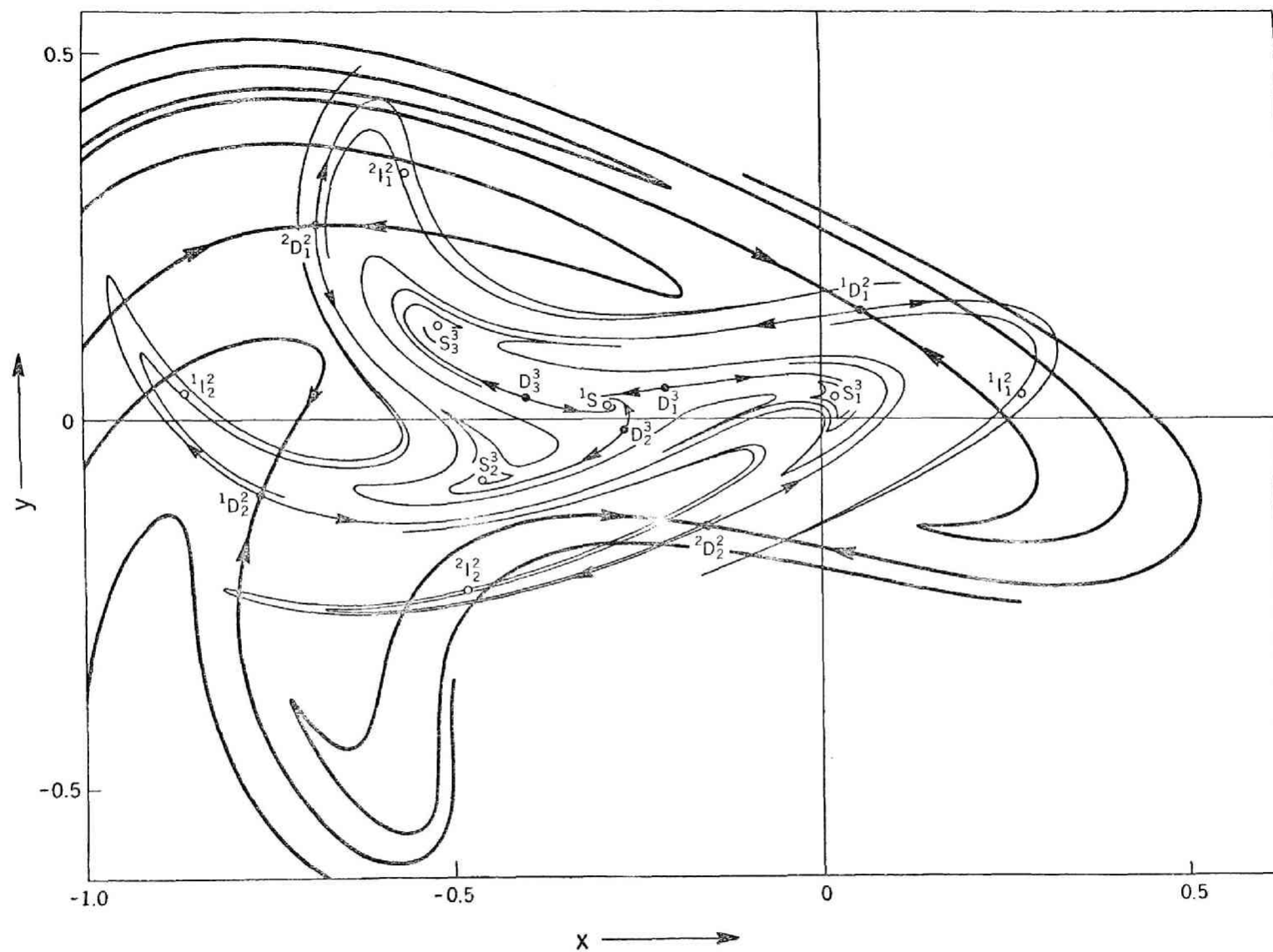


Fig. 3.11. 2- and 3-periodic points and invariant curves of the mapping
for Eqs. (3.3) with $k = 0.05$ and $B = 0.22$.

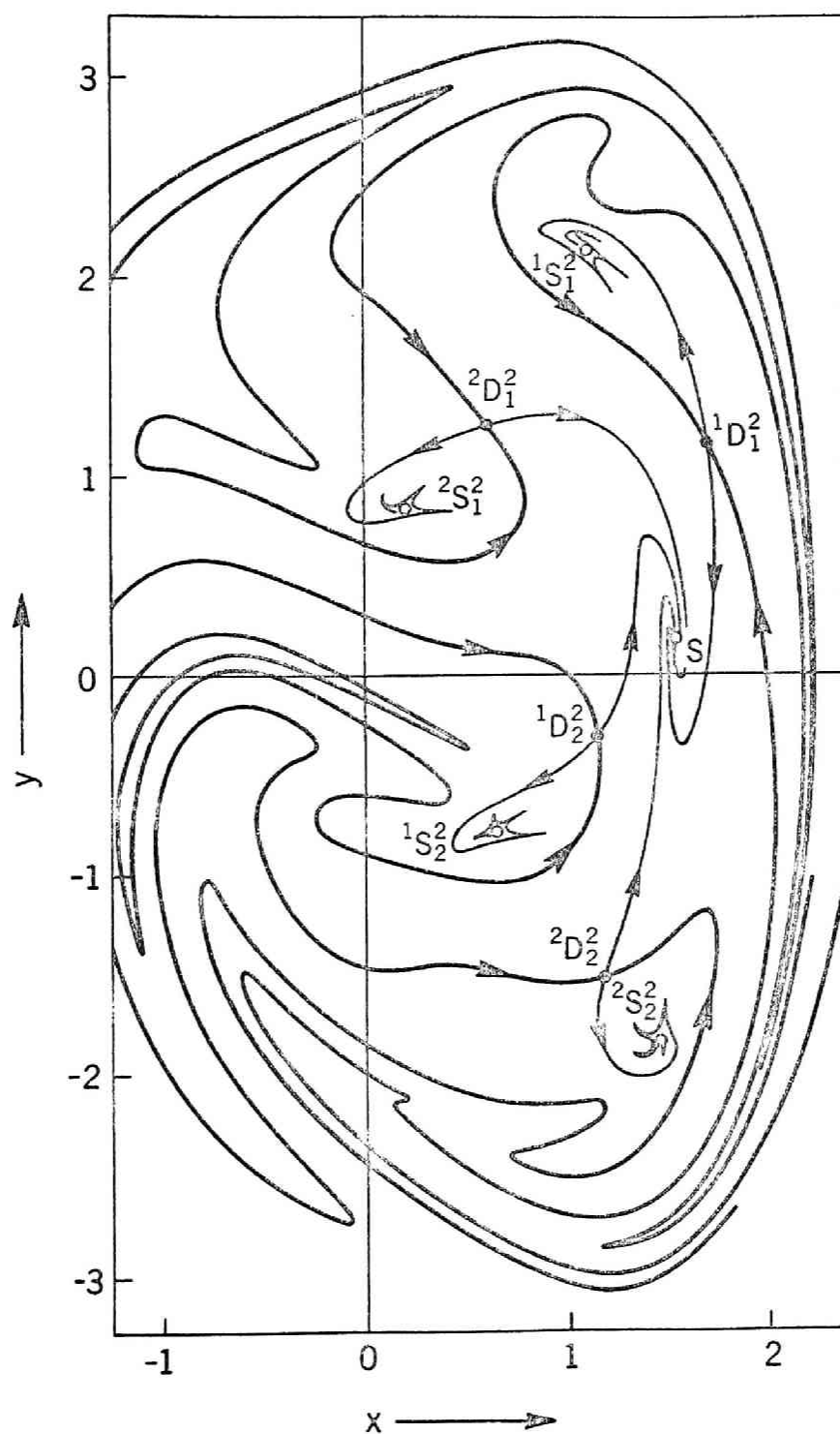


Fig. 3.12. 2-periodic points and invariant curves of the mapping for Eq. (3.10).

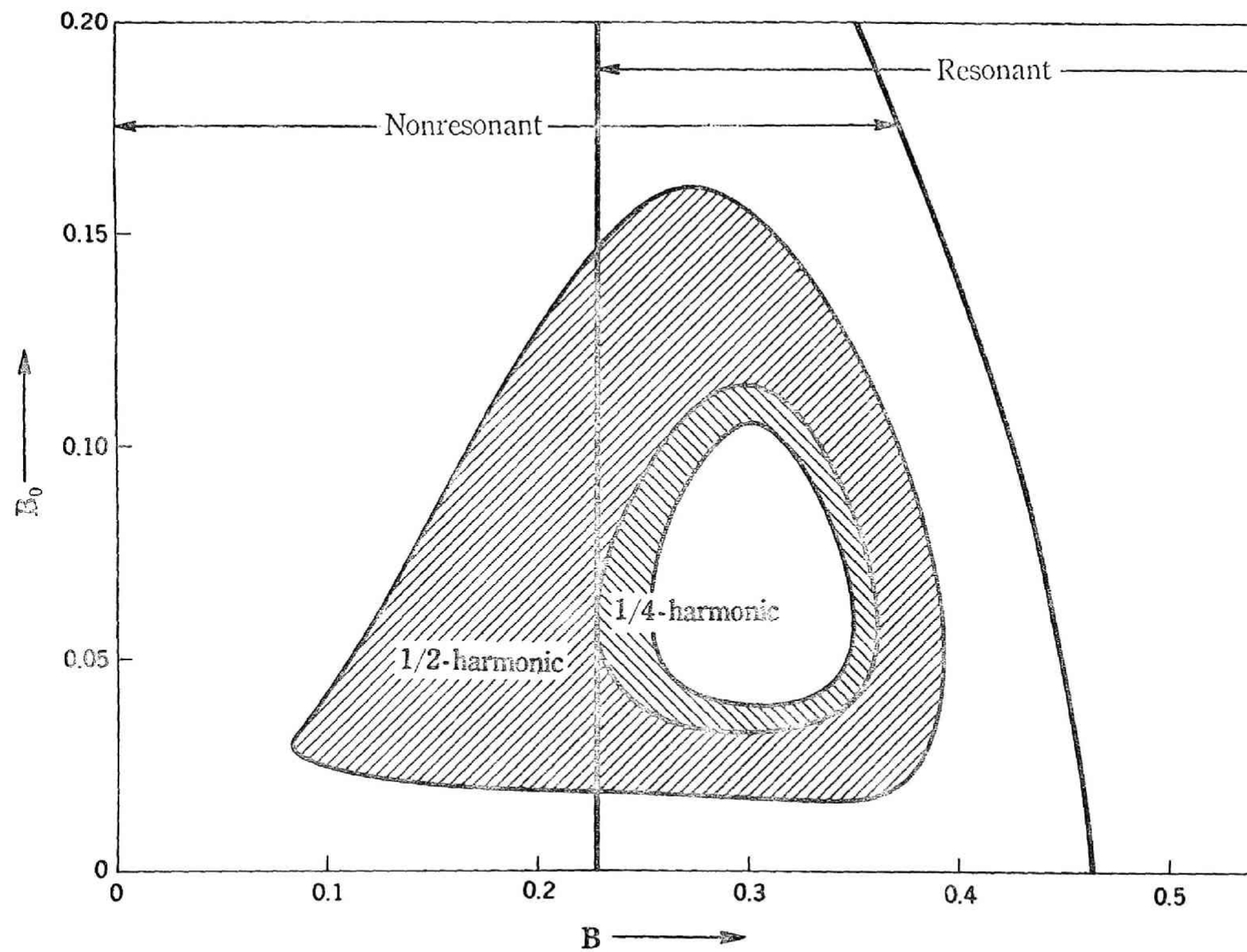
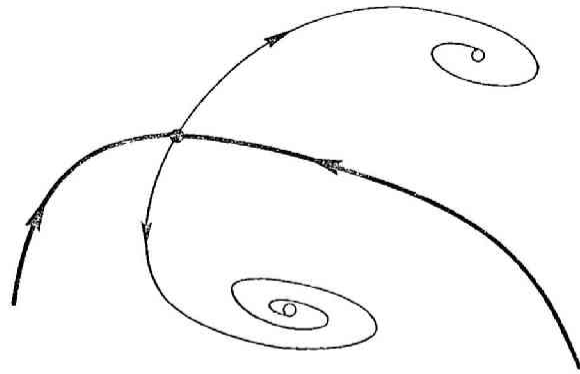
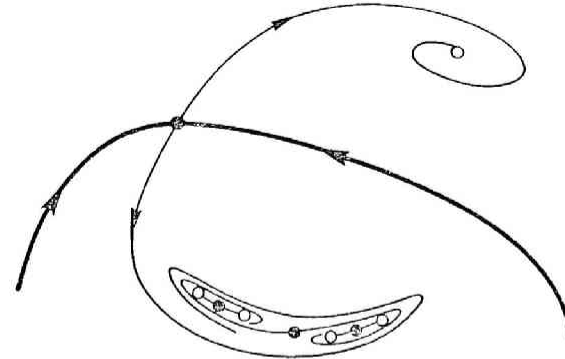


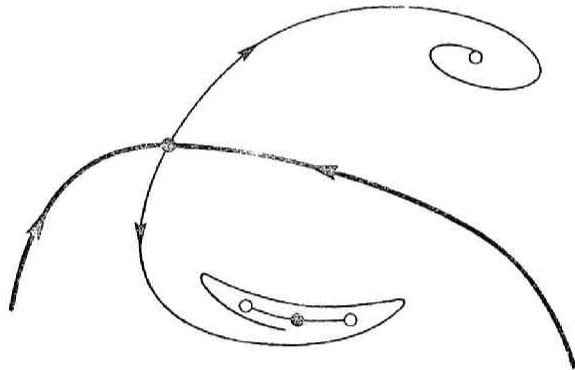
Fig. 3.13. Regions in which harmonic (resonant and nonresonant) and subharmonic solutions are obtained for the system (3.11).



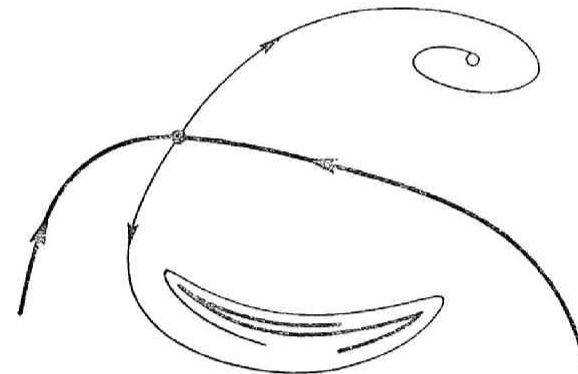
(a)



(c)



(b)



(d)

Fig. 3.14. Successive multiplication of fixed points under varying system parameters.

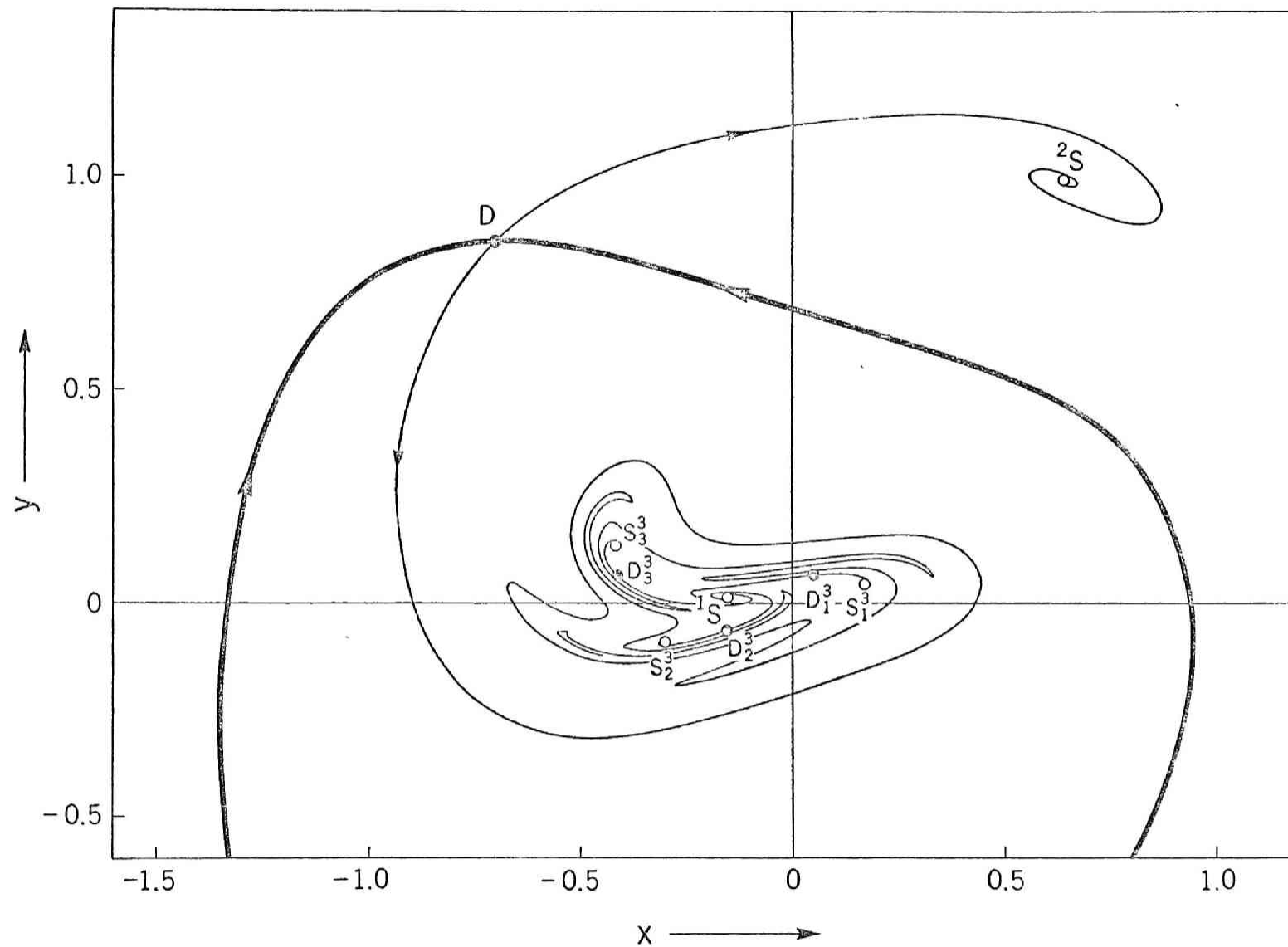


Fig. 3.15. Fixed and 3-periodic points and invariant curves of the mapping for Eq. (3.12).

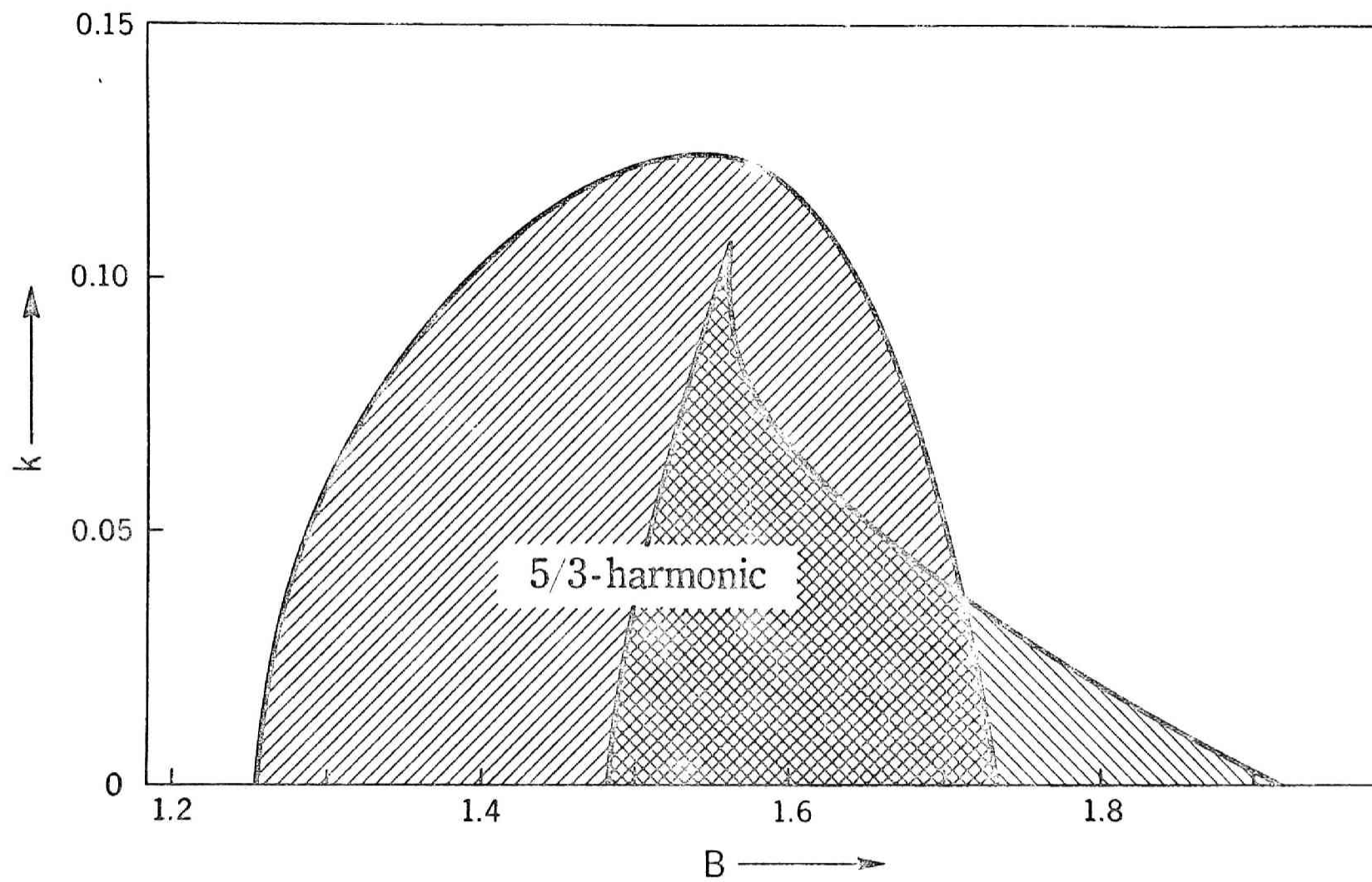


Fig. 3.16. Regions in which $5/3$ -harmonic solutions of different types are obtained.

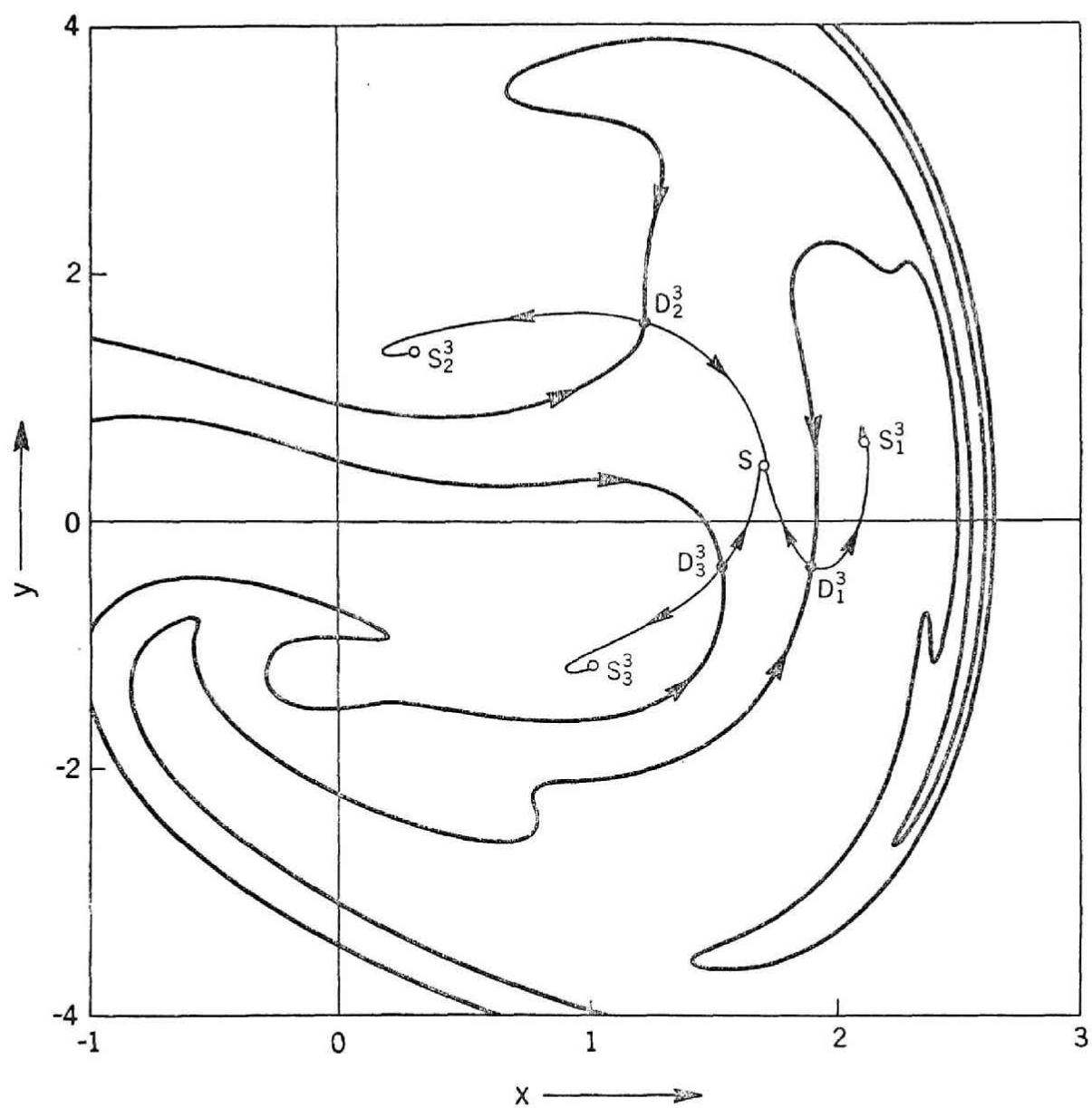


Fig. 3.17. 3-periodic points and invariant curves of the mapping for Eq. (3.13).

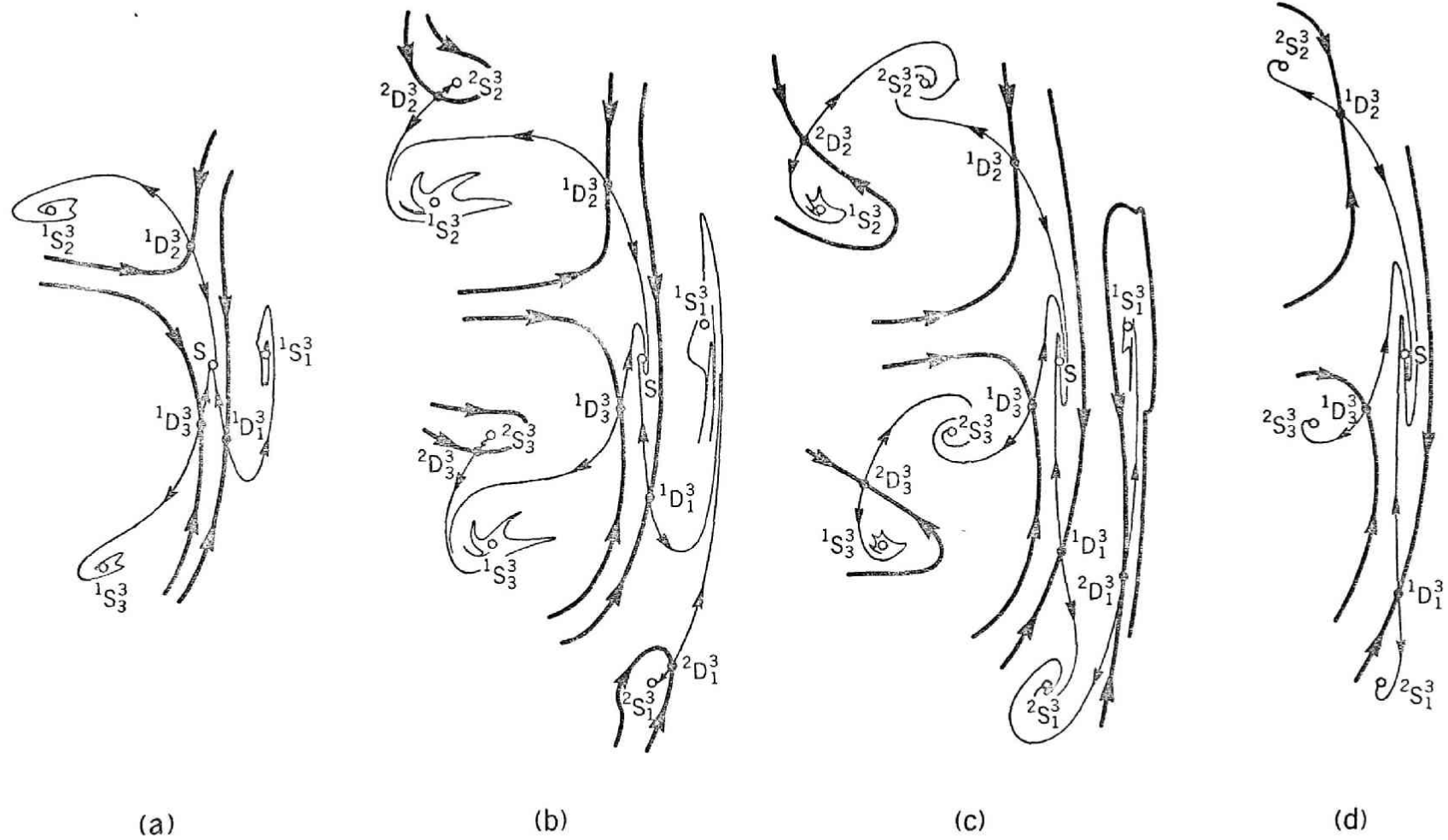


Fig. 3.18. Some representative patterns of phase portrait in the regions of Fig. 3.16.

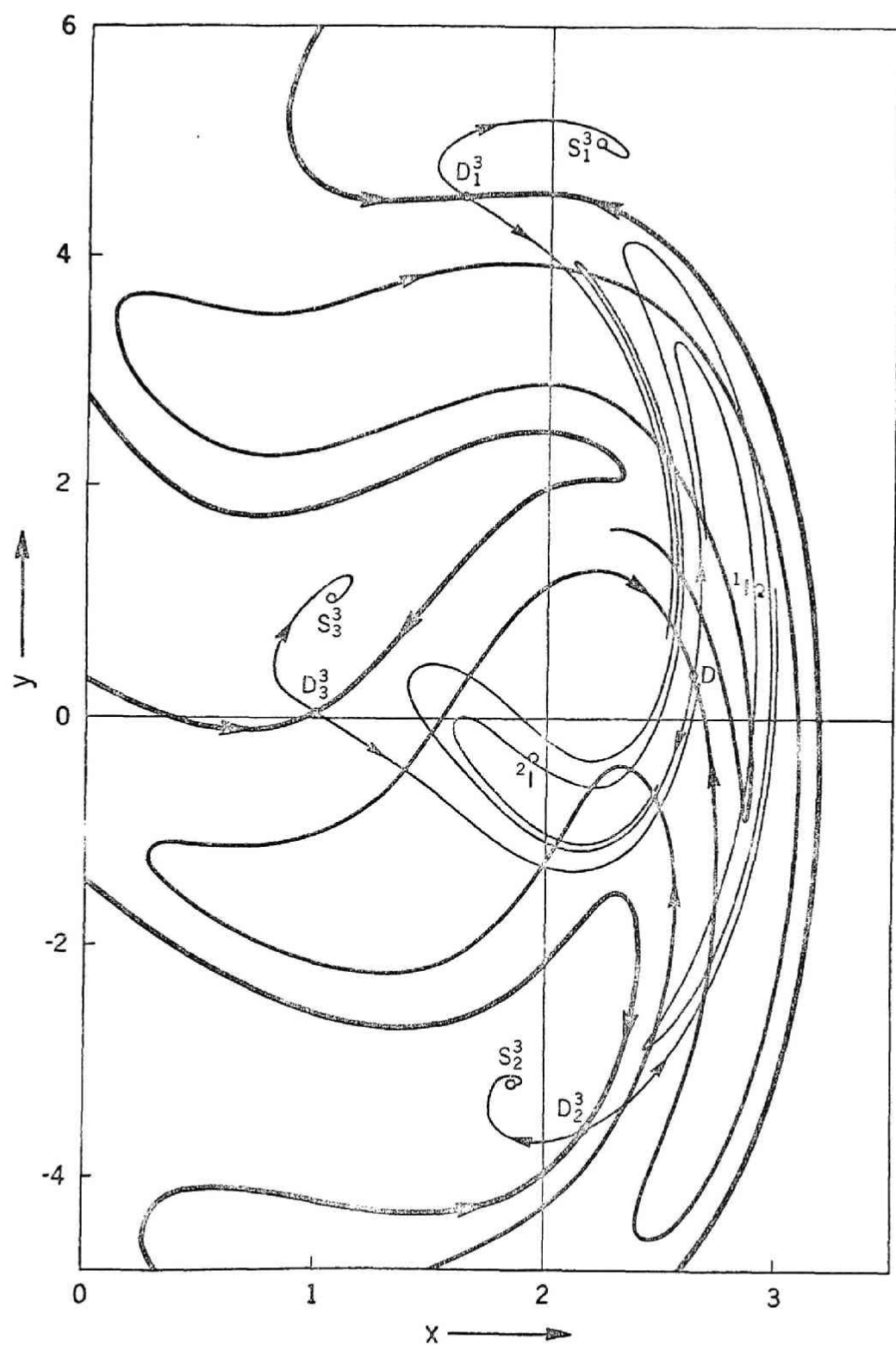


Fig. 3.19. Fixed and 3-periodic points and invariant curves of the mapping for Eq. (3.14).

CHAPTER 4

DOUBLY ASYMPTOTIC SOLUTIONS AND THEIR RELATED PROPERTIES

4.1 Introduction

It is known that Duffing's equation without dissipative term possesses infinitely many periodic solutions with period equal to the integral multiples of that of the external forcing term. Some of these periodic solutions might be center stable types and others be directly or inversely unstable types. It is expected that the equation with a small dissipative term still possesses many periodic solutions. Especially, directly and inversely unstable periodic solutions remain for such small parameter variation because of their structural stability. In this situation it is interesting to investigate the behavior of invariant manifolds of the unstable periodic solutions.

The present chapter is concerned with the doubly asymptotic solutions and their related properties of Duffing's equation. As discussed in Chap. 1, a doubly asymptotic solution is defined by a solution whose trajectory is the intersection of stable and unstable manifolds for some directly or inversely unstable periodic solutions. Therefore it is necessary to investigate the nature of invariant curves of directly or inversely unstable fixed or periodic points under the Poincaré mapping. Mathematically, the investigation of the behavior of invariant curves faces two unavoidable problems: the finding of directly or inversely unstable fixed or periodic points and the determination of invariant curves (ω - and α -branches). Nevertheless, it is very important to consider these problems for the study of transient responses in nonlinear physical systems. As we have already seen in the previous chapters, although these problems are quite difficult, the numerical analysis with the Poincaré

mapping is comparatively simple. Throughout this chapter we shall consider the Poincaré mapping defined by Duffing's equation studied in Chap. 3.

In Sec. 4.2 homoclinic points correlated with a directly unstable fixed point and its related properties are discussed. In Sec. 4.3 homoclinic points correlated with directly unstable periodic points are investigated. Heteroclinic points are discussed in Sec. 4.4.

4.2 Homoclinic points correlated with a directly unstable fixed point

In this section we consider the appearance of homoclinic points and the patterns of phase portrait obtained by the Poincaré mapping defined by Duffing's equation

$$\begin{aligned}\frac{dx}{dt} &= y \\ \frac{dy}{dt} &= -ky - x^3 + B \cos t\end{aligned}\tag{3.3}$$

The investigation is mainly done in the region II of Bk plane in Fig. 3.2, i.e., the region in which three fixed points are obtained.

(a) Homoclinic points in nondissipative systems

Let us consider the Poincaré mapping T defined by the equations

$$\begin{aligned}\frac{dx}{dt} &= y \\ \frac{dy}{dt} &= -x^3 + B \cos t\end{aligned}\tag{4.1}$$

The mapping T is area-preserving and the phase portrait obtained by T is symmetrical with respect to x-axis in the xy plane. As stated in Chap. 3, for $0 < B < 0.44$ (this value is obtained by numerical analysis, see Fig. 3.2 or 3.9), Eqs. (4.1) has at least three fixed points one of which is directly unstable.

Thus for the directly unstable fixed point, nine possible patterns of invariant curves illustrated in Fig. 4.1 may be considered. But actual behavior obtained by analog computations is as follows: For the parameter B small, $0 < B < 0.06$, the pattern of invariant curves (a) in Fig. 4.1 is observed. For $0.06 < B < 0.44$, the pattern (d) is obtained. In fact, it is very difficult to determine the critical value $B = 0.06$ by numerical analysis. Therefore we can only say that the behavior of invariant curves has changed at about $B = 0.06$ if one were to view the solutions of Eqs. (4.1) as output of some electronic circuit.

As representative examples of two cases stated above, we consider first the equation

$$\frac{d^2x}{dt^2} + x^3 = 0.04 \cos t \quad (4.2)$$

Figure 4.2 (a) shows schematically the location of three fixed points and a pair of invariant curves which emanate from and converge to the directly unstable points D . Closed curve surrounding the point 2S is invariant under T . Many such curves are observed in the neighborhood of 2S . These curves may correspond to the almost periodic points of T . On the contrary, around the fixed point 1S , the situation is considerably different. This is shown in Fig. 4.3. In this figure the periodic points around 1S are, from the inside toward the outside, 7-, 5-, 4-, 3-, 2-, 3-, ... periodic points; for notational conventions see Sec. 1.3 in Chap. 1. Invariant curves emanating from and converging to, i.e., α - and ω -branches, of directly unstable points are observed to be closed. Thus every point on the closed curves is doubly asymptotic point of special type. In the neighborhood of these curves many invariant closed curves corresponding to the almost periodic points are also observed though they are not shown in the figure, [13].

For the second example, we consider the equation

$$\frac{d^2x}{dt^2} + x^3 = 0.3 \cos t \quad (4.3)$$

Figure 4.2 (b) shows schematically the location of three fixed points and a pair of invariant curves with respect to the point D. In this example, transversal homoclinic points appear. In the small neighborhood of 1S or 2S closed invariant curves are observed. On the contrary, in the neighborhood of invariant curves with respect to D, the situation is extremely complex. Figure 4.4 shows the phase portrait of interior part in Fig. 4.2 (b). The α - and ω -branches which issue from D intersect repeatedly giving rise to transversal homoclinic points. Beside the fixed points D and 1S of the mapping T, there are infinitely many periodic points. To avoid the complexity of illustration, however, only periodic points of the order 2 and 3 are shown in Fig. 4.4, i.e.,

$$\text{2-periodic points: } ^1D_i^2, ^2D_i^2, ^1I_i^2, ^2I_i^2 \quad (i = 1, 2)$$

$$\text{3-periodic points: } ^1D_i^3, ^2D_i^3, ^1I_i^3, ^2I_i^3 \quad (i = 1, 2, 3)$$

When compared with Fig. 4.3, one sees that the center stable periodic points change into inversely unstable periodic points. For instance, $^jS_i^2$ of Fig. 4.3 changes into $^jI_i^2$ in Fig. 4.4. In this case, successive multiplication of the periodic points, i.e., SI-branching occurs; thus, though not shown in the figure, each $^jI_i^2$ produces a pair of periodic points of the order 4, and so on. The invariant curves of the mapping T^2 issuing from the directly unstable 2-periodic points are also drawn in Fig. 4.4. These curves intersect one another and also with the invariant curves of the mapping T. Thus we can locate infinitely many homoclinic and heteroclinic points in the figure. To see the successive images of a point in the neighborhood of a homoclinic point, let us

consider a homoclinic cycle $H\omega_1 D\alpha_1 H$ illustrated in Fig. 4.5 (a). A point 0 in the neighborhood of the homoclinic point H is successively mapped to points 1, 2, In this particular example the point 0 is illustrated as \hat{a}_{8n} -periodic point. Now we consider a point in the neighborhood of heteroclinic points. Figure 4.5 (b) shows the invariant curves with respect to D , ${}^2D_1^2$ and ${}^2D_2^2$, where the invariant curves for ${}^2D_i^2$ ($i = 1, 2$) are illustrated by fine lines. As an example, let consider heteroclinic points K_1, K_2 and a cycle $K_1\omega_1(D)D\alpha_1(D)K_2\omega_1({}^2D_1^2){}^2D_1^2\alpha_1({}^2D_1^2)K_1$ sketched in the figure. A point 0 in the neighborhood of K_1 is successively mapped to points 1, 2, In the figure the point 0 is illustrated as \hat{a}_{16} -periodic point.

In Fig. 4.4, considering an appropriate domain in the neighborhood of homoclinic points, we have so-called a horseshoe structure under the mapping T^3 .^{*} An example is sketched in Fig. 4.5 (c). In this figure if we start a horseshoe like domain Σ surrounded by arcs PQ, QR, RS and SP, we get the image $T^3(\Sigma)$ surrounded by arcs P_3Q_3, Q_3R_3, R_3S_3 and S_3P_3 , which intersects the domain Σ . Therefore, the 3-periodic points ${}^1I_3^3$ and ${}^1D_3^3$ are contained in this intersection.

We can observe the horseshoe structure more explicitly for the mapping T defined by the following equations:

$$\begin{aligned}\frac{dx}{dt} &= y \\ \frac{dy}{dt} &= -x^3 + 0.3 \cos t - 0.08\end{aligned}\tag{4.4}$$

The phase portrait for the mapping T is shown in Figs. 4.6 and 4.7. Some

* The definition of a horseshoe structure is found in Ref. [32].

representative fixed and periodic points under T are indicated in Fig. 4.7.

If we consider a rectangle domain PQRS illustrated in Fig. 4.8 (a), we get its image $P_1Q_1R_1S_1$ sketched in the same figure; where $P_1 = T(P)$, $Q_1 = T(Q)$, $R_1 = T(R)$ and $S_1 = T(S)$. Thus in this example, the Poincaré mapping T has a typical horseshoe structure. We can see two fixed points D and I in the domain PQRS. Considering the splitted domains $PP'S'S$ and $Q'QRR'$ partially sketched by broken lines in Fig. 4.8 (b), we see that $PP'S'S$ and $Q'QRR'$ contain fixed points D and I, respectively. This assertion is obtained by the index calculation of the domains. Moreover, 2- and 3-periodic points are observed and sketched in Fig. 4.7. As the total number of n -periodic points is 2^n , the number of n -periodic points with least period n , which is the sum of directly and inversely unstable n -periodic points with least period n , is easily calculated. Some of them are listed in Table 4.1. In this example, in addition to fixed and periodic points, there exists a minimal set which is homeomorphic to a Cantor set [33].

It is to be noted that for the symmetrical system (4.3) the center stable fixed point 1S cannot change into an inversely unstable fixed point, since it corresponds to a primary periodic solution. Thus, for symmetrical system, we cannot obtain the phase portrait which is topologically equivalent to that of Fig. 4.6.

(b) Homoclinic points in dissipative systems

We now consider the perturbed system of Eqs. (4.1), that is the Poincaré mapping T defined by Eqs. (3.3). It is expected that homoclinic points still exist for Eqs. (3.3) with the small dissipative constant k . The numerical result for the region in which homoclinic points are obtained is illustrated

Table 4.1. Number of fixed and periodic points in the domain PQRS for Eqs. (4.4)

Period (n)	1	2	3	4	5	6	7	8	9	10	11
Total number of n-periodic pts. (2^n)	2	4	8	16	32	64	128	256	512	1024	2048
Number of n-periodic pts. (least period n)	2	2	6	12	30	54	126	240	504	990	2046
Number of DU points	1	0	3×1	4×1	5×3	6×4	7×9	8×14	9×28	10×48	11×93
Number of IU points	1	2×1	3×1	4×2	5×3	6×5	7×9	8×16	9×28	10×51	11×93

in Fig. 4.9. For small B , $0 < B < 0.06$, it is observed that, when the dissipative constant is present, most of the periodic points of Fig. 4.3 vanish. An example of the phase portrait for $k = 0.02$ and $B = 0.04$ is shown in Fig. 4.10, where only the periodic points of order 3 are preserved. If the dissipative constant k is small enough, some of the periodic points of other order are retained.

On the other hand, for $0.06 < B < 0.44$, the homoclinic points are still observed when $k > 0$. This situation is schematically illustrated in Fig. 4.11. The system parameters in the respective cases are given by

- | | |
|-------------------------|--------------------------|
| (a) $k = 0, B = 0.3$ | (b) $k = 0.005, B = 0.3$ |
| (c) $k = 0.05, B = 0.3$ | (d) $k = 0.1, B = 0.3$ |

From these examples, we see some patterns of invariant curves stated in Sec. 1.7 (b). As a representative example, the phase portrait for Eqs. (3.3) with $k = 0.05$ and $B = 0.3$ is shown in Fig. 4.12. The behavior of invariant curves of the mapping T does not change very much from that of Fig. 4.4. As before, the intersections of these invariant curves give rise to infinitely many homoclinic and heteroclinic points.

4.3 Homoclinic points correlated with directly unstable 3-periodic points

In general, as an intersection of the invariant curves with respect to directly unstable n -periodic points, we can consider two kind of homoclinic point, that is, simple and non-simple ones stated in Sec. 1.6. We now briefly observe the appearance of simple and non-simple homoclinic points for 3-periodic points correlated with the $1/3$ -harmonic solutions discussed in Sec. 3.5 (a).

Figure 4.13 shows the regions in which 3-periodic, simple and non-simple

homoclinic points are obtained in the symmetrical system (3.3). Under the variation of the parameters k and B , the qualitative change of the invariant curves for T^3 occurs as illustrated in Fig. 4.14. The system parameters in the respective cases are given by

- | | |
|--------------------------|-------------------------|
| (a) $k = 0.1, B = 0.2$ | (b) $k = 0.05, B = 0.2$ |
| (c) $k = 0.035, B = 0.2$ | (d) $k = 0.02, B = 0.2$ |

From these examples, we see the appearance of simple and non-simple homoclinic points for 3-periodic points according to the gradual change of the parameter k . In the case (a) and (b), homoclinic point does not appear and only the deformation of invariant curves is observed. In the case (c), we see the appearance of simple homoclinic points, i.e., an $\alpha(D_i^3)$ intersects an $\omega(D_i^3)$ for $i = 1, 2, 3$. In the case (d), both simple and non-simple homoclinic points appear, i.e., in addition to the simple homoclinic points of the case (c), an $\alpha(D_i^3)$ intersects an $\omega(D_j^3)$ for $i, j = 1, 2, 3$.

It is to be noted that the examples stated above are considered only 3-periodic points, but in the cases (b), (c) and (d) Eqs. (3.3) has 2-periodic points whose locations and invariant curves are situated in as surrounding the phase portraits illustrated in Fig. 4.14.

4.4 Heteroclinic points correlated with directly unstable fixed points

As we have seen in Sec. 3.3 (d), Eqs. (3.3) has three directly unstable fixed points in the parameter region V in Fig. 3.2, see also Fig. 3.7 for the phase portraits. Therefore, the equations may have heteroclinic points correlated with these fixed points in the region V . Actually, we can see the appearance of heteroclinic points for small k .

As representative examples, we consider first the equation

$$\frac{d^2x}{dt^2} + 0.03 \frac{dx}{dt} + x^3 = 3.2 \cos t \quad (4.5)$$

The phase portrait for this equation is shown in Fig. 4.15. From this figure, we see that an α -branch of 1D intersects an ω -branch of 2D (or 3D). Therefore, the point 2D (or 3D) is chained to 1D . But no other chain exists in this case. Hence the minimal sets for the mapping T are only seven fixed points in the figure, that is, only seven periodic solutions exist and all other solution tends to one of these periodic solutions as t goes to infinity. The appearance of heteroclinic points causes only the complexity of the shape of related invariant curves.

For the second example, we consider the equation

$$\frac{d^2x}{dt^2} + 0.03 \frac{dx}{dt} + x^3 = 3.4 \cos t \quad (4.6)$$

Figure 4.16 shows the phase portrait for this equation. In this case the transversal intersections appear between an ω -branch of 1D and an α -branch of 2D (or 3D). Therefore, 1D is chained to 2D (or 3D). All other properties are similar to that of the first example.

The third example is given by the equation

$$\frac{d^2x}{dt^2} + 0.01 \frac{dx}{dt} + x^3 = 3.44 \cos t \quad (4.7)$$

Figure 4.17 shows schematically the location of seven fixed points and invariant curves with respect to three directly unstable fixed points. From this figure, we see that any two directly unstable fixed points have a cycle property. Therefore, as stated in Sec. 1.6, there appear homoclinic points correlated with

j_D ($j = 1, 2, 3$). Hence there exist infinitely many periodic points in this example. It is to be noted that, when compared with Fig. 3.7 (c), one sees that the completely stable fixed points 1S and 2S change into inversely unstable fixed points 1I and 2I , respectively. This is the case stated in the last part of Sec. 3.3 (d).

4.5 Heteroclinic points correlated with a fixed and 3-periodic points

In Sec. 4.2 (a), we have seen heteroclinic points correlated with a directly unstable fixed point and a directly unstable 2-periodic point, see Fig. 4.5 (b). In this section we shall investigate an example of the appearance of homoclinic and heteroclinic points for Eqs. (3.3) with a large parameter B . As we have seen in Sec. 3.5 (c), when B is largely increased, Eqs. (3.3) has 3-periodic points. Under the small dissipative constant k , the pattern of invariant curves for a directly unstable fixed and 3-periodic points may be much more complicated than that of the example stated in Sec. 3.5 (c).

As an example we consider the equation

$$\frac{d^2x}{dt^2} + 0.05 \frac{dx}{dt} + x^3 = 6.0 \cos t \quad (4.8)$$

Fixed points and 3-periodic points are the same that of Eq. (3.14), i.e., Eq. (4.8) has one directly unstable and two inversely unstable fixed points, and three completely stable and three directly unstable 3-periodic points. These fixed and periodic points and invariant curves with respect to the directly unstable points are illustrated in Fig. 4.18. From this figure, we see that invariant curves with respect to D have a horseshoe structure, and the points D and D_i^3 ($i = 1, 2, 3$) have a cycle property. Therefore, the properties

of the horseshoe structure discussed in Sec. 4.2 (a) are also applied to this case. Moreover, in addition to the appearance of heteroclinic points correlated with D and D_i^3 , homoclinic points correlated with D_i^3 ($i = 1, 2, 3$) appear.

An example of homoclinic and heteroclinic cycles is shown in Fig. 4.19. For the point D and a homoclinic point H , $H\omega_2(D)D\alpha_2(D)H$ forms a homoclinic cycle. A point a in the neighborhood of the point H is successively mapped to point b, c, d as illustrated in the figure, where the point a is indicated as a 4-periodic point. On the other hand, for the point D , D_1^3 , K_1 and K_2 , $K_1\omega_1(D_1^3)D_1^3\alpha_1(D_1^3)K_2\omega_2(D)D\alpha_1(D)K_1$ forms a heteroclinic cycle. A point 0 in the neighborhood of the point K_1 is successively mapped to points $1, 2, \dots$, where the point 0 is indicated as a 13-periodic point in the figure.

It is to be noted that although this example has many periodic points, only three 3-periodic points S_1^3 , S_2^3 and S_3^3 are observed as completely stable points. Therefore, every solution tends to the periodic solutions correlated with these three completely stable points as t goes to infinity.

4.6 Supplementary remarks

Some examples of doubly asymptotic points and related properties are investigated for Duffing's equation. At the early stage of our study on this equation, the appearance of doubly asymptotic points, especially homoclinic points, was not expected, because our investigation had mainly been done for relatively large dissipative constants. At the present time, however, the existence of doubly asymptotic points seems to be very natural when the dissipative constant is sufficiently small. If we consider Duffing's equation without a dissipative term, then the equation becomes a nonautonomous Hamiltonian system. Therefore, the phase portrait obtained by the Poincaré mapping,

which is defined by the Hamiltonian system, must have very complex structure. Our investigation in Sec. 4.2 is only a part of this phase portrait. There may be expected the existence of many other periodic points and non-periodic points. Hence Duffing's equation with a sufficiently small dissipative constant may have many periodic solutions and homoclinic and heteroclinic solutions.

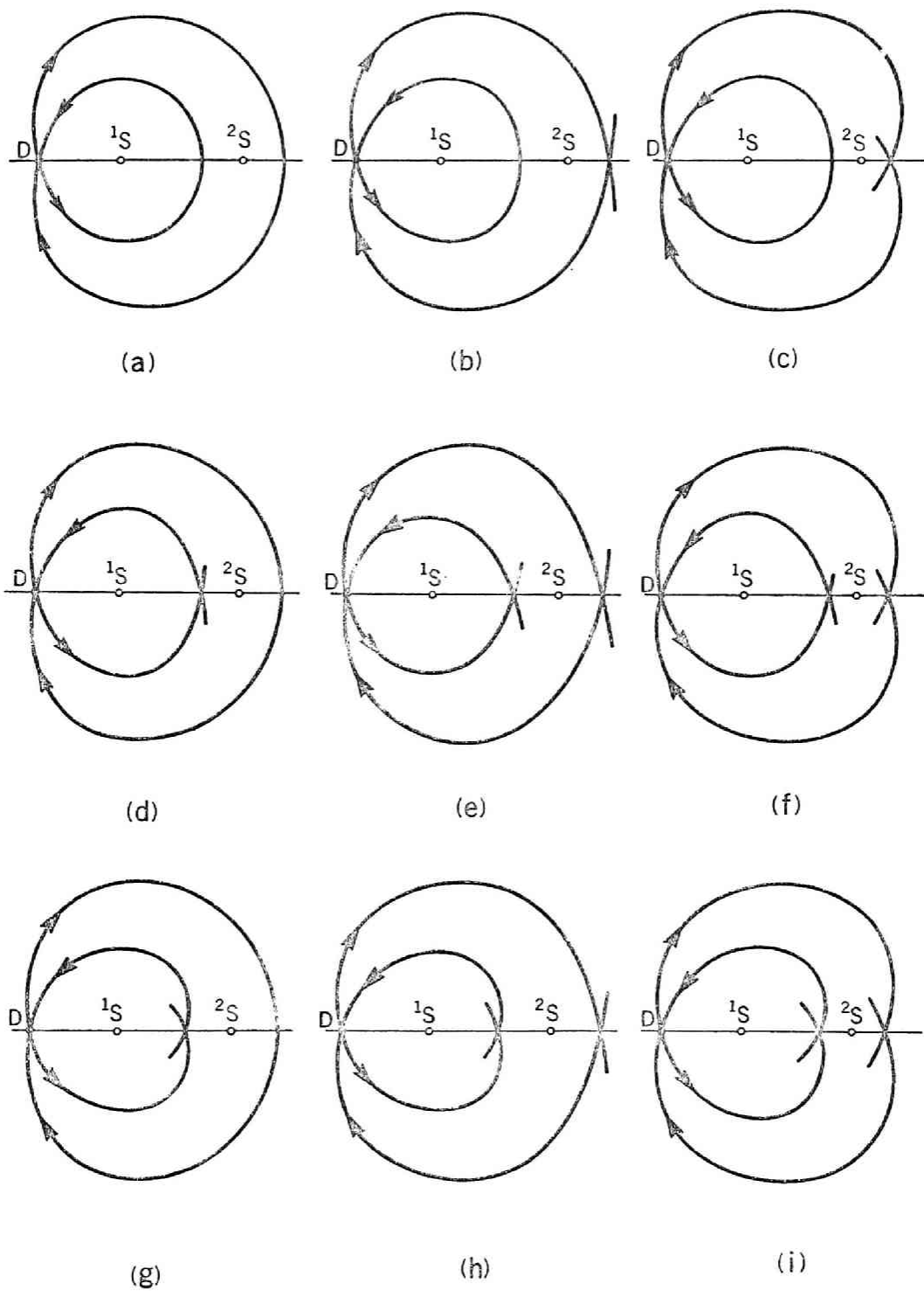
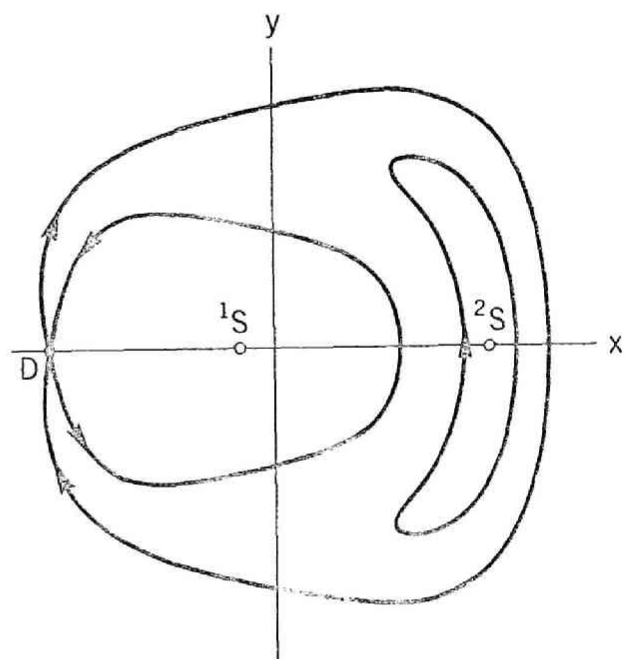
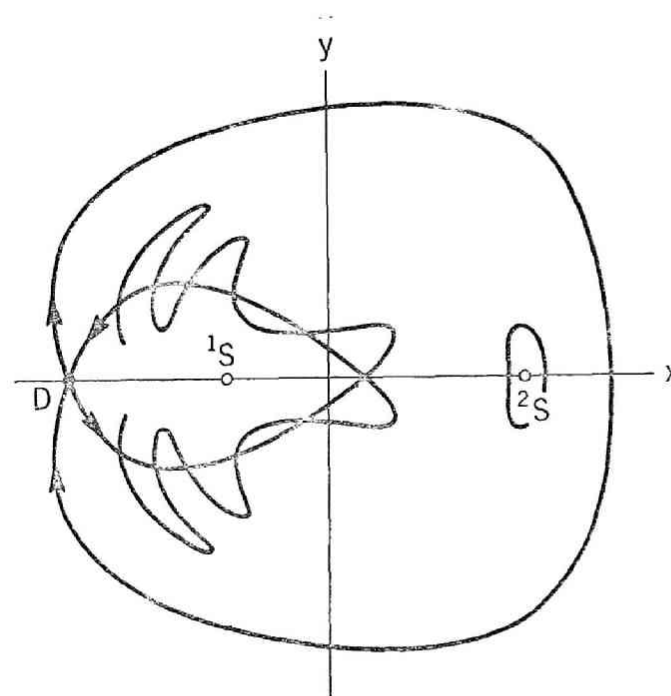


Fig. 4.1. Patterns of invariant curves for Eqs. (4.1).



(a)



(b)

Fig. 4.2. Patterns of the phase portrait for Eqs. (4.1).

(a) $B = 0.04$. (b) $B = 0.3$.

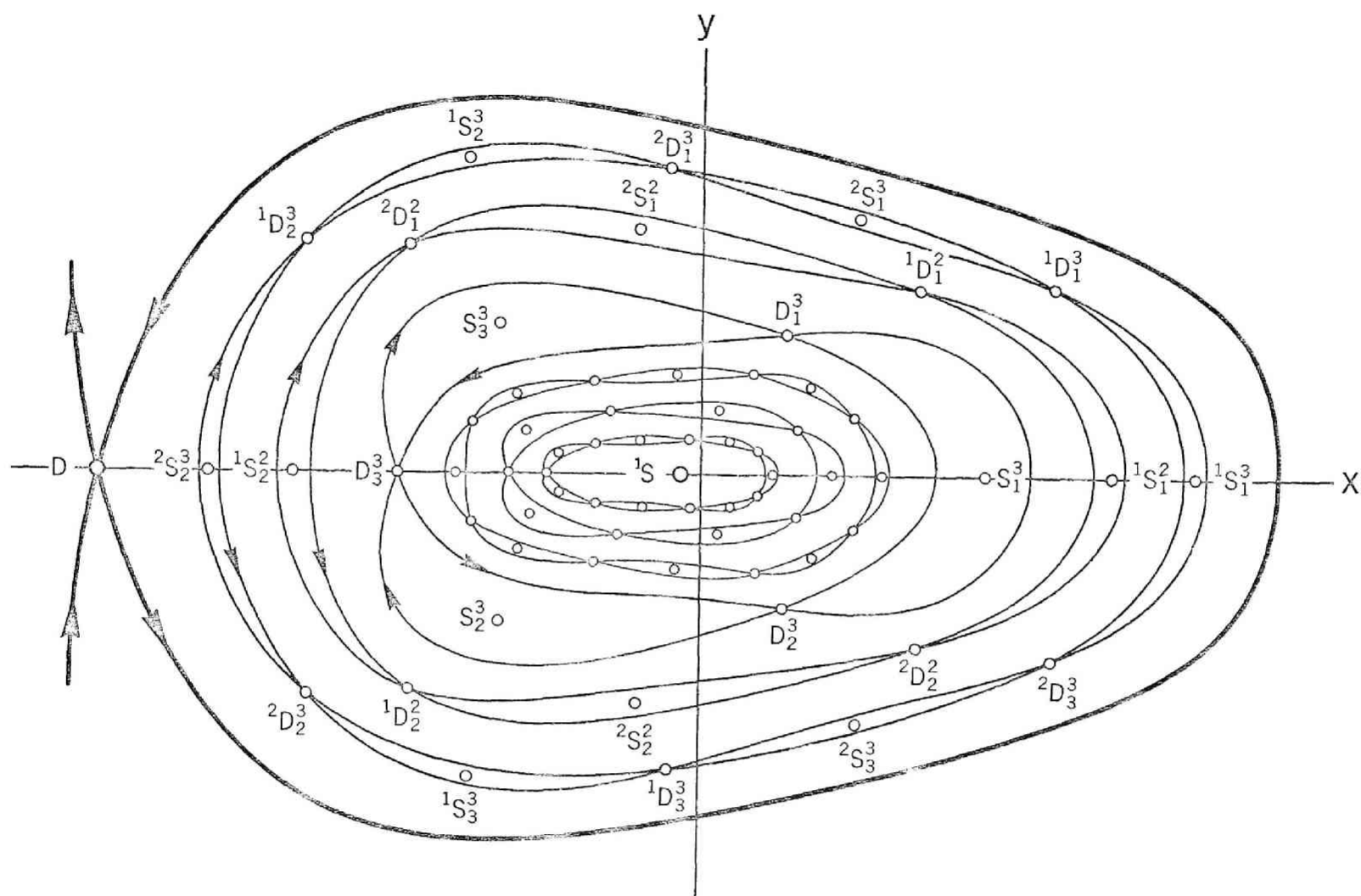


Fig. 4.3. Fixed and periodic points and invariant curves of the mapping for Eq. (4.2).

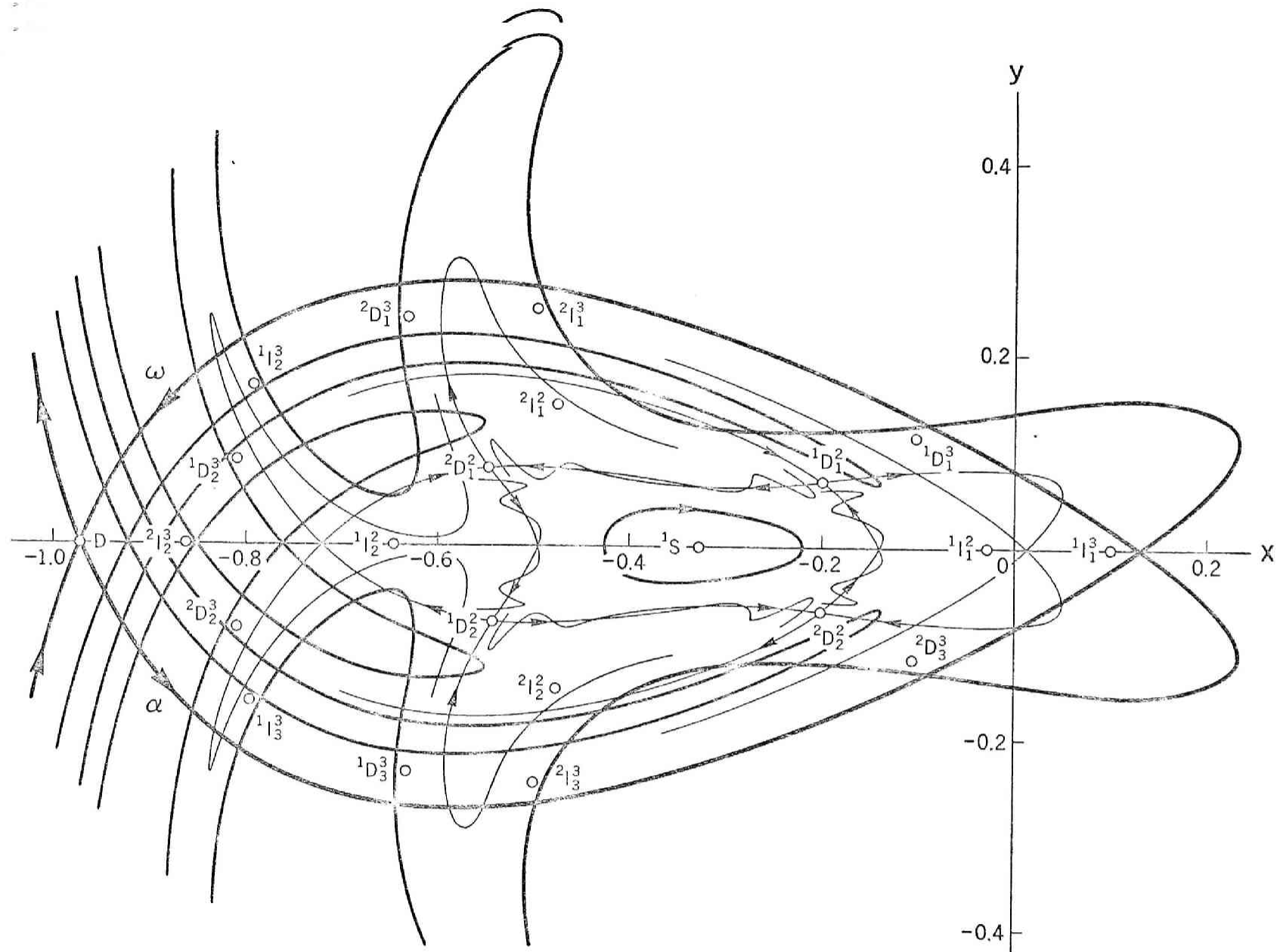
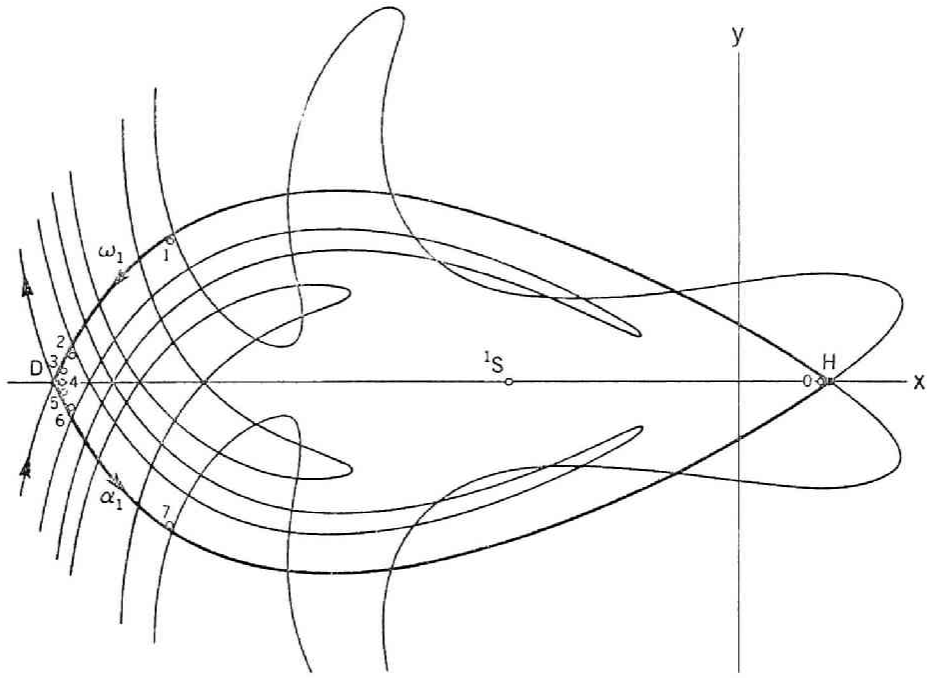
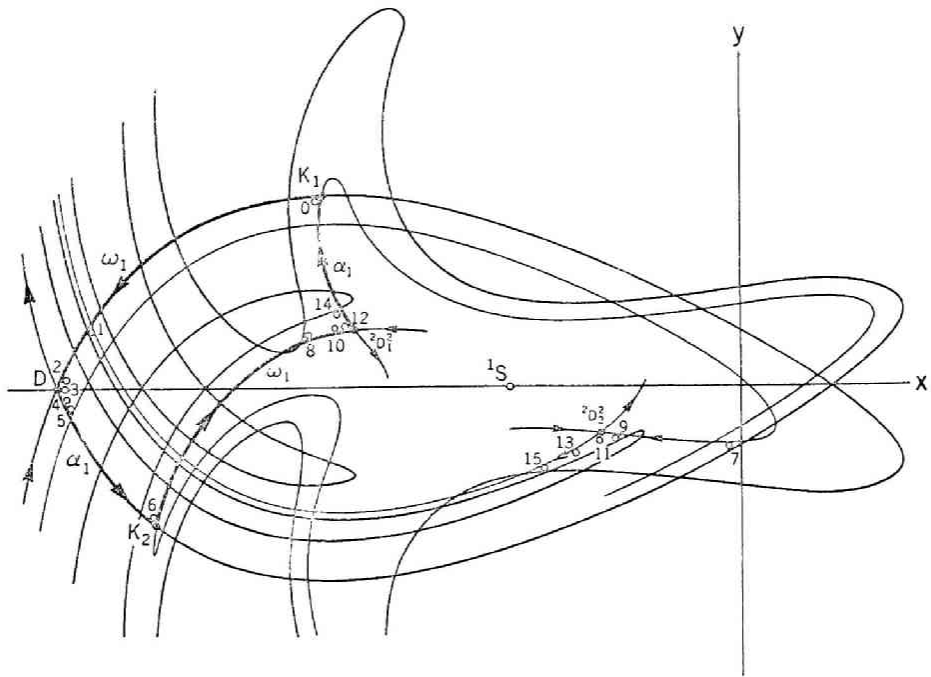


Fig. 4.4. Fixed and periodic points and invariant curves of the mapping for Eq. (4.3).



(a) A homoclinic cycle: $H\omega_1(D)D\alpha_1(D)H$.



(b) A heteroclinic cycle: $K_1\omega_1(D)D\alpha_1(D)K\omega_1({}^2D_1^2){}^2D_1\alpha_1({}^2D_1^2)K_1$.

Fig. 4.5. Examples of homoclinic and heteroclinic cycles of the mapping for Eq. (4.3).

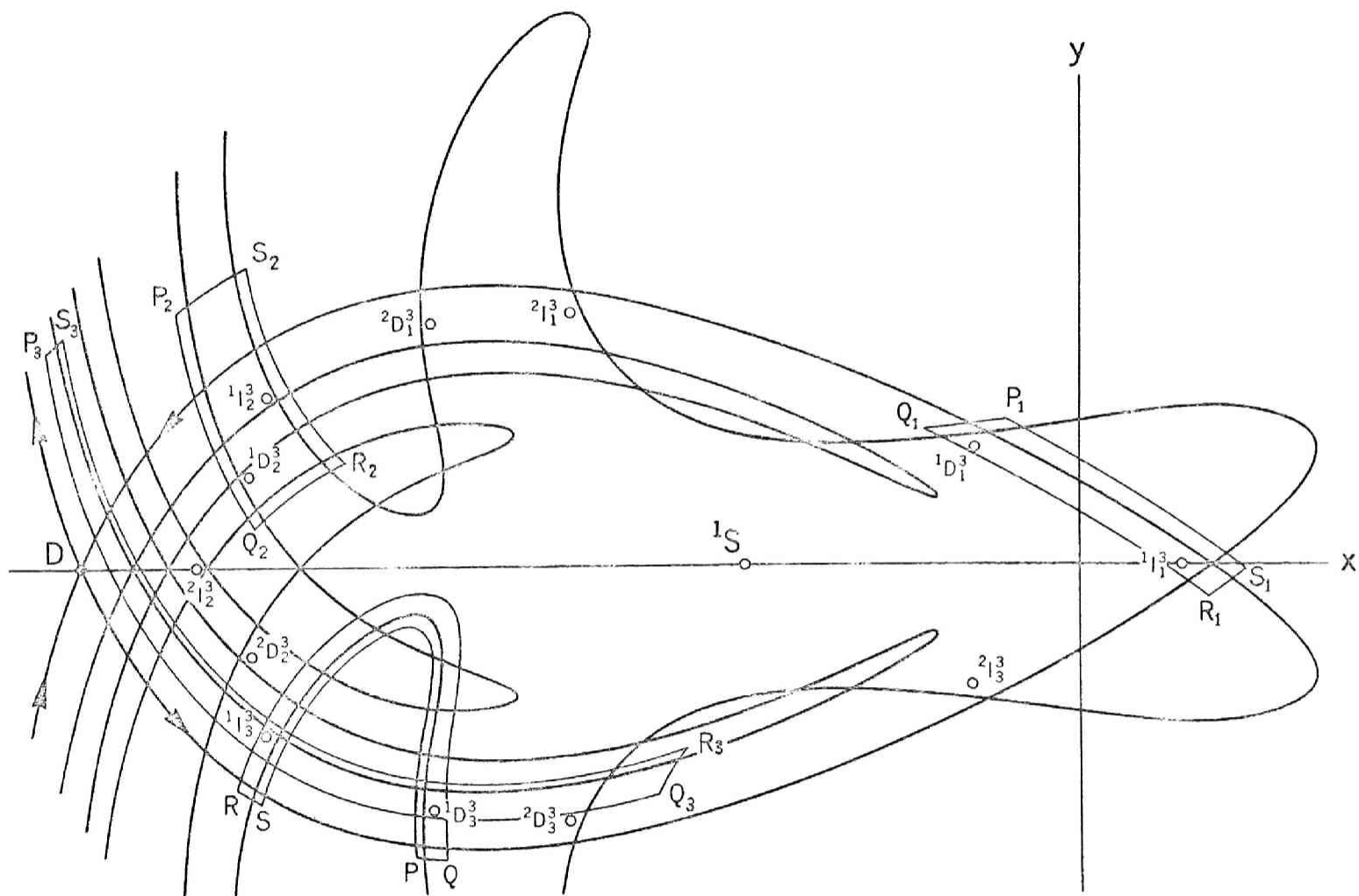


Fig. 4.5 (c). An example of horseshoe domain $PQRS$ of the mapping T^3 for Eq. (4.3).

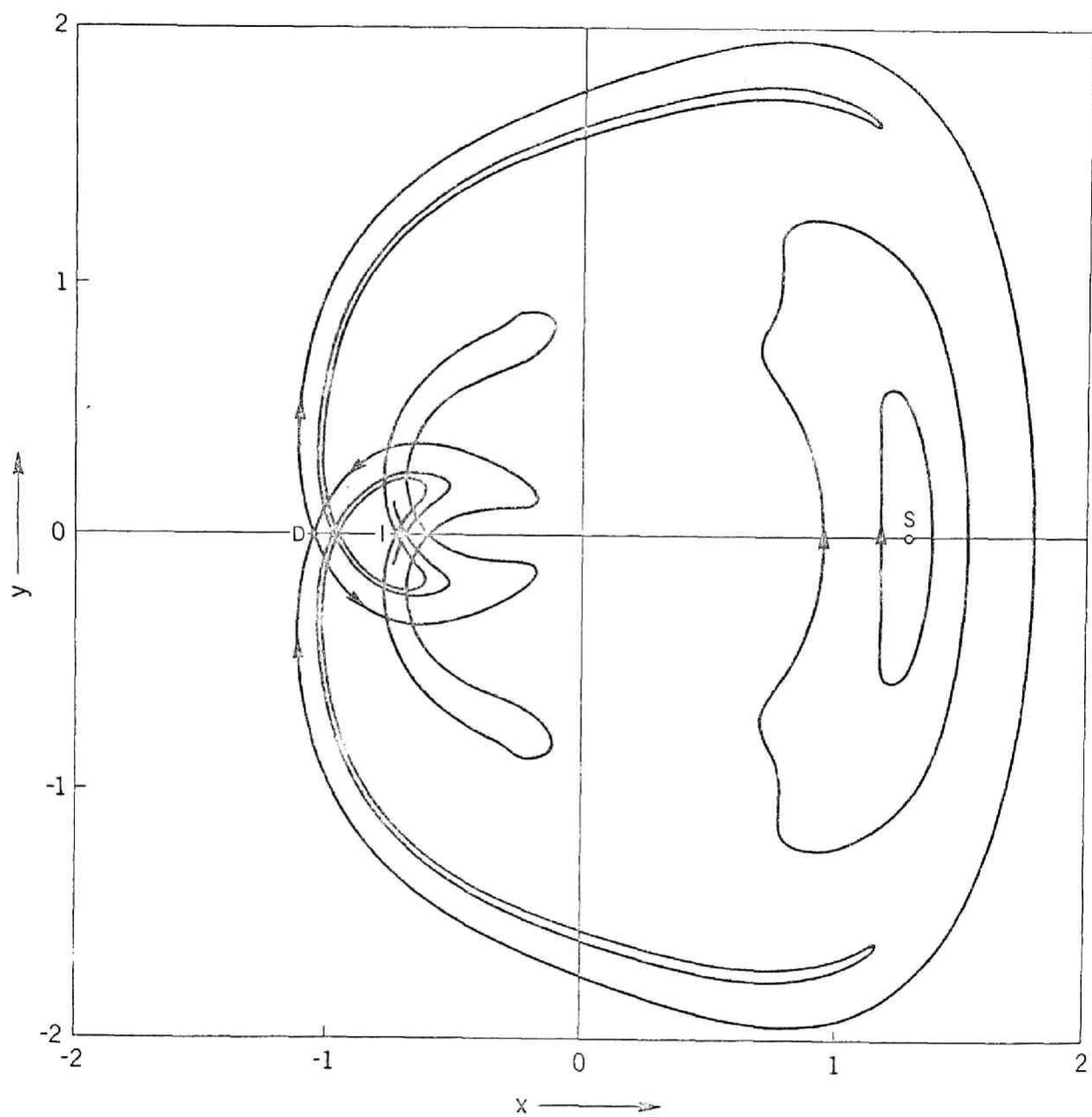


Fig. 4.6. Fixed points and invariant curves of the mapping
for Eqs. (4.4).

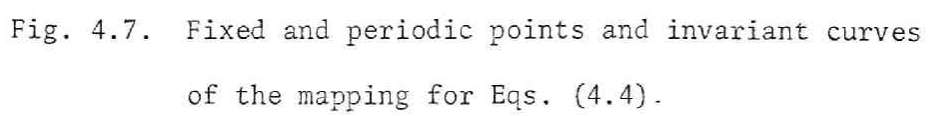
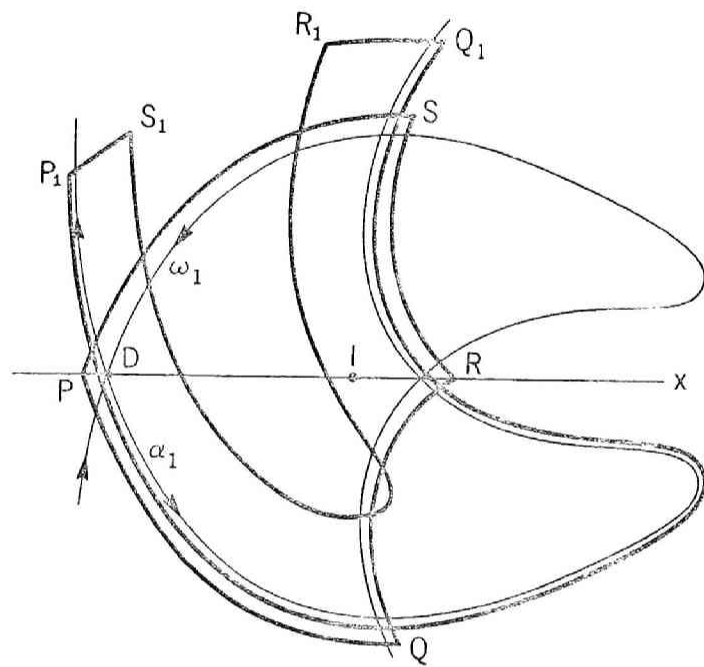
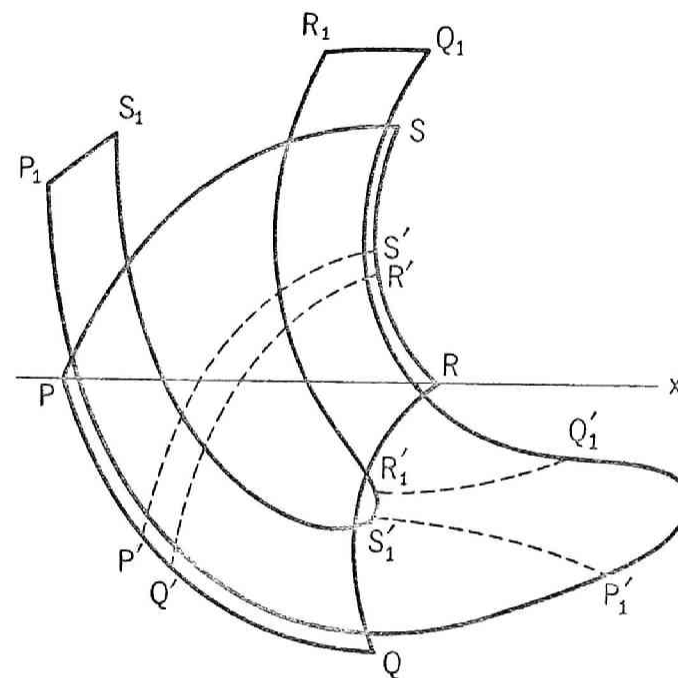


Fig. 4.7. Fixed and periodic points and invariant curves of the mapping for Eqs. (4.4).



(a)



(b)

Fig. 4.8. An example of horseshoe domain of the mapping T for Eqs. (4.4).

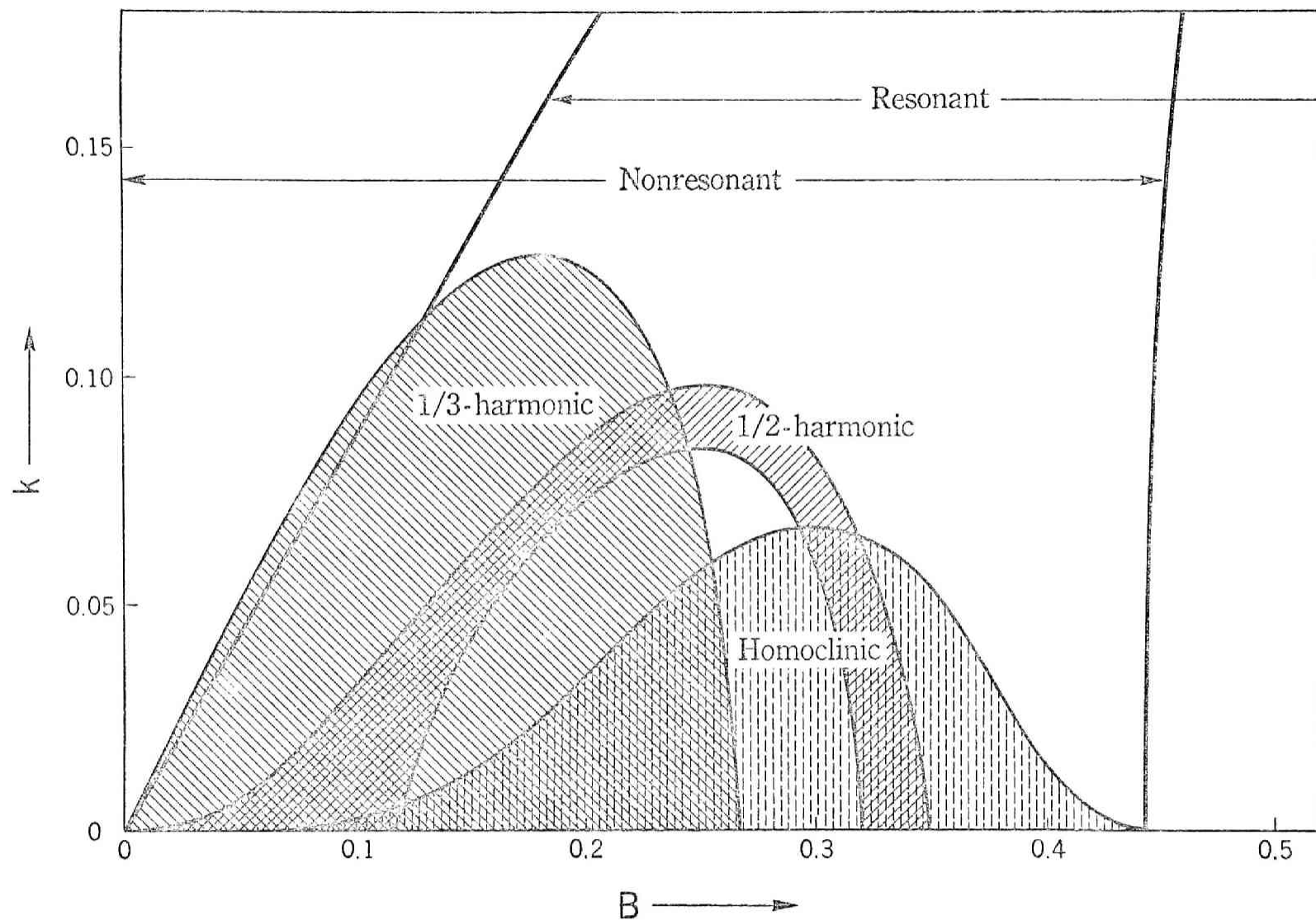


Fig. 4.9. Regions in which fixed, periodic, and homoclinic points are obtained.

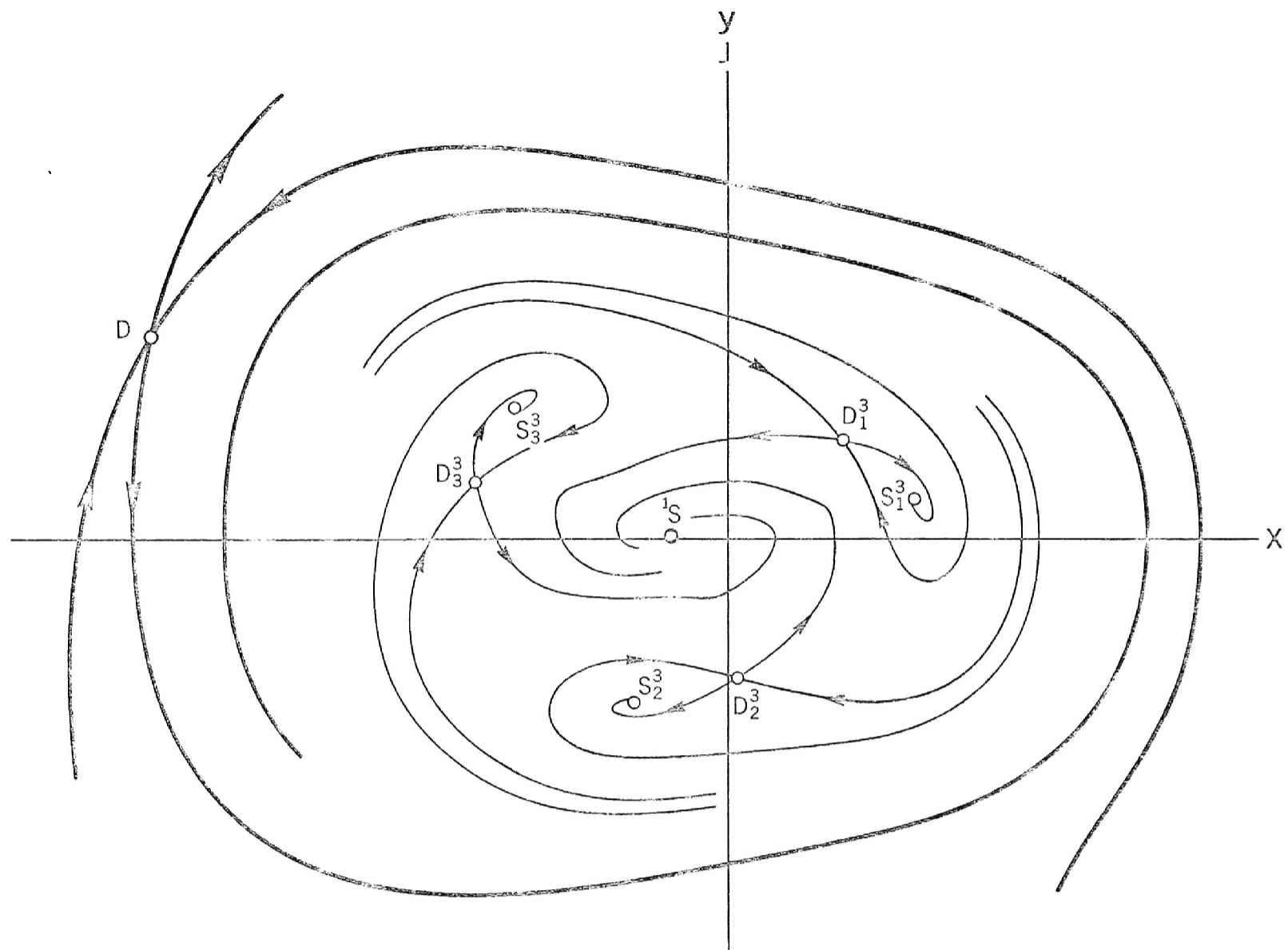
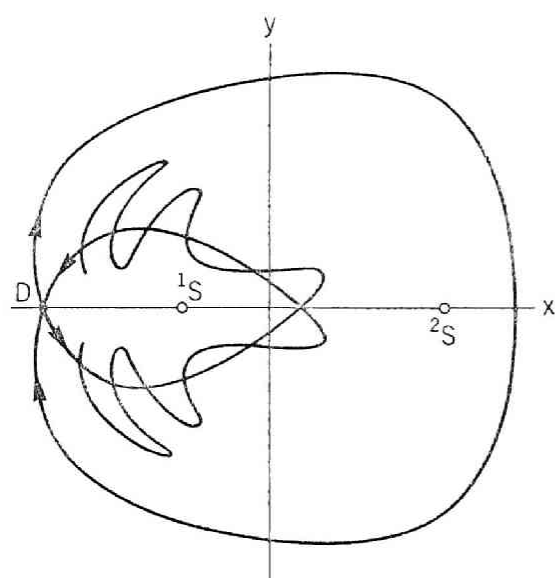
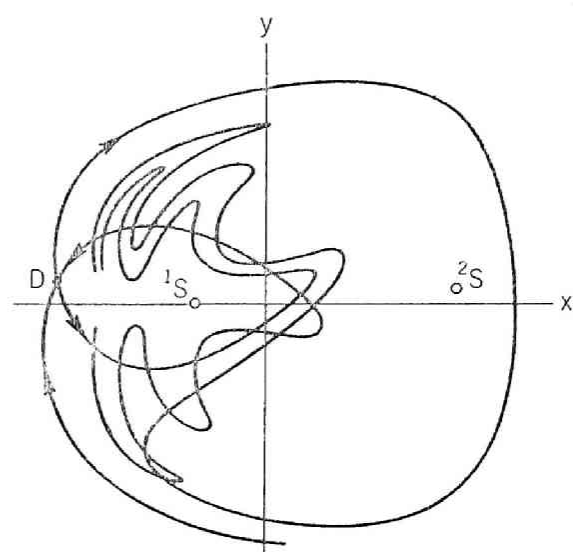


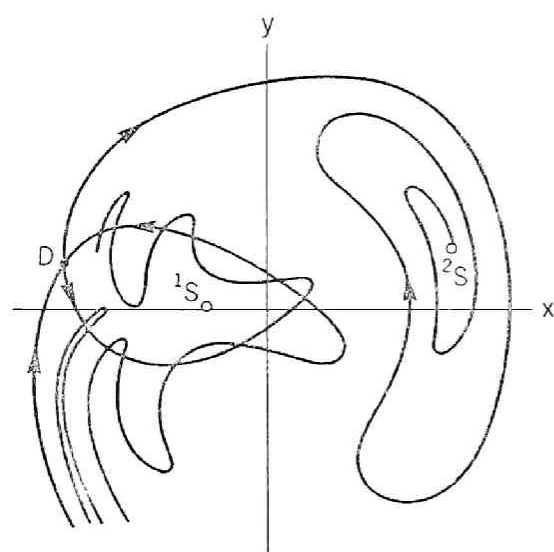
Fig. 4.10. Fixed and periodic points and invariant curves of the mapping
in a dissipative system ($k = 0.02$, $B = 0.04$ in Eqs. (3.3)).



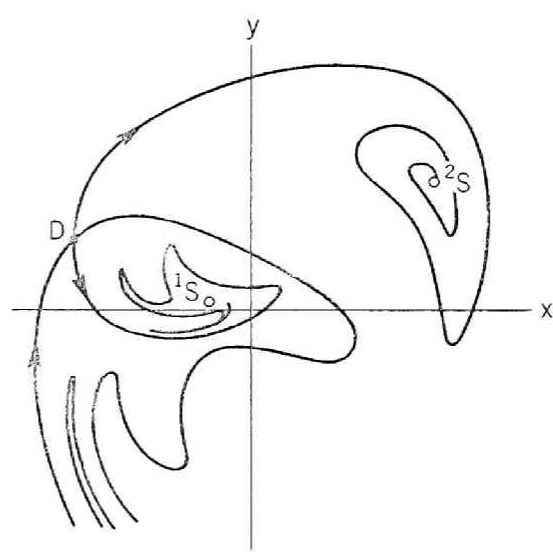
(a)



(b)



(c)



(d)

Fig. 4.11. Fixed points and invariant curves of the mapping for Eqs. (3.3).

(a) $k = 0$, $B = 0.3$

(b) $k = 0.005$, $B = 0.3$

(c) $k = 0.05$, $B = 0.3$

(d) $k = 0.1$, $B = 0.3$.

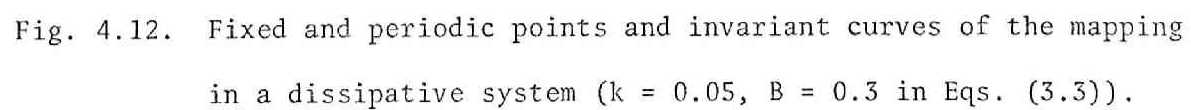


Fig. 4.12. Fixed and periodic points and invariant curves of the mapping in a dissipative system ($k = 0.05$, $B = 0.3$ in Eqs. (3.3)).

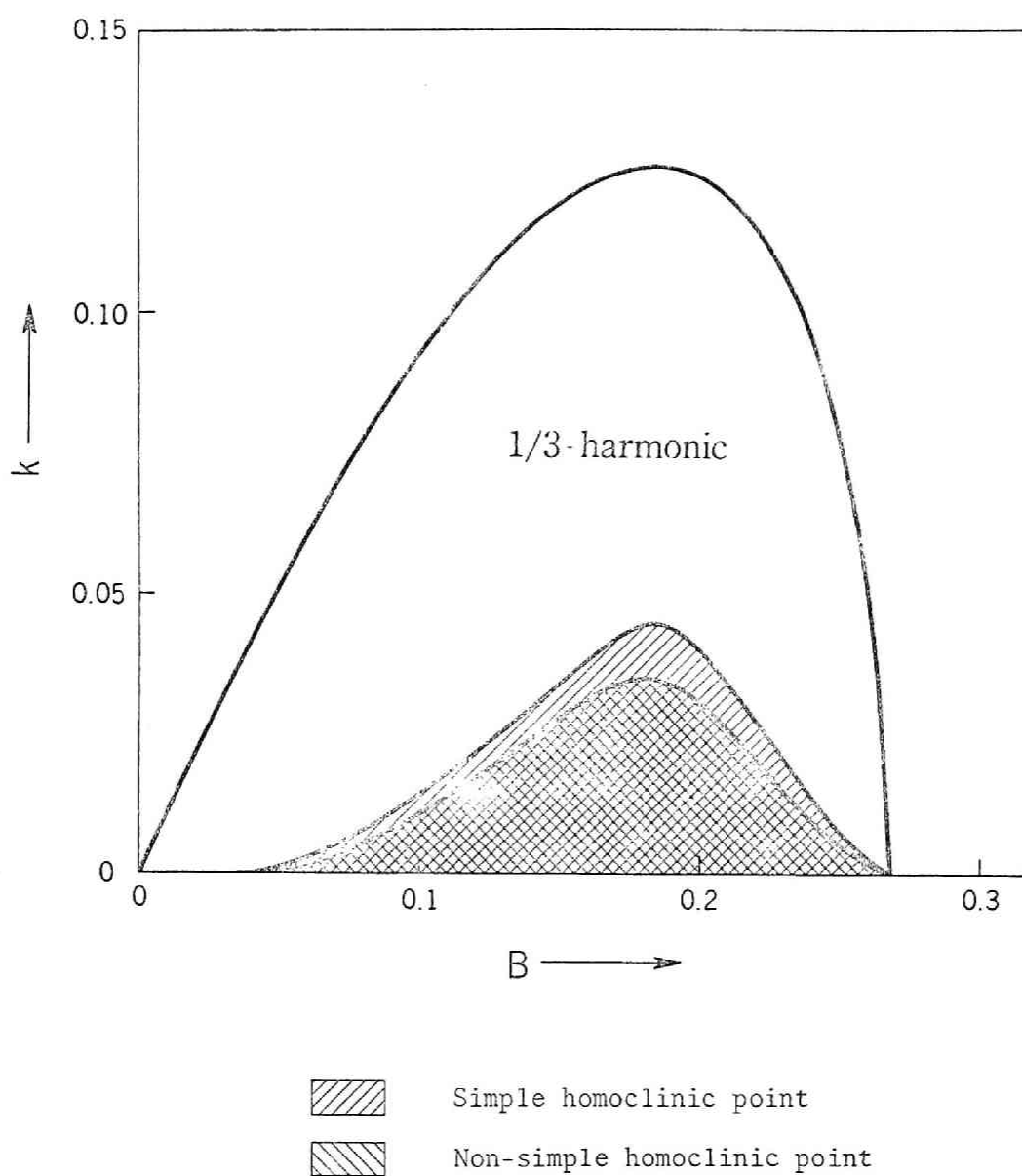
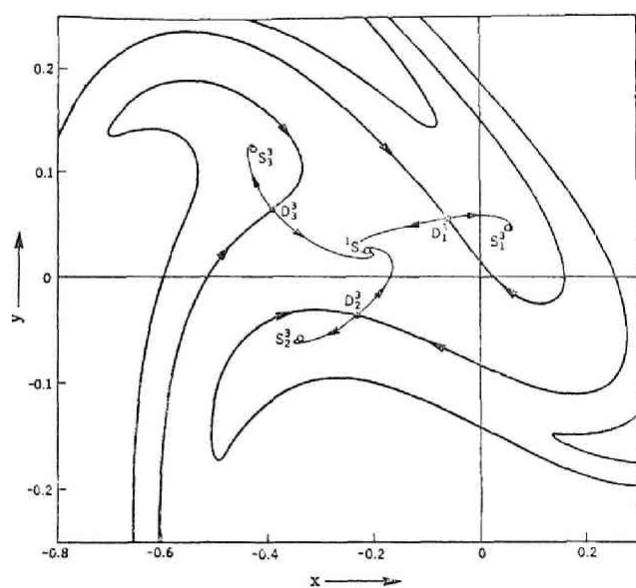
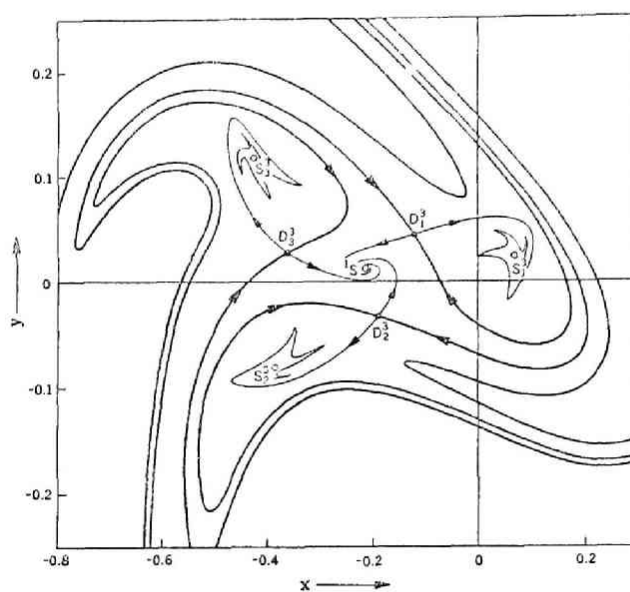


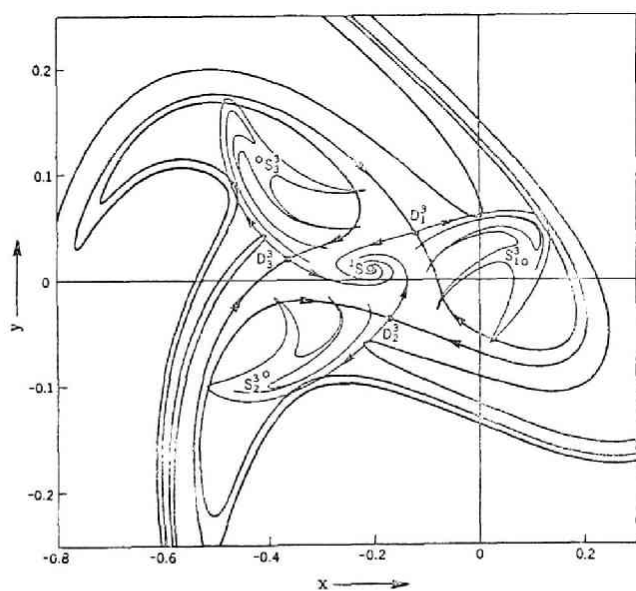
Fig. 4.13. Regions in which 3-periodic, simple homoclinic, and non-simple homoclinic points are obtained.



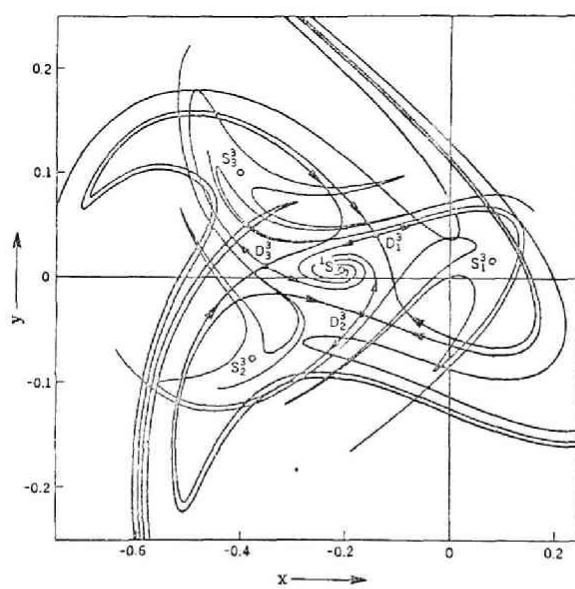
(a) $k = 0.1, B = 0.2$



(b) $k = 0.05, B = 0.2$



(c) $k = 0.035, B = 0.2$



(d) $k = 0.02, B = 0.2$

Fig. 4.14. 3-periodic points and invariant curves of the mapping for Eqs. (3.3).

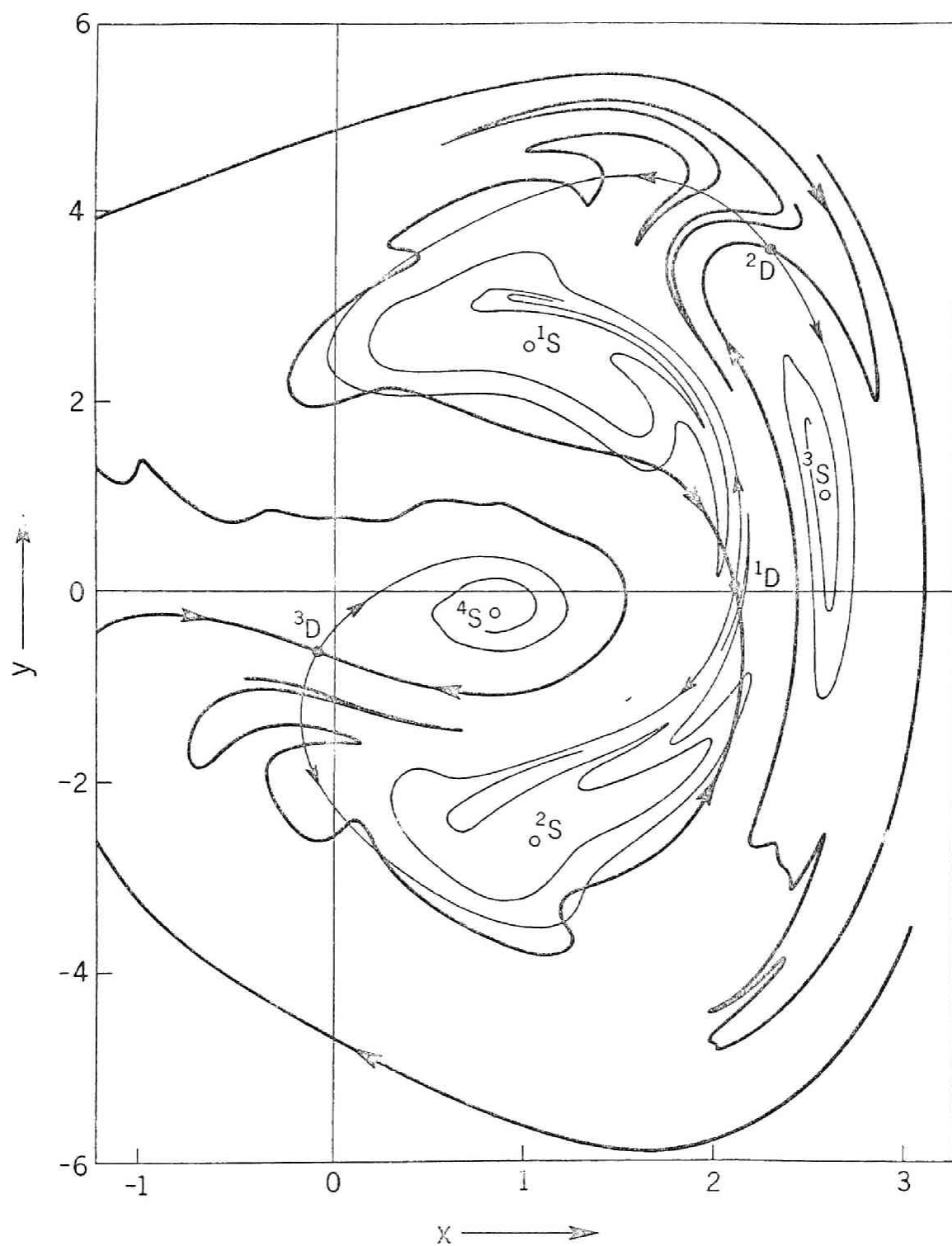


Fig. 4.15. Fixed points and invariant curves of the mapping for Eq. (4.5).

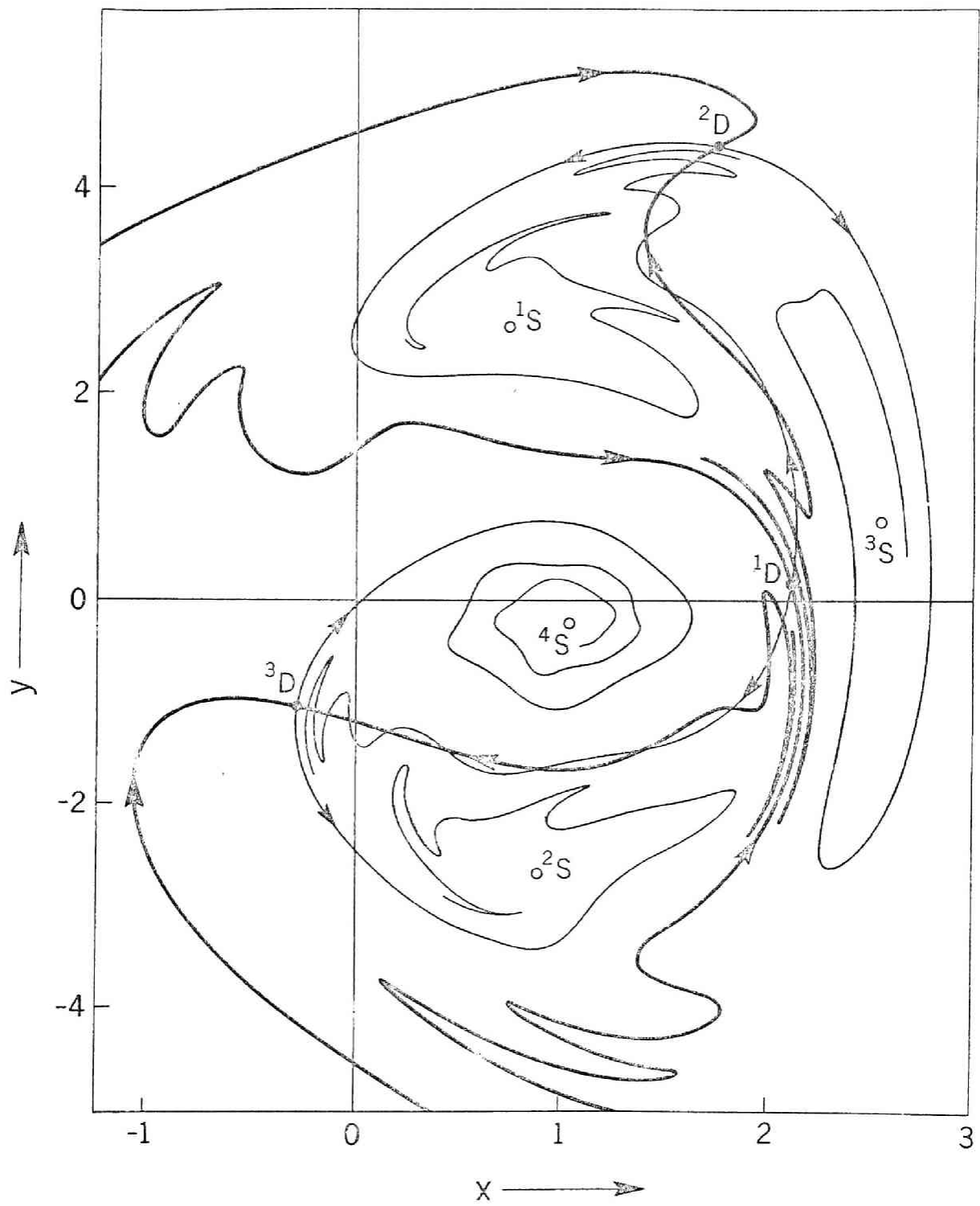


Fig. 4.16. Fixed points and invariant curves of the mapping for Eq. (4.6).

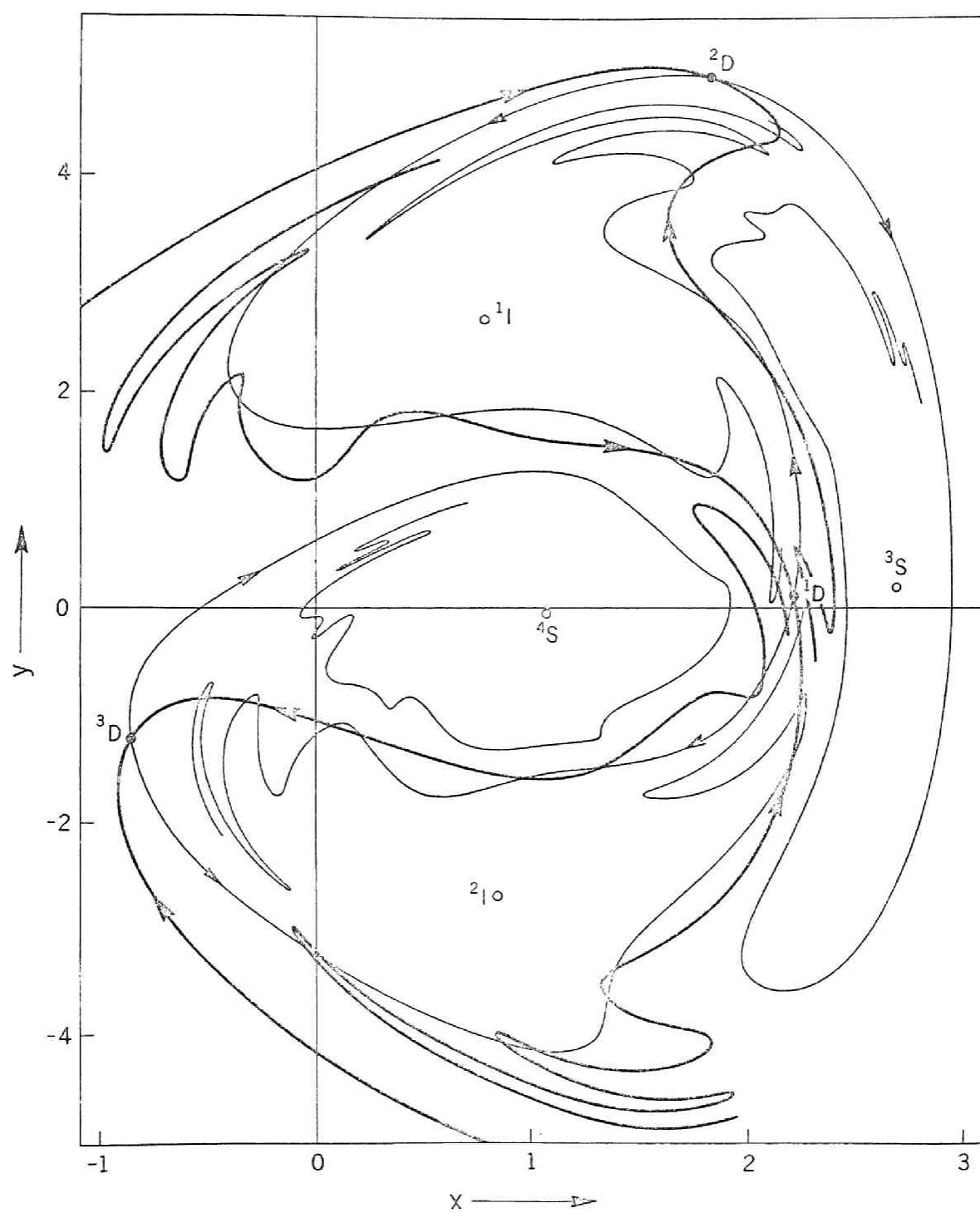


Fig. 4.17. Fixed points and invariant curves of the mapping for Eq. (4.7).

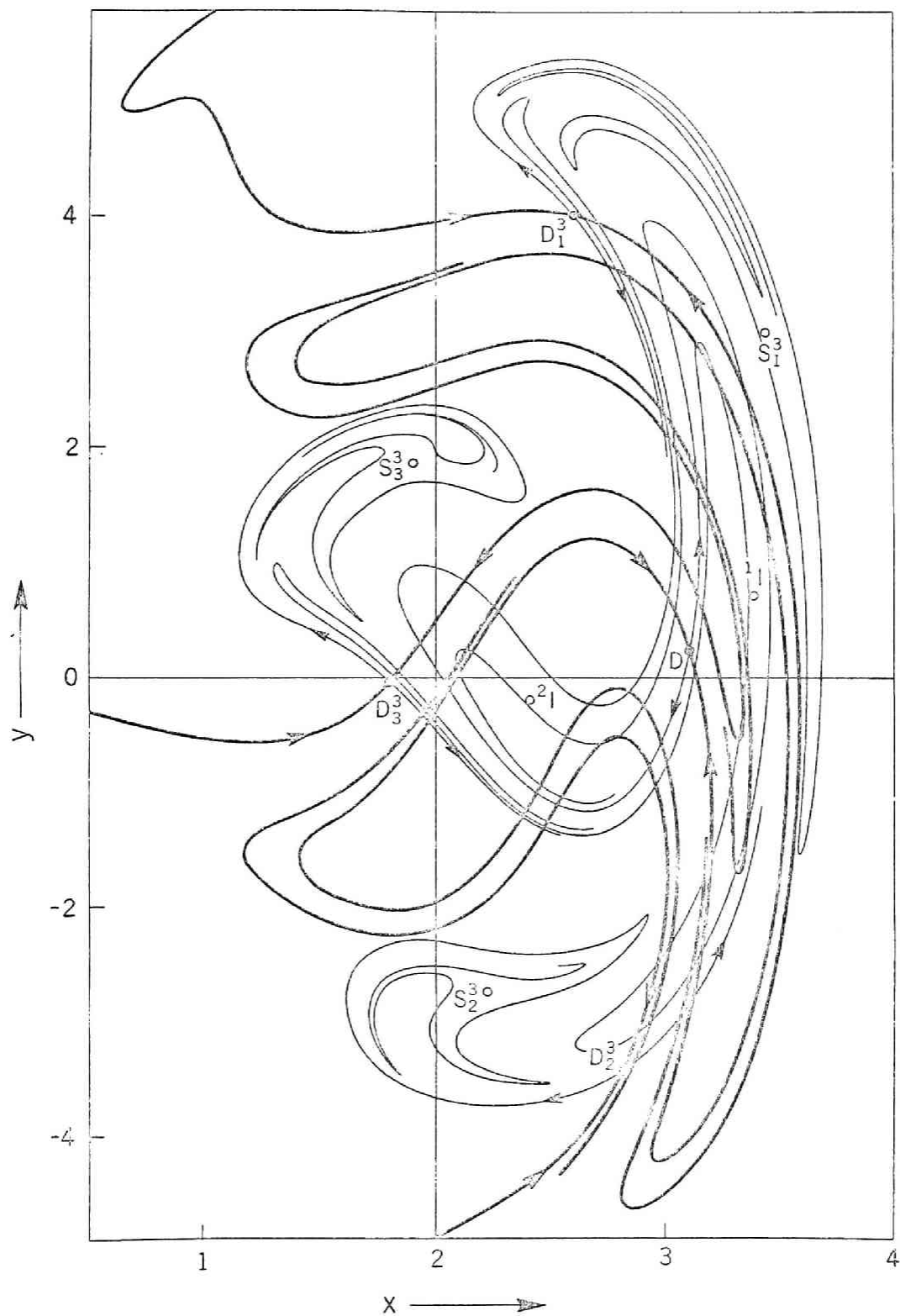


Fig. 4.18. Fixed and 3-periodic points, and invariant curves of the mapping for Eq. (4.8).

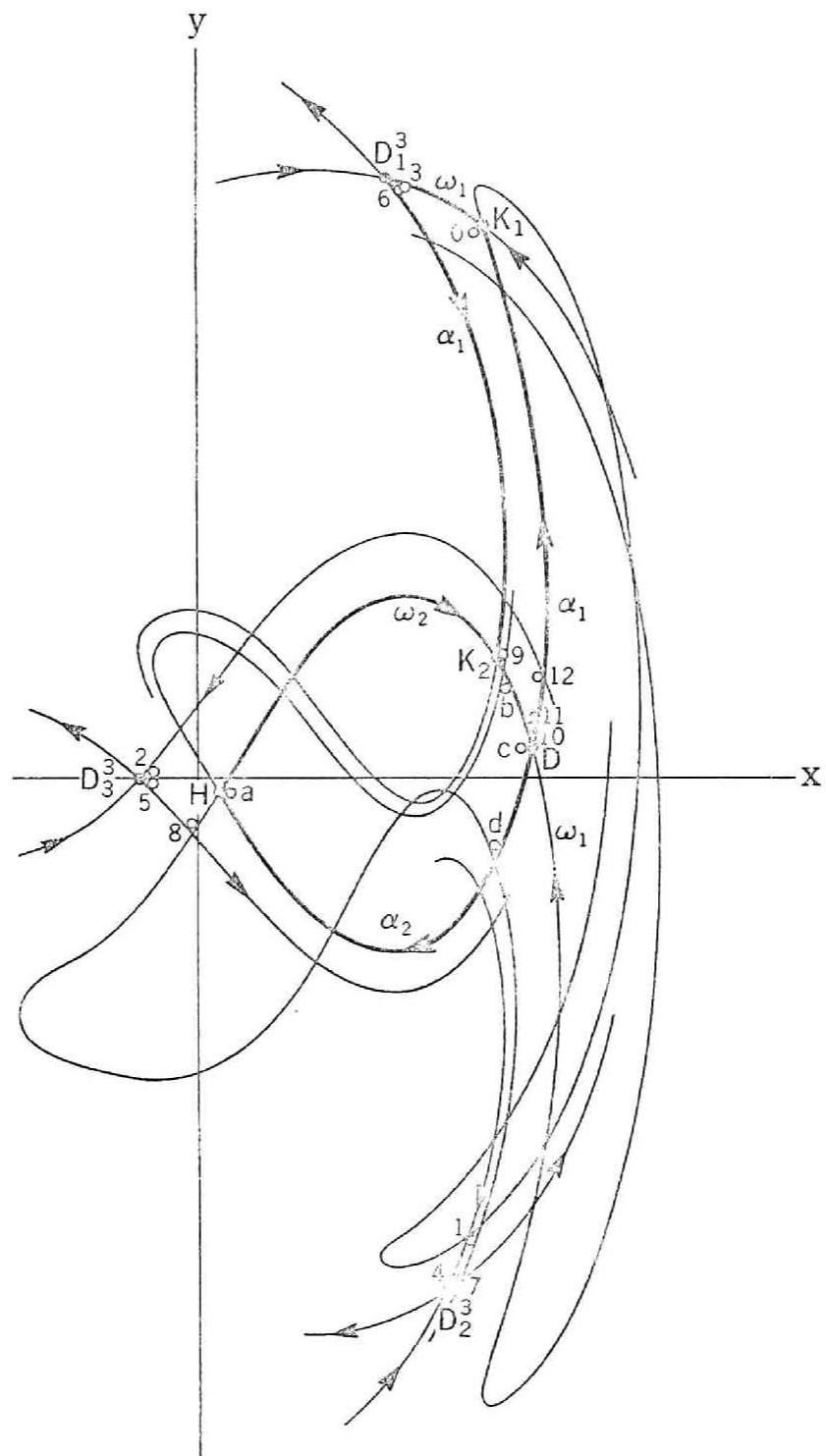


Fig. 4.19. Examples of homoclinic and heteroclinic cycles of the mapping for Eq. (4.8).

REFERENCES

1. Andronov, A. A., A. A. Vitt, and S. E. Khaikin: "Theory of Oscillators," Fizmatgiz, Moscow, 1963 (in Russian); English translation, Pergamon Press, London, 1966.
2. Arnold, V. I.: Instability of dynamical systems with many degrees of freedom, Dokl. Akad. Nauk SSSR, 156-1: 9-12 (1964); Sov. Math. Dokl., 5-3: 581-585 (1964).
3. Arnold, V. I., and A. Avez: "Problèmes ergodiques de la mécanique classique," Gauthier-Villars, Paris, 1967.
4. Birkhoff, G. D.: Nouvelles recherches sur les systemes dynamiques, Mem. Pont. Acad. Sci. Novi. Lyncaeii, 3-1: 85-216 (1935).
5. Birkhoff, G. D.: Sur le problème restreint des trois corps (II), Ann. Scuola Norm. Sup. di Pisa, 2-5: 1-42 (1936).
6. Birkhoff, G. D., and P. A. Smith: Structure analysis of surface transformations, J. de Math., 7-4: 345-379 (1928).
7. Bogoliubov, N. N., and Y. A. Mitropolsky: "Asymptotic Method in the Theory of Nonlinear Oscillations," Fizmatgiz, Moscow, 1963 (in Russian); English translation, Gordon and Breach Science Publishers, Inc., New York, 1961.
8. Cartwright, M. L.: Forced oscillations in nonlinear systems, 149-241 in "Contributions to the Theory of Nonlinear Oscillations," 1 (1950), Ann. Math. Studies, No. 20, Princeton University Press, Princeton, N. J.
9. Cartwright, M. L.: Some decomposition theorems for certain invariant continua and their minimal sets, Fund. Math. 48: 229-250 (1960).
10. Hale, J. K.: "Ordinary Differential Equations," Interscience Publishers, New York, 1969.

11. Hartman, P.: "Ordinary Differential Equations," John Wiley and Sons, Inc., New York, 1964.
12. Hayashi, C.: "Nonlinear Oscillations in Physical Systems," McGraw-Hill Book Company, New York, 1964.
13. Hayashi, C., and Y. Ueda: Behavior of solutions for certain types of nonlinear differential equations of the second order, Sixth Conf. on Nonlinear Oscillations, Poznan, 1972.
14. Hayashi, C., Y. Ueda, and H. Kawakami: Solution of Duffing's equation using mapping concepts, Fourth Conf. on Nonlinear Oscillations, Prague, 1967.
15. Hayashi, C., Y. Ueda, and H. Kawakami: Periodic solutions of Duffing's equation with reference to doubly asymptotic solutions, Fifth Conf. on Nonlinear Oscillations, Kiev, 1969.
16. Hayashi, C., Y. Ueda, and H. Kawakami: Transformation theory as applied to the solutions of non-linear differential equations of the second order, Int. J. Non-Linear Mechanics, 4: 235-255 (1969).
17. Kawakami, H.: Sur les points fixes des itérés d'un difféomorphisme dans le voisinage d'un point homocline, J. Diff. Equations, (to appear).
18. Levenson, M. E.: Harmonic and subharmonic response for the Duffing equation $\ddot{x} + \alpha x + \beta x^3 = F \cos \omega t$ ($\alpha > 0$), J. Appl. Phys., 20: 1045-1051 (1949).
19. Levinson, N.: Transformation theory of non-linear differential equations of the second order, Ann. Math., 45: 723-737 (1944); Correction 49: 738 (1948).
20. Loud, W.: Periodic solutions of $x'' + cx' + g(x) = \epsilon f(t)$, Mem. Am. Math. Soc., No. 31, 1959.
21. Massera, J. L.: The number of subharmonic solutions of non-linear differential equations of the second order, Ann. Math., 50: 118-126 (1949).

22. Minorsky, N.: "Nonlinear Oscillations," D. Van Nostrand Company, Inc., Princeton, N. J., 1962.
23. Neimark, Y. I.: Motions close to doubly-asymptotic motion, Dokl. Akad. Nauk SSSR, 172-5: 1021-1024 (1967); Sov. Math. Dokl., 8-1: 228-231 (1967).
24. Neimark, Y. I.: On one class of dynamical systems, Fifth Conf. on Nonlinear Oscillations, Kiev, 1969.
25. Nishikawa, Y.: "A Contribution to the Theory of Nonlinear Oscillations," Nippon Printing and Publishing Co., Ltd., Osaka, 1964.
26. Pliss, V. A.: "Nonlocal Problems of the Theory of Oscillations," Academic Press Inc., New York, 1966.
27. Pliss, V. A.: The behavior of the solutions of structurally stable periodic and autonomous systems, Dokl. Akad. Nauk SSSR, 182-3: 500-502 (1968); Sov. Math. Dokl., 9-5: 1161-1163 (1968).
28. Pliss, V. A.: On separatrices of periodic saddle motions for periodic systems of the second-order differential equations, Dokl. Akad. Nauk SSSR, 197-2: 275-276 (1971); Sov. Math. Dokl., 12-2: 441-442 (1971).
29. Poincaré, H.: "Les Méthodes nouvelles de la Mécanique Céleste," Vol. 3, Gauthier-Villars, Paris, 1899; Dover Edition 1957.
30. Silnikov, L. P.: On the problem of Poincaré-Birkhoff, Math. Sb., 74(116)-3: 378-397 (1967).
31. Silnikov, L. P.: The existence of a countable set of periodic motions in the neighborhood of a homoclinic curve, Dokl. Akad. Nauk SSSR, 172-2: 298-301 (1967); Sov. Math. Dokl., 8-1: 102-106 (1967).
32. Smale, S.: Diffeomorphisms with many periodic points, 63-80 in "Differential and Combinatorial Topology," Princeton University Press, Princeton, N.J., 1965.

33. Smale, S.: Differentiable dynamical systems, Bull. Amer. Math. Soc., 73: 747-817 (1967).
34. Smale, S.: Stable manifolds for differential equations and diffeomorphisms, Ann. Scuola Norm. Sup. di Pisa, 17-3: 97-116 (1963).
35. Ueda, Y.: "Some Problems in the Theory of Nonlinear Oscillations," Nippon Printing and Publishing Company Co., Ltd., Osaka, 1968.

